DOE/NASA/3132-78/1
NASA CR-135344

EMPLOYING STATIC EXCITATION CONTROL AND TIE LINE REACTANCE TO STABILIZE WIND TURBINE GENERATORS

H. H. Hwang, H. V. Mozeico, and Tenhuei Guo
University of Hawaii
Honolulu, Hawaii 96822

April 1978

Prepared for the
NATIONAL AERONAUTICS AND SPACE ADMINISTRATION
Lewis Research Center
Cleveland, Ohio 44135

Grant NAS 3-3132

As a part of the
U.S. DEPARTMENT OF ENERGY
Division of Solar Energy
Federal Wind Energy Program

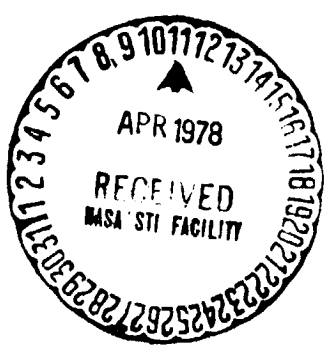

1. Report No.	2. Government Accession No.	3. Recipient's Catalog No.
NASA CR-135344		

4. Title and Subtitle	5. Report Date
EMPLOYING STATIC EXCITATION CONTROL AND TIE LINE REACTANCE TO STABILIZE WIND TURBINE GENERATORS	April 1978
	6. Performing Organization Code

7. Author(s)	8. Performing Organization Report No.
H. H. Hwang, H. V. Mozeico, and Tenhuei Guo	
	10. Work Unit No.

9. Performing Organization Name and Address	11. Contract or Grant No.
University of Hawaii Honolulu, Hawaii 96822	NSG-3132
	13. Type of Report and Period Covered
12. Sponsoring Agency Name and Address U. S. Department of Energy Division of Solar Energy Washington, D.C. 20545	Contractor Report
	14. Sponsoring Agency Code
	DOE/NASA/3132-78/1

15. Supplementary Notes

Final report. Prepared under Interagency Agreement E(49-26)-1004. Project Manager, Leonard J. Gilbert, Wind Energy Project Office, NASA Lewis Research Center, Cleveland, Ohio 44135.

16. Abstract

This study presents an analytical representation of a wind turbine generator which employs blade pitch angle feedback control. A mathematical model is formulated. With the functioning MOD-0 wind turbine serving as a practical case study, results of computer simulations of the model as applied to the problem of dynamic stability at rated load are presented. The effect of the tower shadow is included in the input to the system. Different configurations of the drive train, and optimal values of the tie line reactance are used in the simulations. Computer results reveal that a static excitation control system coupled with optimal values of the tie line reactance will effectively reduce oscillations of the power output, without the use of a slip clutch.

17. Key Words (Suggested by Author(s))	18. Distribution Statement
Wind power Alternator Windmill	Unclassified - unlimited STAR Category 44 DOE Category UC-60

19. Security Classif. (of this report)	20. Security Classif. (of this page)	21. No. of Pages	22. Price*
Unclassified	Unclassified		

* For sale by the National Technical Information Service, Springfield, Virginia 22161

TABLE OF CONTENTS

INTRODUCTION

ERDA-NASA has planned a graduated wind turbine project, with turbines ranging from 100-kw to 1500-kw [1]. The project currently has a 100-kw wind turbine at the NASA Plum Brook Station near Sandusky, Ohio, which became operational in 1975. This wind turbine, designated the Mod-0, is used as a practical case study in this paper (Fig. 1).

The Mod-0 is a horizontal-axis, propeller type machine. The rotor is downwind of the tower and rotates at a constant speed of 40 rpm. The alternator is a 125 kva, 3 phase, 60 hz, 1800 rpm, 480 volt, Y-connected synchronous machine. Figure 2 shows details of the wind turbine drive train assembly, and yaw system.

The control of a system which generates power from as unsteady an input as the wind presents a formidable problem. Even with constant wind velocity, the input at a wind turbine's blades varies due to the cyclical obstruction of the wind by the turbine's supporting tower. Control of the pitch of the turbine's blades relative to their plane of rotation is perhaps the most promising method to stabilize the effects of such an input upon the mechanical stresses of the turbine and the electromagnetic transients of the generator.

The first purpose of this study is to analyze the current control method for wind turbine generators, i.e. blade pitch angle control and a slip clutch [2]. Secondly, an investigation is conducted via computer simulation of the effects of techniques proposed in this paper upon the dynamic stability of the Mod-0.

SYSTEM EQUATIONS

Figure 3 is a schematic diagram of the system under study. Speed control is used only for the starting up and synchronization operations. The power control system is used for stabilizing the output under load conditions. The blade pitch control system is shown in Fig. 4.

Synchronous Machine Equations

Park's equation [3], with appropriate modifications, [4,5], are used.

It is reasonable to assume that the transformer emfs $(\frac{d\lambda_d}{dt}, \frac{d\lambda_q}{dt})$ are negligible as compared to the speed voltages $(\omega_o\lambda_d, \omega_o\lambda_q)$. Also, the synchronous generator frequency may be assumed to be the same as the system frequency, ω_o, as long as synchronism is retained.

$$\frac{de'_q}{dt} = (V_f - e_{q1})/T'_{do} \tag{1}$$

$$\frac{de''_q}{dt} = -\frac{e_{q2}}{T''_{do}} \frac{x'_d - x''_d}{x_d - x''_d} \tag{2}$$

$$\frac{de''_d}{dt} = -e_d/T''_{qo} \tag{3}$$

$$i_d = \frac{(R_a e''_d + x''_q e''_q) - (R_a V_d + x''_q V_q)}{R_a^2 + x''_d x''_q} \tag{4}$$

$$i_q = \frac{(R_a e''_q - x''_d e''_d) - (R_a V_q - x''_d V_d)}{R_a^2 + x''_d x''_q} \tag{5}$$

$$\lambda_d = e''_q - i_d x''_d \tag{6}$$

$$\lambda_q = -e''_d - i_q x''_q \tag{7}$$

$$e_d = \frac{x_q}{x''_q} e''_d + \frac{(x_q - x''_q)}{x''_q} \lambda_q \tag{8}$$

$$e_{q1} = \frac{x_d - x''_d}{x'_d - x''_d} e'_q - \frac{x_d - x'_d}{x'_d - x''_d} e''_q \tag{9}$$

$$e_{q2} = -\frac{x_d - x''_d}{x'_d - x''_d} e'_q + \frac{x'_d}{x''_d} \frac{x_d - x'_d}{x'_d - x''_d} e''_q - \frac{x_d - x''_d}{x''_d} \lambda_d \tag{10}$$

The armature current is given by

$$i_a = \sqrt{i_d^2 + i_q^2} \tag{11}$$

The electromagnetic torque is:

$$T_e = [e''_q i_q + e''_d i_d - i_d i_q (x''_d - x''_q)] \tag{12}$$

Equations (1-12) are in per unit based upon the machine rating. In these equations, the total tie line and transformer reactances, X_L, are included in the machine impedances. Therefore, voltages V_d and V_q in Eqs. (4) and (5) are the d-axis and q-axis components of the bus voltage.

Equations of Motion

The electromagnetic torque (referred to the rotor shaft) in lb-ft is

$$T_L = \frac{NP}{2} \frac{1}{\omega_o} (\text{kva base})(738) T_e \tag{13}$$

Two configurations for the equations of motion, or swing equations are formulated. The first representation of the drive train system is by a π-mechanical network (Fig. 5).

The corresponding equations are:

$$\frac{d\delta_m}{dt} = \Omega - \Omega_N = \Omega_e \tag{14}$$

$$\frac{d\delta_w}{dt} = ZW \tag{15}$$

$$\frac{d\Omega}{dt} = \frac{2K(\delta_w - \delta_m) - 2T_L - B\Omega}{J} \tag{16}$$

$$\frac{dZW}{dt} = \frac{2T - 2K(\delta_w - \delta_m) - B(\Omega_N + ZW)}{J} \tag{17}$$

where δ_m is in mechanical radians and T is in lb-ft.

In the Mod-0, a Falk coupling is installed between the low speed shaft and the step up gearbox (not shown in Fig. 2). The torsional stiffness coefficient, K_f, of the Falk coupling is a function of the power output, P_o, in kw.

$$K_f = (0.000042\ P_o^2 + 0.0057\ |P_o| + 0.06) \tag{18}$$

The spring constant, K, in Fig. 5 is

$$K = \frac{1}{1.919253 + \frac{1}{K_f}} \times \frac{10^8}{12} \text{ lb-ft/rad} . \tag{19}$$

If the Falk coupling is removed,

$$K = 4.342 \times 10^6 \text{ lb-ft/rad} . \tag{20}$$

The second configuration represents the drive train system by a π-network with slip clutch, B_c, Fig. 6. In this case, Eqs. (14) and (15) remain the same and Eqs. (16) and (17) are replaced by

$$\frac{d\Omega}{dt} = \frac{T_2 - T_L}{J_2} \tag{21}$$

$$\frac{dZW}{dt} = \frac{2T - 2K(\delta_w - \delta_r) - B(\Omega_c + ZW)}{J_1} \tag{22}$$

$$\frac{d\delta r}{dt} = ZR \tag{23}$$

$$\frac{dZR}{dt} = \frac{2K(\delta_w - \delta_r) - 2T_c - B(\Omega_c + ZR)}{J_1} \tag{24}$$

The Slip, S is defined as

$$S = 1 - \frac{\Omega_N + \Omega_e}{\Omega_c + ZR} \tag{25}$$

where Ω_N and Ω_c are the reference shaft speeds (referred to the turbine rotor shaft) on the right hand and left hand sides of the slip clutch in Fig. 6, respectively.

The mechanical torque transferred by the slip clutch in lb-ft is approximated by a function of the slip S:

$$T_2 = aS^4 + bS^3 + cS^2 + dS \tag{26}$$

$$T_c = \frac{T_2}{1-S} \tag{27}$$

Equations of the Blade Pitch Control System

The Mod-0 feedsback the power output of the alternator to the blade pitch control system to stabilize the output under load conditions. Here the pitch controller, Fig. 4, consists only of an integrator, without the proportional components ($K_1 = 0$).

The following equations are formulated according to Fig. 4.

$$\frac{dX_1}{dt} = K_2(P_N - P_o) \tag{28}$$

where

$$P_o = (\text{kva base})(V_d i_d + V_q i_q) \tag{29}$$

and P_N is the reference power input.

$$\frac{dX_2}{dt} = Y \tag{30}$$

$$\frac{dX_3}{dt} = X_4 \tag{31}$$

$$\frac{dX_4}{dt} = \omega_N^2 X_2 - \omega_N^2 X_3 - 2\xi\omega_N X_4 \tag{32}$$

The input and output variables of the flow limiter are:

$$X = \frac{1}{\tau_p}(X_1 - X_2) \tag{33}$$

$$Y = \text{limit}\left(-\frac{\pi}{22.5}, \frac{\pi}{22.5}, X\right) \tag{34}$$

The change in pitch angle is

$$\Delta\theta = \frac{180}{\pi} X_3 \tag{35}$$

The pitch angle is

$$\theta = \theta_N + \Delta\theta \tag{36}$$

The corresponding torque developed by the rotor in lb-ft is:

$$T = f(V_w, \Omega_r, \theta) \tag{37}$$

Equation (37) is a nonlinear function of wind speed in mph, rotor speed in rpm, and pitch angle in mechanical degrees, [6]. The turbine blade pitch angle physically can vary only from -90 degrees to zero degrees so that the slope of the torque angle curves is always positive. Figure 7 shows the turbine torque-pitch angle curves for 15, 18 and 20 mph.

Equations of Generator Excitation Control System

A static excitation regulator is used to hold the terminal voltage, the output power factor, and the armature current of the generator within satisfactory limits. The excitation control system is approximated by the following equations:

$$\frac{d\Delta V_f}{dt} = z \tag{38}$$

$$\frac{dz}{dt} = \frac{\mu_e}{\tau_e} \Delta V_t - \frac{z}{\tau_e} \tag{39}$$

$$V_f = V_{fn} + \Delta V_f \tag{40}$$

$$\Delta V_t = (V_N - V_t) - K_3\left(0.8\, i_a - \frac{P_o}{V_t(\text{kva base})}\right) \tag{41}$$

$$V_{td} = V_d - X_L i_q \tag{42}$$

$$V_{tq} = V_q + X_L i_d \tag{43}$$

$$V_t = \sqrt{V_{td}^2 + V_{tq}^2} \tag{44}$$

$$V_d = \sin\delta, \quad V_q = \cos\delta \tag{45}$$

$$\delta = \frac{180}{\pi} \frac{NP}{2} \delta_m \tag{46}$$

The first term in Eq. (41) corrects for the deviation of the generator terminal voltage, V_t, from its reference value, V_N. The second term corrects for power factor deviation. At rated output, the practical power factor is equal to 0.8, lagging current. V_{td} and V_{tq} in Eqs. (42) and (43) are the d-axis and q-axis components of V_t.

DIGITAL SIMULATION

The system equations formulated in the preceding sections are nonlinear and interrelated. They are solved numerically by the fourth order Adams-Bashforth (predictor) and Adams-Moulton (corrector) method, [7], for which a fixed stepsize of $h = 0.005$ is used.

Initially, the wind generator is supplying rated power (100-kw) to the bus at 0.8 power factor, lagging current, and rated frequency. The tower shadow cuts in at time t=0. All case studies simulated here were run for 30 simulated seconds. Only the last 14 seconds of the simulation are plotted here, in order to allow the initially stable system time to adjust to the artificially abrupt imposition of the tower shadow at time=0. All time references on the graphs are relative to these last 14 seconds.

System Input

In all the cases under study, a constant wind speed of 18 mph is assumed. However, practical experience with the Mod-0 has revealed that a significant cyclical perturbation occurs, caused by the obstruction of the wind by the supporting tower of the turbine [8]. The rotor blades, which are downwind of the tower, enter into this 'tower shadow' of reduced wind velocity during each revolution. The shadow's arc is estimated to be 30 degrees.

Data from the NASA-Lewis Research Center reveals that the Mod-0 sustains approximately a 28 percent decrease in torque as a blade passes through the tower shadow, Fig. 8. The effective wind speed at the blades is calculated by using Eq. (37) and holding both the rotor speed and the blade pitch angle constant. Thus the 28 percent decrease in torque is equivalent to a 10 percent decrease in wind velocity at the blade when in the shadow, Fig. 9. A cosine function models the tower shadow effect.

Case Studies

	Case	Falk Coupling	Slip Clutch	X_L, Per Unit
Original Mod-0	1	Yes	No	0.02
Current Mod-0	2	Yes	Yes	0.02
Hypothetical Cases	3	No	No	0.02
	4	No	Yes	0.02
	5	No	Yes	0.40
	6	No	Yes	0.47
	7	No	Yes	0.50
	8	No	Yes	0.55
	9	No	Yes	0.60
	10	Yes	Yes	0.47
	11	No	No	0.20
	12	No	No	0.30
	13	No	No	0.35
	14	No	No	0.40
	15	No	No	0.43
	16	No	No	0.47
	17	No	No	0.50
	18	No	No	0.55

Case 1. Falk coupling, no slip clutch, $X_L = 0.02$ p.u.

This case represents the Mod-0 as originally conceived, without a slip clutch. Early operational experience with this configuration was unsatisfactory. Later, a slip clutch was added to the Mod-0 (see Case 2). The configuration here includes the Mod-0's Falk coupling, and its existing tie-line and transformer reactances, X_L.

The following table summarizes the maximum and minimum values for the last 14 simulated seconds of Case 1:

	Alternator Output (KW)	Armature Current (p.u.)	Power Angle (El. Deg.)	Rotor Speed (rpm)	Pitch Angle (deg.)	Turbine Torque (ft-lb)	Generator Torque (ft-lb)	Field Voltage (p.u.)	Power Factor
Maximum	139.4	1.305	34.33	40.12	-0.267	22898	25295	2.911	0.852
Minimum	67.8	0.733	20.65	39.90	-0.524	16420	12167	2.830	0.715
Max-Min	71.6	0.572	13.68	0.22	0.257	6478	13128	0.081	0.137

Graphic representations for Case 1 are given in Figs. 10a-g.

Unlike all the other cases, Case 1 was simulated for 40 seconds rather than 30 seconds. Thus, as compared to the subsequent cases, an additional 10 seconds was provided here to allow this particularly unstable configuration to react to the abrupt imposition of the tower shadow.

Note that although the input is periodically uniform, the graphs of this configuration reveal a moderate harmonic response.

Case 2. Falk coupling, slip clutch, $X_L = 0.02$ p.u.

This case represents the existing Mod-0 with its added slip clutch.

The addition of the slip clutch has reduced the oscillations of all the variables tabulated below, except turbine torque, by a factor greater than 3. However, the response of the system here is characterized by a more severe harmonic response to the input, Figs. 11a-h.

The following table summarizes the maximum and minimum values for the last 14 simulated seconds of Case 2:

	Alternator Output (KW)	Armature Current (p.u.)	Power Angle (El. Deg.)	Rotor Speed (rpm)	Pitch Angle (deg.)	Turbine Torque (ft-lb)	Generator Torque (ft-lb)	Field Voltage (p.u.)	Power Factor
Maximum	112.2	1.085	29.70	40.04	+0.010	23093	20206	2.878	0.818
Minimum	89.5	0.906	25.47	39.97	-0.063	16632	16076	2.856	0.779
Max-Min	22.7	0.179	4.23	0.07	0.073	6461	4130	0.022	0.039

Case 3. No Falk coupling, no slip clutch, $X_L = 0.02$ p.u.

This case is a theoretical one, differing from Case 1 only in the removal of the Mod-0's Falk coupling. The improvement in performance caused by this hypothetical stiffer shaft is considerable. The difference between maximum and minimum values here is very similar in magnitude to the corresponding values of Case 2. However, contrary to the harmonic response exhibited in the simulation

of the Mod-0 with a slip clutch (Case 2), maximum and minimum values for each cycle in Case 3 are very nearly constant, Figs. 12a-g.

The following table summarizes the maximum and minimum values for the last 14 simulated seconds of Case 3:

	Alternator Output (KW)	Armature Current (p.u.)	Power Angle (El. Deg.)	Rotor Speed (rpm)	Pitch Angle (deg.)	Turbine Torque (ft-lb)	Generator Torque (ft-lb)	Field Voltage (p.u.)	Power Factor
Maximum	108.4	1.055	29.34	40.04	-0.367	22759	19533	2.880	0.820
Minimum	85.4	0.871	24.78	39.95	-0.448	16449	15352	2.857	0.775
Max-Min	23.0	0.184	4.56	0.09	0.081	6310	4181	0.023	.045

Case 4. No Falk coupling, slip clutch, $X_L = 0.02$ p.u.

This hypothetical case attempts to combine the successful methods of Cases 2 and 3. The configuration here differs from the existing Mod-0 only in the removal of the Falk coupling. Differences between maxima and minima for the variables tabulated below (except for wind turbine torque) are approximately one half of the corresponding values for Case 2 or Case 3. Additionally, the harmonics which appeared in Case 2 have been eliminated by removing the Falk coupling.

Figure 13a-h are the plots obtained from Case 4.

The following table summarizes the maximum and minimum values for the last 14 simulated seconds of Case 4:

	Alternator Output (KW)	Armature Current (p.u.)	Power Angle (El. Deg.)	Rotor Speed (rpm)	Pitch Angle (deg.)	Turbine Torque (ft-lb)	Generator Torque (ft-lb)	Field Voltage (p.u.)	Power Factor
Maximum	105.7	1.036	28.48	40.02	-0.006	23075	19021	2.873	0.807
Minimum	93.4	0.937	26.26	39.98	-0.046	16640	16790	2.861	0.788
Max-Min	12.3	.099	2.22	0.04	0.040	6435	2231	0.012	0.019

The subsequent Cases 5-9 attempt to refine the hypothetical Case 4, i.e., Cases 5-9 simulate the Mod-0 with the slip clutch and without the Falk coupling. However, in each of these cases the tie line and transformer reactances, X_L, has a different value.

The previous simulations revealed that the terminal voltage, V_t, was nearly equal to the constant bus voltage. Under such conditions, the field excitation voltage, V_f, cannot be effectively controlled by the voltage regulator when necessary. Since the power factor, armature current, and power angle must be held within narrow limits, the patent means of adjusting V_f to reduce output oscillations caused by the tower shadow is to vary X_L within an acceptable range. Changing X_L will not only allow V_t to vary within reasonable limits, but also can store or release energy to smooth the output oscillations.

Cases 4-9 simulate the Mod-0 with only the value of X_L (and hence the initial conditions as well) different in each case.

Case 5. No Falk coupling, slip clutch, $X_L = 0.40$ p.u.

As the plots (Fig. 14a,b) show, the deviations from rated alternator output have been reduced by about 20 percent, as compared to Case 4, as a result of increasing X_L from 0.02 to 0.40 p.u. The differences between maximum and minimum values of armature current, blade pitch angle, generator torque and power factor have also been reduced. However, the field voltage and rotor speed have both increased their differences between maximum and minimum values. The former is not surprising since the purpose of increasing X_L is improved performance of the static excitation control system.

The power angle has increased the magnitude of the difference between its maximum and minimum values by nearly 50 percent. However, the increase in X_L has also resulted in a significant increase in the mean value of the power angle. Therefore, let us consider the relative change in the power angle,

$$RC(\text{power angle}) = \frac{\text{maximum (power angle)} - \text{minimum (power angle)}}{[\text{maximum (power angle)} + \text{minimum (power angle)}]/2}$$

We find that RC(power angle) of Case 4 = 0.0811 electrical degrees, and RC(power angle) of Case 5 = 0.0787 electrical degrees. Using the relative change criterion, the power angle has less fluctuation here than in Case 4. The relative change criterion for all other variables is consistent with the difference between maximum and minimum values.

The following table summarizes the maximum and minimum values for the last 14 simulated seconds of Case 5:

	Alternator Output (KW)	Armature Current (p.u.)	Power Angle (El. Deg.)	Rotor Speed (rpm)	Pitch Angle (deg.)	Turbine Torque (ft-lb)	Generator Torque (ft-lb)	Field Voltage (p.u.)	Power Factor
Maximum	104.4	0.888	39.88	40.03	-0.067	22968	18693	2.723	0.806
Minimum	94.7	0.821	36.86	39.98	-0.100	16571	16938	2.710	0.791
Max-Min	9.7	0.067	3.02	0.05	0.033	6397	1755	0.013	0.015

Case 6. No Falk coupling, slip clutch, $X_L = 0.47$ p.u.

In this case, X_L is again increased. As the plots of Case 6 (Fig. 15a-h) show, maximum and minimum values for each cycle are still reasonably constant, although a very slight harmonic can be detected. As compared to Case 5, performance has improved here with regard to the alternator output, the armature current, the blade pitch angle, the generator torque, the power factor, and the power angle (using the relative change criterion, RC(power angle) of Case 6 is 0.0776 electrical degrees). Performance has been degraded marginally with respect to the rotor speed, and the field voltage.

The following table summarizes the maximum and minimum values for the last 14 simulated seconds of Case 6:

	Alternator Output (KW)	Armature Current (p.u.)	Power Angle (El. Deg.)	Rotor Speed (rpm)	Pitch Angle (deg.)	Turbine Torque (ft-lb)	Generator Torque (ft-lb)	Field Voltage (p.u.)	Power Factor
Maximum	104.2	0.872	42.06	40.03	-0.073	22958	18640	2.715	0.805
Minimum	95.0	0.809	38.92	39.98	-0.105	16563	16981	2.693	0.791
Max-Min	9.2	0.063	3.14	0.05	0.032	6395	1659	0.022	0.014

Case 7. No Falk coupling, slip clutch, X = 0.50 p.u.

In this case, the small increase in X_L has resulted in marginal improvements over Case 6 with respect to the alternator output, armature current, blade pitch angle, and generator torque. However, performance fell off somewhat with respect to the power angle (using either absolute difference or relative change criteria), the rotor speed, the field voltage and the power factor. Furthermore, as the plots of Case 7 (Fig. 16a,b) show, the slight harmonic observed in Case 6 persists in Case 7.

The following table summarizes the maximum and minimum values for the last 14 simulated seconds of Case 7:

	Alternator Output (KW)	Armature Current (p.u.)	Power Angle (El. Deg.)	Rotor Speed (rpm)	Pitch Angle (deg.)	Turbine Torque (ft-lb)	Generator Torque (ft-lb)	Field Voltage (p.u.)	Power Factor
Maximum	104.1	0.867	43.03	40.03	-0.076	22954	18619	2.712	0.806
Minimum	95.0	0.805	39.79	39.97	-0.107	16561	16984	2.688	0.791
Max-Min	9.1	0.062	3.24	0.06	0.031	6393	1635	0.024	0.015

Case 8. No Falk coupling, slip clutch, X_L = 0.55 p.u.

In this case, the increase in X_L has resulted in smaller differences between maximum and minimum values of alternator output and generator torque as compared to the corresponding values of Case 7. However, the differences between maximum and minimum values of field voltage, rotor speed and power angle have continued to increase over the previous case. Also note in the plots (Fig. 17a,b) that the harmonics have become more conspicuous.

The following table summarizes the maximum and minimum values for the last 14 simulated seconds of Case 8:

	Alternator Output (KW)	Armature Current (p.u.)	Power Angle (El. Deg.)	Rotor Speed (rpm)	Pitch Angle (deg.)	Turbine Torque (ft-lb)	Generator Torque (ft-lb)	Field Voltage (p.u.)	Power Factor
Maximum	104.0	0.858	44.71	40.03	-0.079	22949	18591	2.715	0.806
Minimum	95.1	0.797	41.27	39.97	-0.110	16557	16994	2.672	0.791
Max-Min	8.9	0.061	3.44	0.06	0.031	6392	1597	0.043	0.015

Case 9. No Falk coupling, slip clutch, $X_L = 0.60$ p.u.

As the plots of Case 9 (Fig. 18a,b) show, the harmonics have here become quite prominent. Therefore, simulation of further increases of X_L with this configuration was abandoned after Case 9.

As compared to Case 8, the increase in X_L here did result with a smaller difference between maximum and minimum values of alternator output, armature current, and generator torque. However, the differences were larger with respect to the power angle, rotor speed, pitch angle, field voltage and power factor.

The following table summarizes the maximum and minimum values for the last 14 simulated seconds of Case 9:

	Alternator Output (KW)	Armature Current (p.u.)	Power Angle (El. Deg.)	Rotor Speed (rpm)	Pitch Angle (deg.)	Turb.ne Torque (ft-lb)	Generator Torque (ft-lb)	Field Voltage (p.u.)	Power Factor
Maximum	104.0	0.850	46.47	40.03	-0.081	22946	18574	2.726	0.807
Minimum	95.2	0.791	42.75	39.97	-0.113	16553	16998	2.650	0.791
Max-Min	8.8	0.059	3.72	0.06	0.032	6393	1576	0.076	0.016

As Case 5-9 demonstrate, changes to the tie-line and limiting reactances, X_L, can significantly improve the overall performance of the hypothetical Mod-0 (i.e., the Mod-0 without a Falk coupling). How would such a change in X_L effect the existing Mod-0?

Case 10. Falk coupling, slip clutch, $X_L = 0.47$ p.u.

A comparison of the plots obtained in this case, Fig. 19a-h, with those of the simulation of the existing Mod-0 (Case 2), reveals no significant enhancement of the stabilization process. For the 2 cases, differences between maximum and minimum values of alternator output, blade pitch angle, and generator torque, as well as armature current and power angle (relative change), are approximately the same. The rotor speed for Case 10 is significantly worse. Moreover, the harmonics which plagued Case 2 have become further aggravated with the increase in X_L.

The following table summarizes the maximum and minimum values for the last 14 simulated seconds of Case 10:

	Alternator Output (KW)	Armature Current (p.u.)	Power Angle (El. Deg.)	Rotor Speed (rpm)	Pitch Angle (deg.)	Turbine Torque (ft-lb)	Generator Torque (ft-lb)	Field Voltage (p.u.)	Power Factor
Maximum	111.4	0.922	44.46	40.07	-0.054	22965	19940	2.723	0.814
Minimum	89.1	0.769	36.93	39.94	-0.125	16561	15917	2.690	0.782
Max-Min	22.3	0.153	7.53	0.13	0.071	6405	4023	0.033	0.032

The remaining Case 11-18 use the previous technique of parameterization of X_L, using Case 3 as a basis. Recall that Case 3 achieved substantial success by simply removing the Falk coupling and slip clutch.

Case 11. No Falk coupling, no slip clutch, $X_L = 0.20$ p.u.

The plots of Case 11, Fig. 20a,b, clearly demonstrate the increased stability brought about by the 10 fold increase in X_L. In Case 11, differences between maximum and minimum values for all variables listed (except turbine torque) in the table below are about one third less than the corresponding values in Case 3. Moreover, maximum and minimum values for Case 11 remain very nearly constant in each cycle.

The following table summarizes the maximum and minimum values for the last 14 simulated seconds of Case 11:

	Alternator Output (KW)	Armature Current (p.u.)	Power Angle (El. Deg.)	Rotor Speed (rpm)	Pitch Angle (deg.)	Turbine Torque (ft-lb)	Generator Torque (ft-lb)	Field Voltage (p.u.)	Power Factor
Maximum	105.6	0.953	34.18	40.04	-0.408	22681	18963	2.779	0.812
Minimum	89.9	0.839	30.17	39.96	-0.467	16408	16111	2.766	0.781
Max-Min	15.7	0.114	4.01	0.08	0.059	6273	2852	0.013	0.031

Case 12. No Falk coupling, no slip clutch, $X_L = 0.30$ p.u.

The plots, Fig. 21a,b, and the table below illustrate the enhanced stability of the alternator output, armature current, power angle, and generator torque. The peak values of the plots remain very nearly constant.

The following table summarizes the maximum and minimum values for the last 14 simulated seconds of Case 12:

	Alternator Output (KW)	Armature Current (p.u.)	Power Angle (El. Deg.)	Rotor Speed (rpm)	Pitch Angle (deg.)	Turbine Torque (ft-lb)	Generator Torque (ft-lb)	Field Voltage (p.u.)	Power Factor
Maximum	104.9	0.933	36.03	40.04	-0.416	22666	18833	2.822	0.787
Minimum	91.2	0.840	32.16	39.96	-0.468	16402	16351	2.808	0.758
Max-Min	13.7	0.093	3.87	0.08	0.052	6264	2482	0.014	0.029

Case 13. No Falk coupling, no slip clutch, $X_L = 0.35$ p.u.

Plots of Case 13, Fig. 22a,b, demonstrate the further improvement of system response.

The following table summarizes the maximum and minimum values for the last 14 simulated seconds of Case 13:

	Alternator Output (KW)	Armature Current (p.u.)	Power Angle (El. Deg.)	Rotor Speed (rpm)	Pitch Angle (deg.)	Turbine Torque (ft-lb)	Generator Torque (ft-lb)	Field Voltage (p.u.)	Power Factor
Maximum	104.7	0.924	37.05	40.04	-0.420	22660	18789	2.844	0.777
Minimum	91.7	0.838	33.14	39.96	-0.469	16397	16438	2.821	0.748
Max-Min	13.0	0.086	3.91	0.08	0.049	6263	2351	0.023	0.029

Case 14. No Falk coupling, no slip clutch, $X_L = 0.40$ p.u.

Plots of Case 14, Fig. 23a,b, illustrate the improvement of system response.

The following table summarizes the maximum and minimum values for the last 14 simulated seconds of Case 14:

	Alternator Output (KW)	Armature Current (p.u.)	Power Angle (El. Deg.)	Rotor Speed (rpm)	Pitch Angle (deg.)	Turbine Torque (ft-lb)	Generator Torque (ft-lb)	Field Voltage (p.u.)	Power Factor
Maximum	104.4	0.888	39.95	40.04	-0.434	22631	18705	2.730	0.808
Minimum	92.4	0.806	36.14	39.96	-0.480	16379	16541	2.705	0.787
Max-Min	12.0	0.082	3.81	0.08	0.046	6252	2164	0.025	0.021

Case 15. No Falk coupling, no slip clutch, $X_L = 0.43$ p.u.

Plots of Case 15, Fig. 24a-g, demonstrate the continued reduction of the difference between extreme values of all variables, except rotor speed and field voltage. System response here is comparable to the case with a slip clutch, no Falk coupling, and with X_L still 0.02 p.u. (Case 4). However, a very slight harmonic response is noticeable here, particularly at the low end of the time scale.

The following table summarizes the maximum and minimum values for the last 14 simulated seconds of Case 15:

	Alternator Output (KW)	Armature Current (p.u.)	Power Angle (El. Deg.)	Rotor Speed (rpm)	Pitch Angle (deg.)	Turbine Torque (ft-lb)	Generator Torque (ft-lb)	Field Voltage (p.u.)	Power Factor
Maximum	104.3	0.881	40.89	40.04	-0.437	22627	18681	2.731	0.808
Minimum	92.7	0.801	37.04	39.96	-0.483	16375	16586	2.695	0.787
Max-Min	11.6	0.080	3.85	0.08	0.046	6252	2095	0.036	0.021

Case 16. No Falk coupling, no slip clutch, X_L = 0.47 p.u.

In this case, X_L is increased by only 0.04 p.u. over the previous Case 15. The plots of Case 16, Fig. 25a-g, reveal a slight reduction in the differences between maximum and minimum values of alternator output, armature current and generator torque from the corresponding values in Case 15. However, the power angle, power factor, and field voltage were better in Case 15. Most significantly, the slight harmonics which appeared at the low end of the time scale in Case 15 extend over the entire time scale in Case 16, and are of greater amplitude.

The following table summarizes the maximum and minimum values for the last 14 simulated seconds of Case 16:

	Alternator Output (KW)	Armature Current (p.u.)	Power Angle (El. Deg.)	Rotor Speed (rpm)	Pitch Angle (deg.)	Turbine Torque (ft-lb)	Generator Torque (ft-lb)	Field Voltage (p.u.)	Power Factor
Maximum	104.3	0.873	42.27	40.04	-0.439	22622	18678	2.739	0.809
Minimum	92.8	0.795	38.12	39.96	-0.486	16369	16609	2.677	0.786
Max-Min	11.5	0.078	4.15	0.08	0.047	6253	2069	0.062	0.023

Case 17. No Falk coupling, no slip clutch, X_L = 0.50 p.u.

Plots of Case 17, Fig. 26a,b, show that the harmonic response of the system has become aggravated with this most recent increase in X_L.

The following table summarizes the maximum and minimum values for the last 14 simulated seconds of Case 17:

	Alternator Output (KW)	Armature Current (p.u.)	Power Angle (El. Deg.)	Rotor Speed (rpm)	Pitch Angle (deg.)	Turbine Torque (ft-lb)	Generator Torque (ft-lb)	Field Voltage (p.u.)	Power Factor
Maximum	104.4	0.867	43.46	40.04	-0.439	22623	18697	2.754	0.812
Minimum	92.8	0.791	38.81	39.96	-0.490	16364	16610	2.649	0.784
Max-Min	11.6	0.076	4.65	0.08	0.051	6259	2087	0.105	0.028

Case 18. No Falk coupling, no slip clutch, $X_L = 0.55$ p.u.

Plots of Case 18, Fig. 27a,b, clearly demonstrate the degenerate response of the control system as caused by the increased value of X_L. Although the system is still functioning within acceptable bounds, the difference between extreme values for all tabulated variables has increased to about the same level as Case 12 (X_L=0.30). Unlike Case 12, however, the extreme values for each cycle oscillate significantly, no longer reflecting the periodic input.

The difference between maximum and minimum values of the field voltage is greater in Case 18 than in any of the previous cases, while the power factor is only surpassed in Case 1.

The following table summarizes the maximum and minimum values for the last 14 simulated seconds of Case 18:

	Alternator Output (KW)	Armature Current (p.u.)	Power Angle (El. Deg.)	Rotor Speed (rpm)	Pitch Angle (deg.)	Turbine Torque (ft-lb)	Generator Torque (ft-lb)	Field Voltage (p.u.)	Power Factor
Maximum	105.5	0.862	46.21	40.05	-0.427	22642	18876	2.868	0.823
Minimum	91.9	0.783	39.33	39.95	-0.506	16342	16435	2.522	0.771
Max-Min	13.6	0.079	6.88	0.10	0.079	6300	2441	0.346	0.052

Case	Falk Coupling	Slip Clutch	X_L (p.u.)	Alternator Output (KW)			Armature Current (p.u.)			Power Angle (el. deg.)			Rotor Speed (rpm)			Generator Torque (ft-lb)		
				max	min	max-min	max	min	max-min	max	min	max-min	max	min	max-min	max	min	max-min
1	Yes	No	0.02	139.4	67.8	71.6	1.305	0.733	0.572	34.33	20.65	13.68	40.12	39.90	0.22	25295	12167	13128
2	Yes	Yes	0.02	112.2	89.5	22.7	1.085	0.906	0.179	29.70	25.47	4.23	40.04	39.97	0.07	20206	16076	4130
3	No	No	0.02	108.4	85.4	23.0	1.055	0.871	0.184	29.34	24.78	4.56	40.04	39.95	0.09	19533	15352	4181
4	No	Yes	0.02	105.7	93.4	12.3	1.036	0.937	0.099	28.48	26.26	2.22	40.02	39.98	0.04	19021	16790	2231
5	No	Yes	0.40	104.4	94.7	9.7	0.888	0.821	0.067	39.88	36.86	3.02	40.03	39.98	0.05	18693	16938	1755
6	No	Yes	0.47	104.2	95.0	9.2	0.872	0.809	0.063	42.06	38.92	3.14	40.03	39.98	0.05	18640	16981	1659
7	No	Yes	0.50	104.1	95.0	9.1	0.867	0.805	0.062	43.03	39.79	3.24	40.03	39.97	0.06	18619	16984	1635
8	No	Yes	0.55	104.0	95.1	8.9	0.858	0.797	0.061	44.71	41.27	3.44	40.03	39.97	0.06	18591	16994	1597
9	No	Yes	0.60	104.0	95.2	8.8	0.850	0.791	0.059	46.47	42.75	3.72	40.03	39.97	0.06	18574	16998	1576
10	Yes	Yes	0.47	111.4	89.1	22.3	0.922	0.769	0.153	44.46	36.93	7.53	40.07	39.94	0.13	19940	15917	4027
11	No	No	0.20	105.6	89.9	15.7	0.953	0.839	0.114	34.18	30.17	4.01	40.04	39.96	0.08	18963	16111	2852
12	No	No	0.30	104.9	91.2	13.7	0.933	0.840	0.093	36.03	32.16	3.87	40.04	39.96	0.08	18833	16351	2482
13	No	No	0.35	104.7	91.7	13.0	0.924	0.838	0.086	37.05	33.14	3.91	40.04	39.96	0.08	18789	16438	2351
14	No	No	0.40	104.4	92.4	12.0	0.883	0.806	0.082	39.95	36.14	3.81	40.04	39.96	0.08	18705	16541	2164
15	No	No	0.43	104.3	92.7	11.6	0.881	0.801	0.080	40.89	37.04	3.85	40.04	39.96	0.08	18681	16586	2095
16	No	No	0.47	104.3	92.8	11.5	0.873	0.795	0.078	42.27	38.12	4.15	40.04	39.96	0.08	18678	16609	2069
17	No	No	0.50	104.4	92.8	11.6	0.867	0.791	0.076	43.46	38.81	4.65	40.04	39.96	0.08	18697	16610	2087
18	No	No	0.55	105.5	91.9	13.6	0.862	0.783	0.079	46.21	39.33	6.88	40.05	39.95	0.10	18876	16435	2441

Note: Case 1 was simulated for 40 seconds. All other cases were simulated for 30 seconds.

MAXIMUM AND MINIMUM VALUES FOR CASES 1-18

CONCLUSIONS

1. Removal of the Falk coupling results in a stiffer shaft, which dramatically increases system stability. Its removal is therefore recommended.

2. The slip clutch effectively aids system stability both with and without the Falk coupling. Once the Falk coupling is removed, output oscillations caused by the tower shadow (28 percent decrease in turbine torque) can be held by the slip clutch to within 7 percent of the rated value. However, the slip clutch is an expensive method of control. Furthermore, the clutch makes it impractical for implementation by the larger machines yet to be built by ERDA-NASA.

3. The reactances X_L significantly affects the dynamic stability. For values of the tie line and transformer reactance, X_L, at the level currently being used in the Mod-0, the excitation control system has little effect on stabilization. Additional reactance (or a longer transmission line) is needed to permit the static excitation control system to realize its control capabilities. The simulations reveal that increasing X_L to within a narrow range around 0.43 p.u. (for the configuration without a a slip clutch), or 0.47 p.u. (for the configuration with a slip clutch), can reduce the variation of power output caused by the tower shadow (for a hypothetical Mod-0 without a Falk coupling) from 12 percent (Case 2) for the current Mod-0 to 7 percent (without a slip clutch) or 5 percent (with a slip clutch) of the rated value.

   Optimization of the tie line and transformer reactances is an inexpensive, easily implemented technique which can be applied to both large and small machines.

4. As Case 10 demonstrates, the technique of using optimal X_L does not appear to be compatible with a drive train configuration containing a Falk coupling. For that reason, it is recommended that X_L not be increased to the range discussed above for the existing Mod-0, which has a Falk coupling.

5. For values of X_L less than the optimal range, control system effectiveness is reduced. However, the system does reflect the constant amplitude of the periodic input.

   For values of X_L exceeding the optimal range, the system no longer reflects the constant amplitude of the periodic input, becoming beset with severe harmonics.

6. Comparison of the effects of the slip clutch (Case 4) with that of optimization of X_L (Case 15) reveals very similar variations of power output for the two techniques. Therefore, by virtue of its lesser expense, greater durability and wider range of applications, the optimization of the tie-line and transformer reactance seems the better method for smoothing the output power of a wind turbine generator.

7. Combining the optimal value of X_L with a slip clutch yields the best method for stabilizing the system (Case 6). However the small improvements realized by the installation of the slip clutch (Case 6 vs. Case 15) do not seem to warrant the added expense of the fluid drive. It is therefore recommended that the technique advanced here -- a static excitation control system with an optimal value of X_L and removal of the Falk coupling -- replace the slip clutch in future wind turbine generators.

NOMENCLATURE

The symbols used correspond insofar as possible to standard definitions.

Other symbols used are

λ_f, λ_{11q}	flux linkage of field and damper circuit in j-axis
M_{af}, M_{alj}	maximum mutual inductance between armature circuit and field (or damper circuit in j axis)
L_{ff}, L_{11j}	self inductance of field circuit and damper circuit in j axis, respectively
ω_o	base angular velocity
P	number of poles of the synchronous machine
N	gear ratio between high and low speed shaft
V_{fn}, V_f	reference or instantaneous field voltage referred to the stator
B	damping coefficient of the complete rotating system in lb-ft-sec
J	inertia of the complete rotating system (referred to low speed shaft) in lb-ft-sec^2
Ω	angular speed of alternator shaft (referred to wind turbine rotor shaft) in radians per second
δ_j	angular displacement of j section of the rotor shaft in mechanical radians from selected reference axis
K_1	controller proportional gain in seconds
K_2	controller integral gain per kw-sec
θ	pitch angle of blade in mechanical radians
θ_N	reference pitch angle of blade in mechanical radians
ξ	damping ratio
τ_p	control hydraulic actuator time constant in seconds
ω_N	undamped natural angular frequency in radians per second

$$e_{q1} = \omega_o M_{af} i_f, \quad e_{q2} = \omega_o M_{ald} i_{11d}, \quad e_d = -\omega_o M_{alq} i_{11q}$$

$$e''_q = \omega_o \frac{M_{ald}}{L_{11d}} \lambda_{11d}, \quad e'_q = \omega_o \frac{M_{af}}{L_{ff}} \lambda_f, \quad e''_d = -\omega_o \frac{M_{alq}}{L_{11q}} \lambda_{11q}$$

SYSTEM CONSTANTS

$R_a = 0.018$, $x_d = 2.21$, $x_q = 1.064$, $x'_d = 0.165$ p.u.,

$x''_d = 0.128$, $x''_q = 0.193$, $V_b = 1.000$ p.u.,

$T'_{do} = 1.94212$, $T''_{do} = 0.01096$, $T''_{qo} = 0.06230$ sec

$N = 45$, $B = 959$ lb-ft-sec

$J = 101{,}100$, $J_1 = 95{,}760$, $J_2 = 5340$ lb-ft-sec^2

$K_1 = 0$, $K_2 = 6 \times 10^{-4}$ per kw-sec

$\omega_N = 100$ radians per sec, $\tau_p = \frac{1}{2 \times 2.7 \times \pi}$ sec, $\xi = 0.02$

$\mu_e = 30.000$, $\tau_e = 0.0500$ sec, $K_3 = 0.2000$

$a = 7.1 \times 10^{10}$, $b = 3.3 \times 10^{9}$, $c = -1.1 \times 10^{8}$, $d = 1.8 \times 10^{6}$

$\Omega_N = 4.189$, $\Omega_c = 4.257$ radians per sec

ACKNOWLEDGMENTS

We are grateful to Dr. W.A. Lewis for his valuable suggestions. This work is supported by NASA-Lewis Research Center and the Hawaii Natural Energy Institute. Thanks to the Center for Engineering Research for typing this manuscript.

REFERENCES

1. Ronald L. Thomas, "Large Experimental Wind Turbines--Where We are Now," NASA TMX-71890.

2. Craig C. Johnson and Richard T. Smith, "Dynamics of Wind Generators on Electric Utility Networks," IEEE Trans. on Aerospace and Electronic Systems, Vol. AES 12, No. 4, July 1976, pp. 483-493.

3. R.H. Park, "Two Reaction Theory of Synchronous Machines, Generalized Method of Analysis, Part 1," AIEE Transactions, Vol. 48, July 1929, pp. 716-730.

4. David W. Olive, "Digital Simulation of Synchronous Machine Transients," IEEE Trans. on Power Apparatus and Systems, Vol. PAS-87, August 1968, pp. 1669-1975.

5. H.H. Hwang and Leonard J. Gilbert, "Synchronization of Wind Turbine Generators Against an Infinite Bus Under Gusting Wind Conditions," presented at IEEE Power Engineering Society 1977 Summer Meeting and to appear in IEEE Trans. on Power Apparatus and Systems, paper no. F77675-2.

6. Robert E. Wilson and Peter B.S. Lissman, Applied Aerodynamics of Wind Power Machines, Oregon State University, May 1975.

7. Germund Dahlquist, Ake Bröck, and translated by Ned Anderson, Numerical Methods, New Jersey: Prentice-Hall, 1974, Chapter 8, pp. 347-348.

8. John C. Glasgow and Bradford S. Linscott, "Early Operation Experience on ERDA/NASA 100-kw Wind Turbine," NASA TMX-71601.

APPENDIX: DERIVATIONS OF INITIAL CONDITIONS

Synchronous Machines

The following conditions can be found in Fig. 28.

$$\phi_b = \frac{1}{2}\left[\phi_t + \sin^{-1}\left(\sin\phi_t - \frac{2P_o X_L}{V_b^2}\cos\phi_t\right)\right] \tag{47}$$

$$I_a = \frac{P_o}{V_b \cos\phi_b} \tag{48}$$

$$V_t = \frac{V_b \cos\phi_b}{\cos\phi_t} \tag{49}$$

$$\delta = \tan^{-1}\left\{\frac{[(X_q+X_L)\cos\phi_b - R_a\sin\phi_b]I_a}{V_b + [(X_q+X_L)\sin\phi_b + R_a\cos\phi_b]I_a}\right\} \tag{50}$$

$$V_f = V_b \cos\delta + R_a I_a(\delta+\phi_b) + (X_d+X_L)I_a \sin(\delta+\phi_b) \tag{51}$$

$$I_d = I_a \sin(\delta+\phi_b) \tag{52}$$

$$I_q = I_a \cos(\delta+\phi_b) \tag{51}$$

Under steady-state, the derivatives of Eqs. (1), (2), and (3) are zero, and initial values of e_d, e_{q2}, and e_{q1}, are

$$e_d = e_{q2} = 0 \tag{52}$$

$$e_{q1} = V_f \tag{53}$$

Solving Eqs. (6-10) simultaneously, there yields

$$e''_q = -(x_d - x''_d)I_d + V_f \tag{54}$$

$$e''_d = (x_q - x''_q)I_q \tag{55}$$

$$e'_q = \left(V_f + \frac{x_d - x'_d}{x'_d - x''_d}\, e''_q\right)\frac{x'_d - x''_d}{x_d - x''_d} \tag{56}$$

Mechanical Networks

$$\delta_m = \frac{\pi}{90}\frac{\delta}{NP} \tag{57}$$

δ_w is found in Fig. 5

$$\delta_w = \frac{T}{K} + \delta_m - \frac{B\Omega_N}{2K} \tag{58}$$

The following initial values are easily derived from Fig. 6

$$T = T_c + B\Omega_c \tag{59}$$

$$\delta_r = \delta_m \tag{60}$$

$$\delta_w = \frac{T}{K} + \delta_r - \frac{B\Omega_c}{2K} \tag{61}$$

Fig. 1 ERDA-NASA 100-kw Wind Turbine

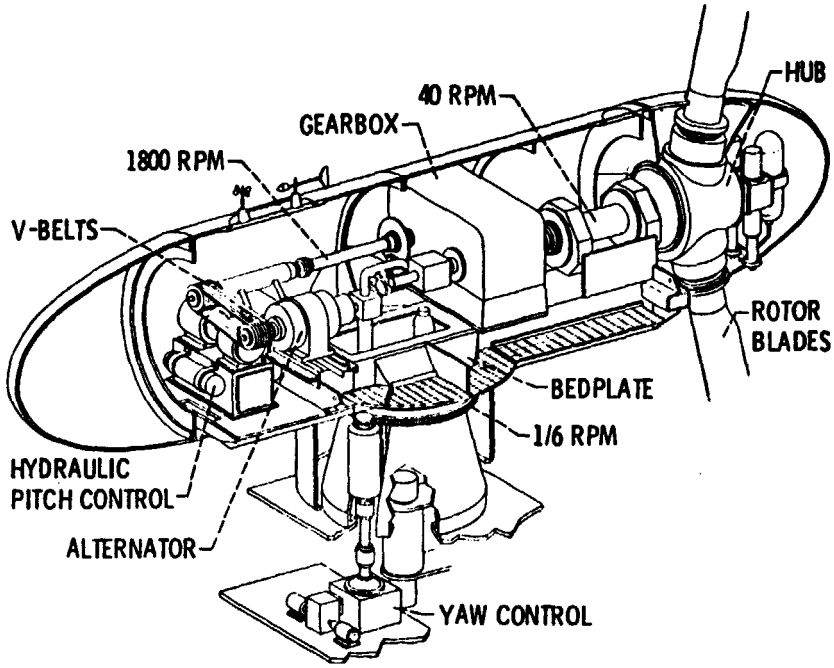

Fig. 2 100-kw Wind Turbine Drive Train Assembly and Yaw System

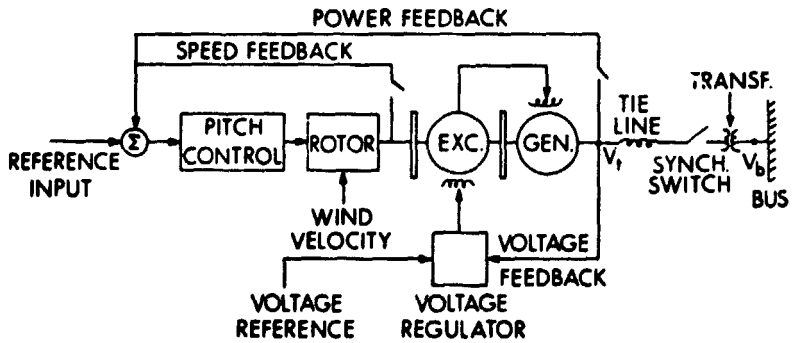

Fig. 3 A Schematic of the System Under Study

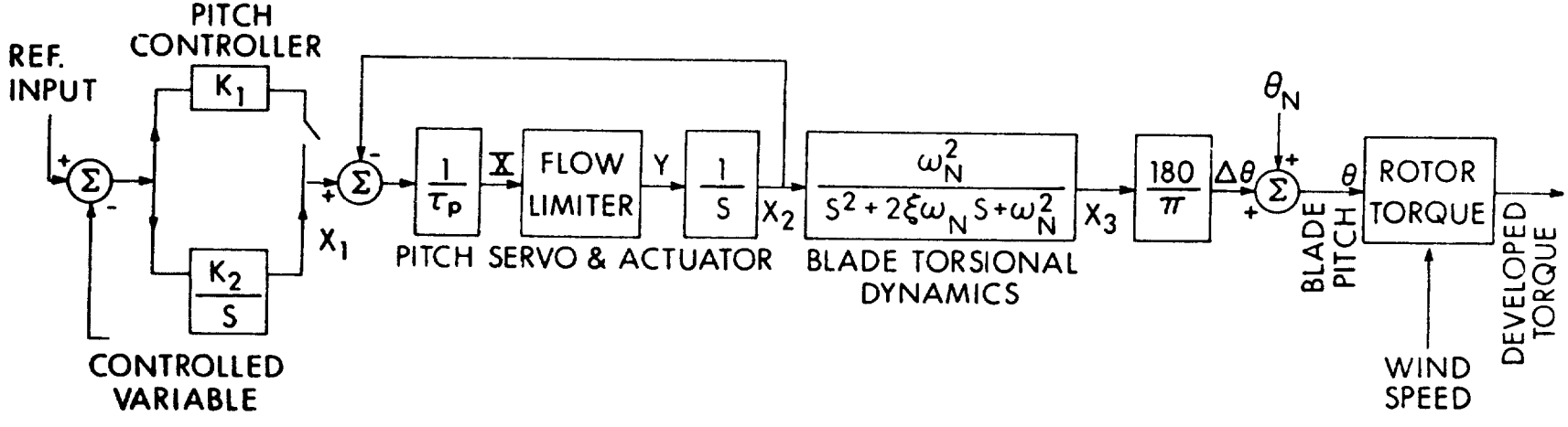

Fig. 4 The Pitch Control System of ERDA-NASA 100-kw Wind Turbine

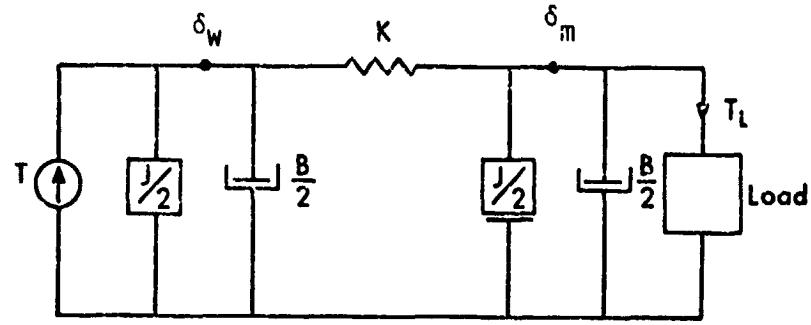

Fig. 5 π-mechanical Network

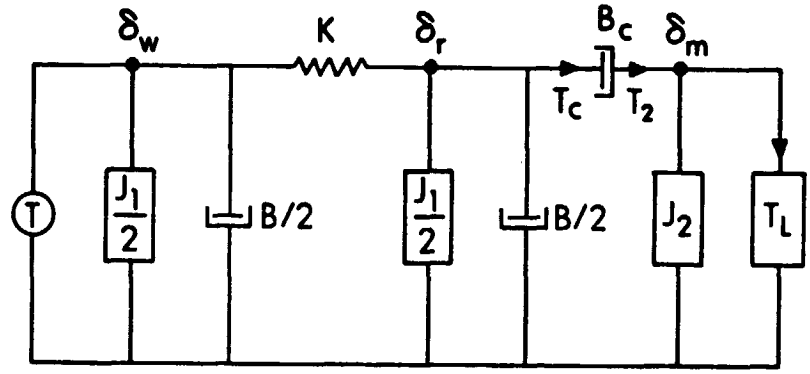

Fig. 6 π-mechanical Network with Slip Clutch

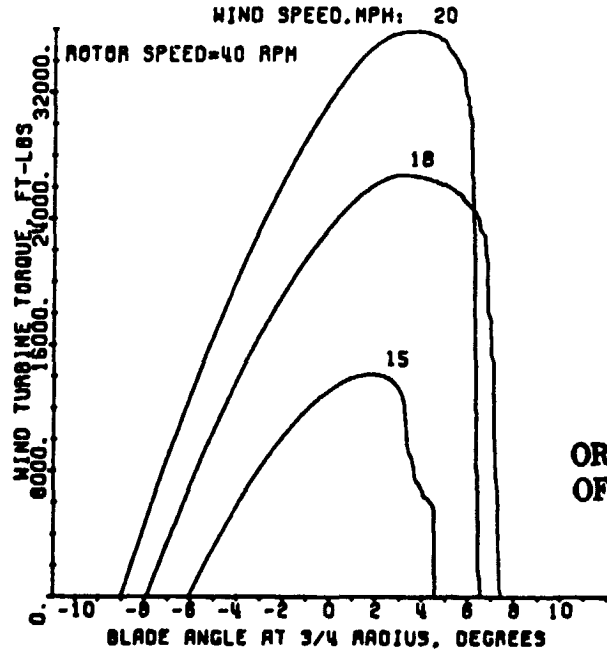

ORIGINAL PAGE IS
OF POOR QUALITY

Fig. 7 The Turbine Torque-Pitch Angle Curve

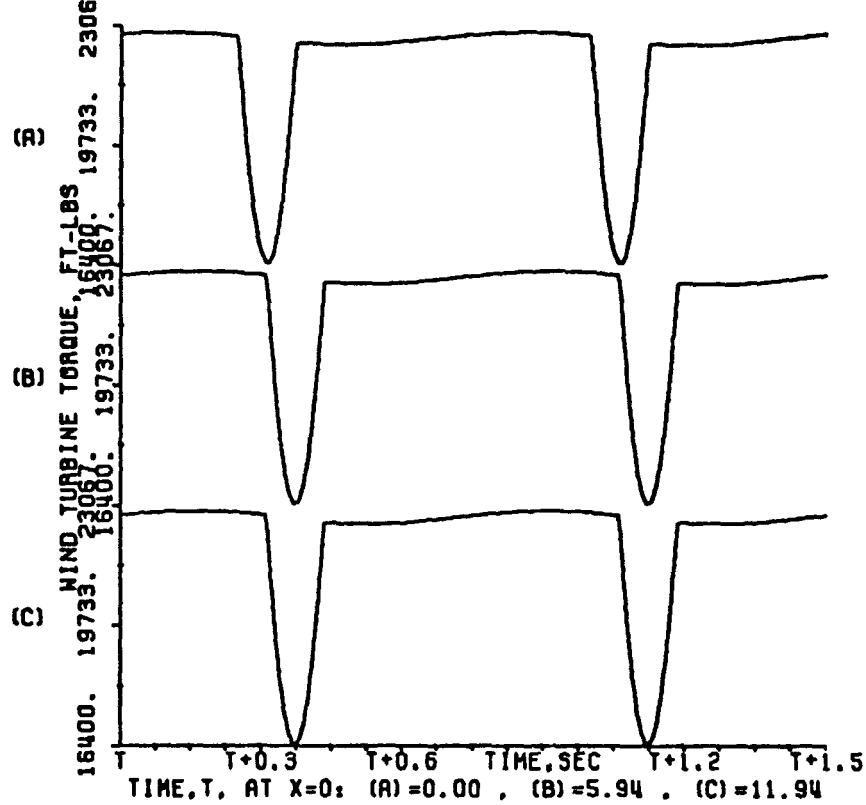

Fig. 8 Turbine Torque vs. Time for 3 Distinct Revolutions of the Blades

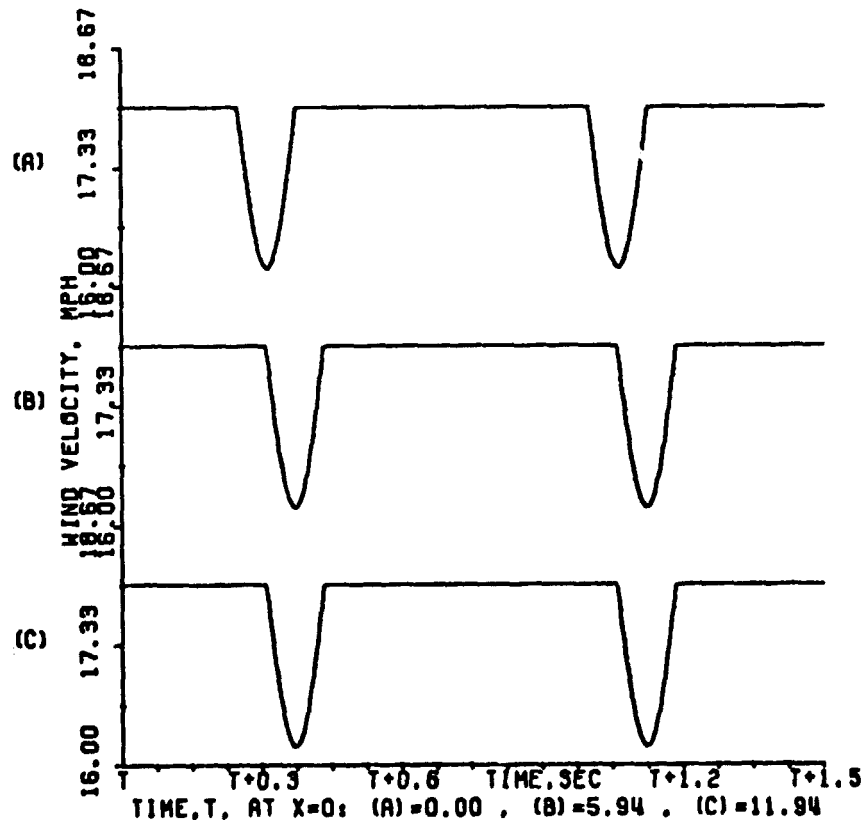

Fig. 9 Wind Speed vs. Time, corresponding to Fig. 8

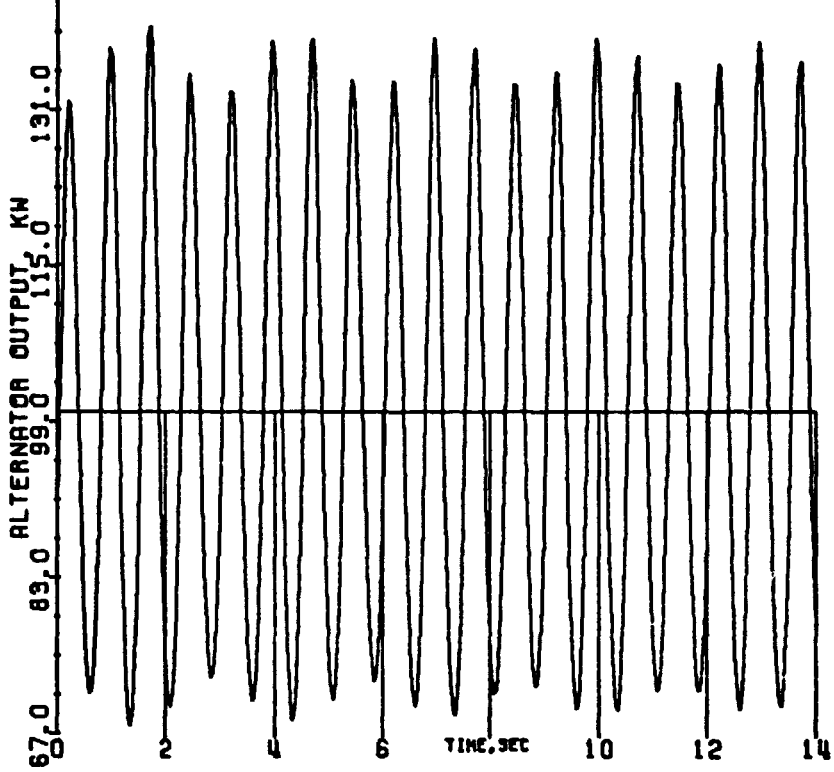

Fig. 10a: Case 1, Alternator Output
Falk coupling, no slip clutch, X_L = 0.02 p.u.

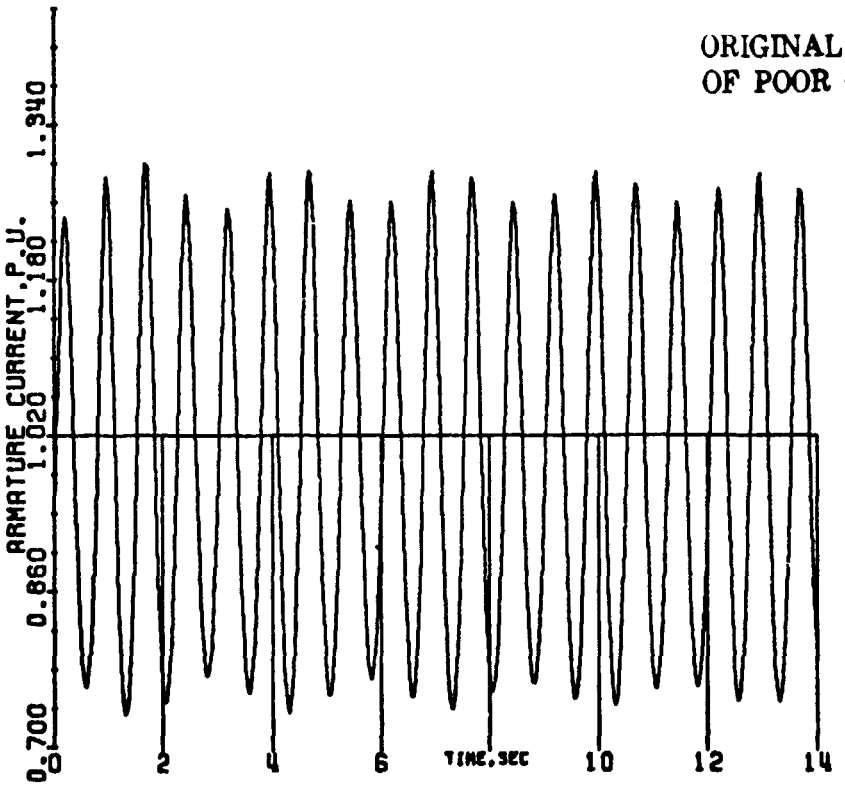

Fig. 10b: Case 1, Armature Current
Falk coupling, no slip clutch, X_L = 0.02 p.u.

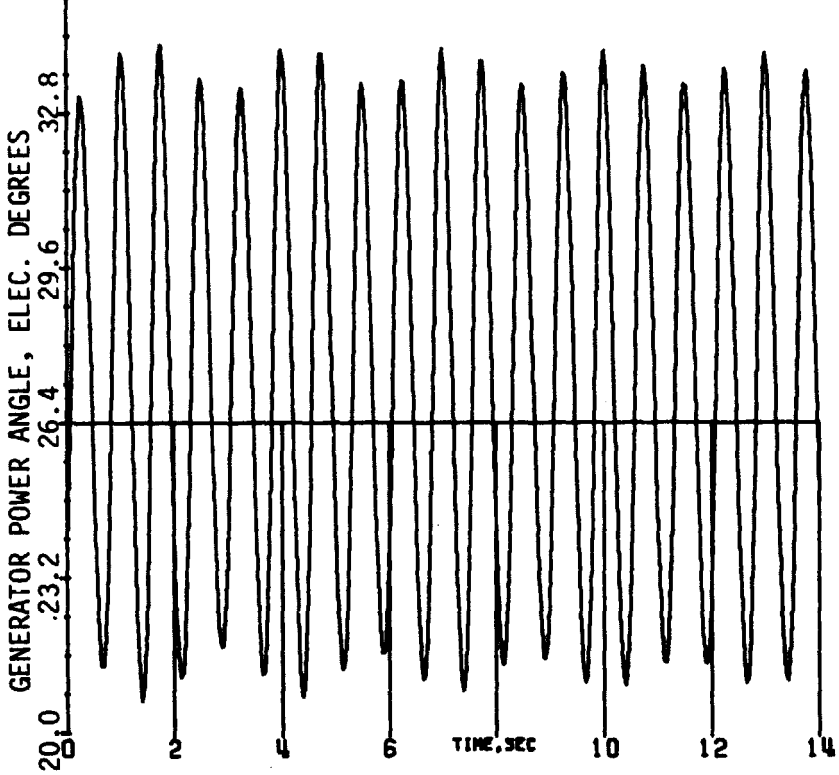

Fig. 10c: Case 1, Generator Power Angle
Falk coupling, no slip clutch, $X_L = 0.02$ p.u.

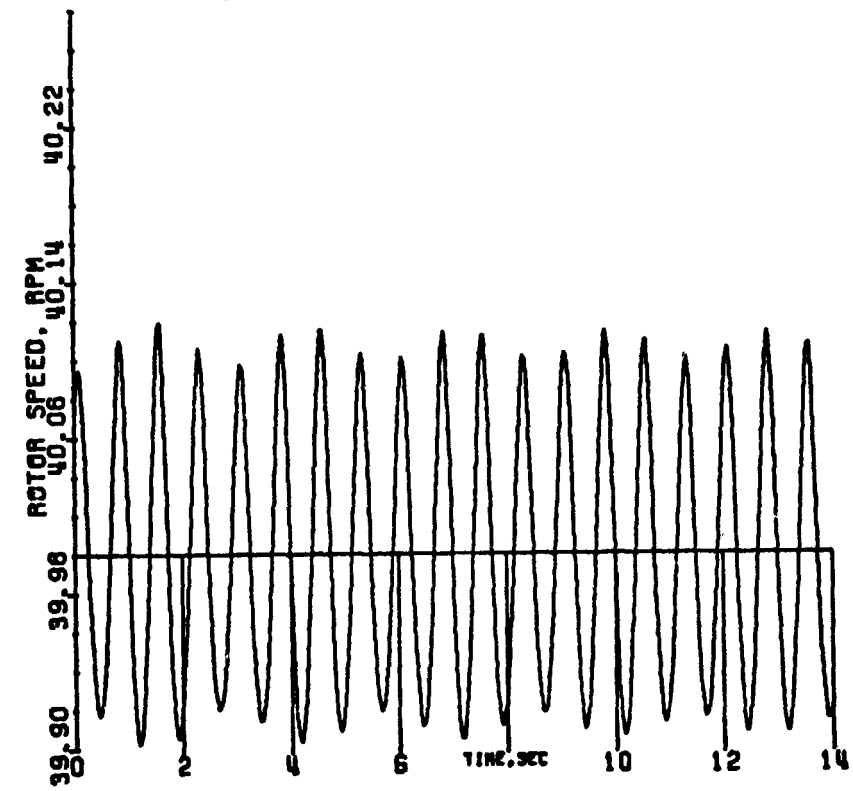

Fig. 10d: Case 1, Rotor Speed
Falk coupling, no slip clutch, $X_L = 0.02$ p.u.

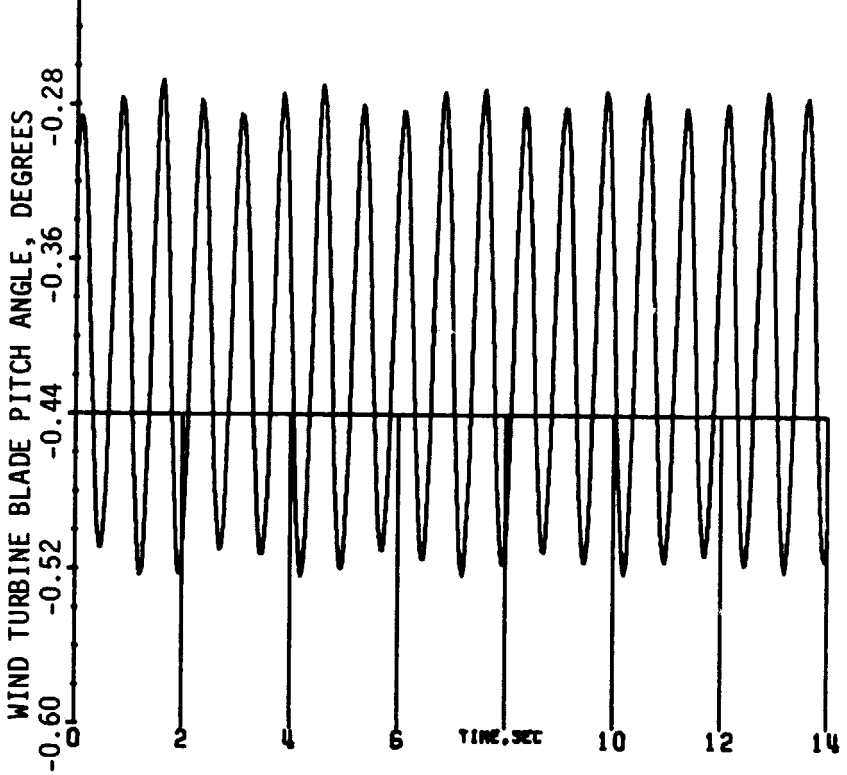

Fig. 10e: Case 1, Blade Pitch Angle
Falk coupling, no slip clutch, $X_L = 0.02$ p.u.

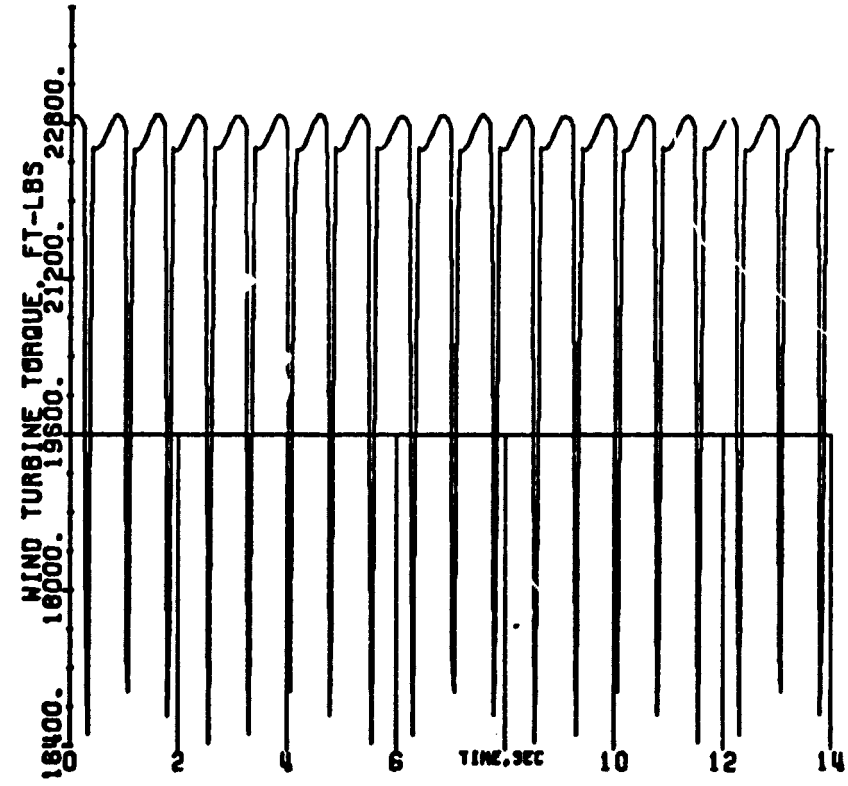

Fig. 10f: Case 1, Wind Turbine Torque
Falk coupling, no slip clutch, $X_L = 0.02$ p.u.

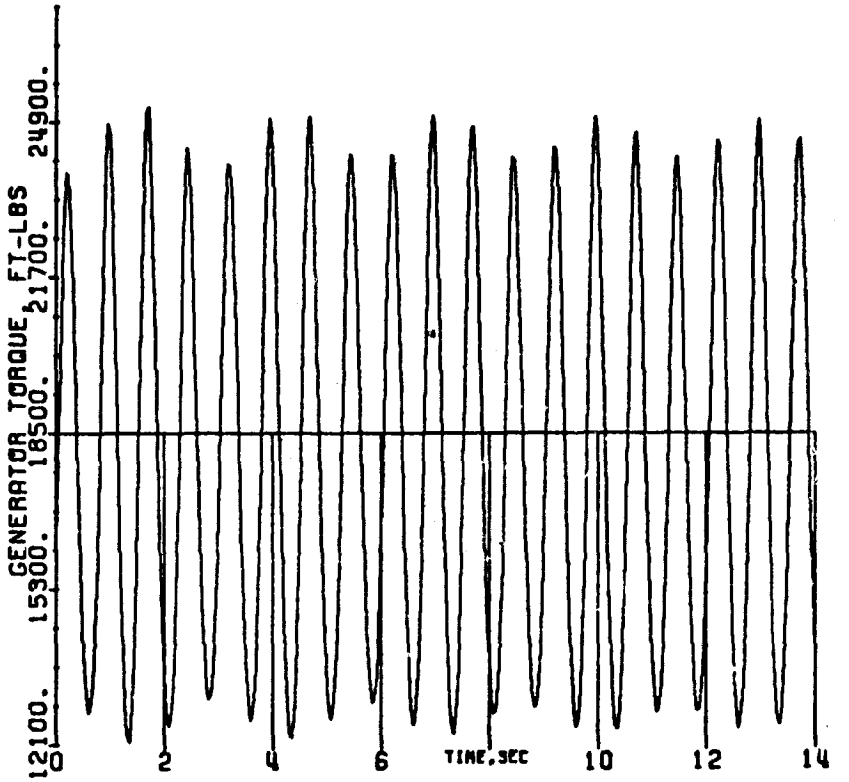

Fig. 10g: Case 1, Generator Torque
Falk coupling, no slip clutch, $X_L = 0.02$ p.u.

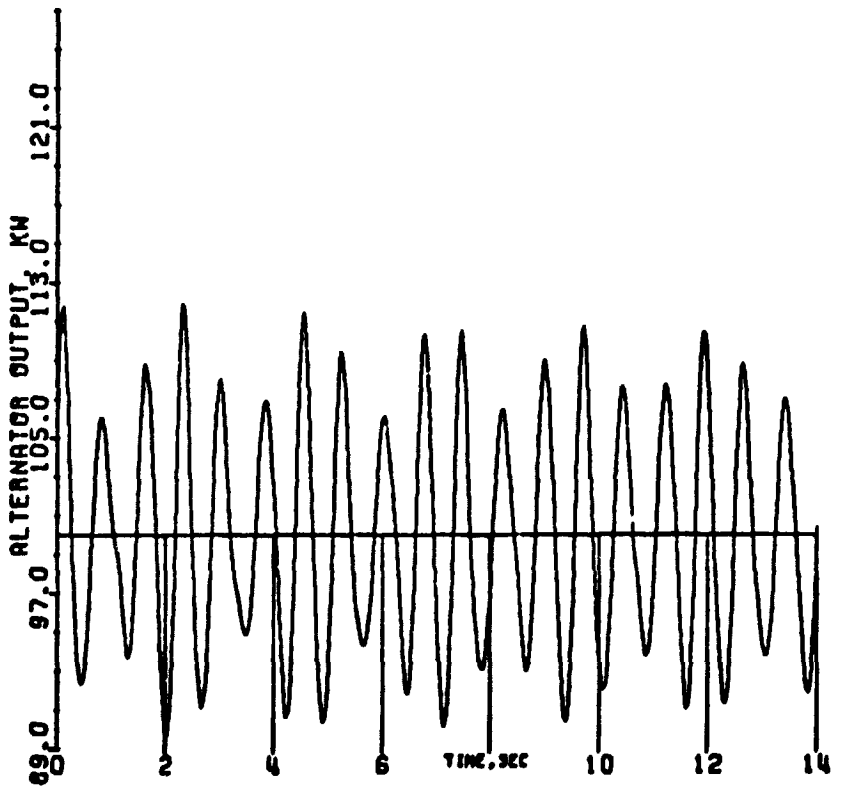

Fig. 11a: Case 2, Alternator Output
Falk coupling, slip clutch, $X_L = 0.02$ p.u.

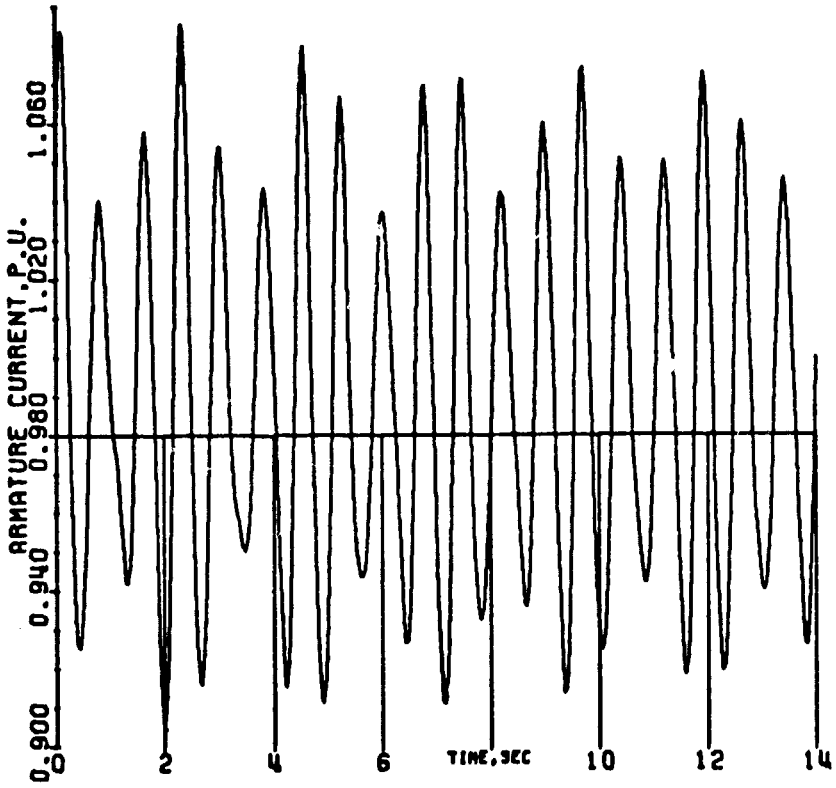

Fig. 11b: Case 2, Armature Current
Falk coupling, slip clutch, X_L = 0.02 p.u.

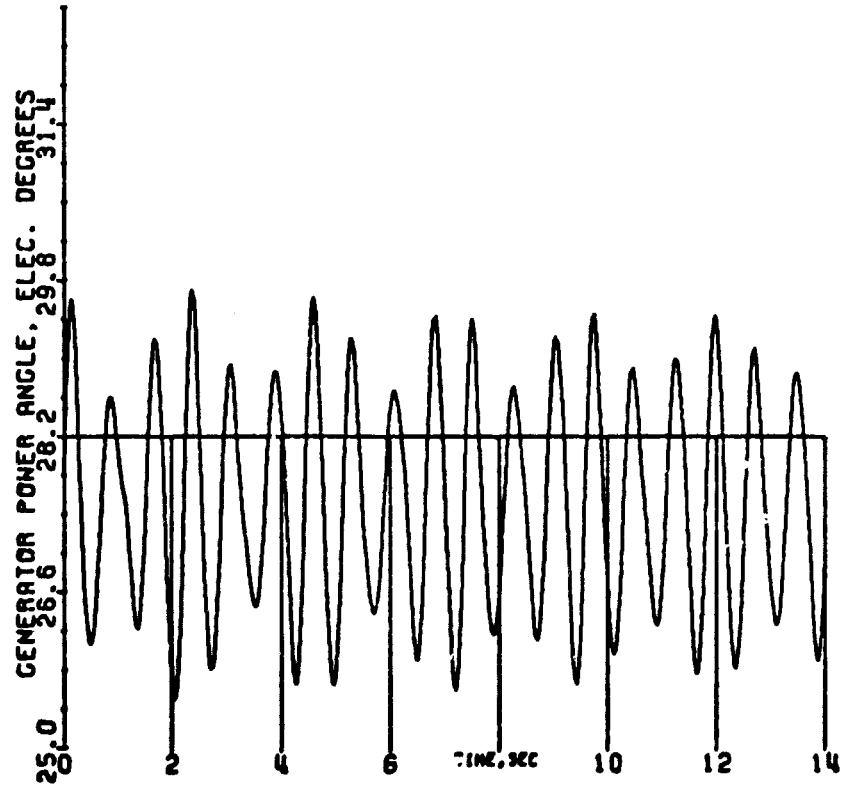

Fig. 11c: Case 2, Generator Power Angle
Falk coupling, slip clutch, X_L = 0.02 p.u.

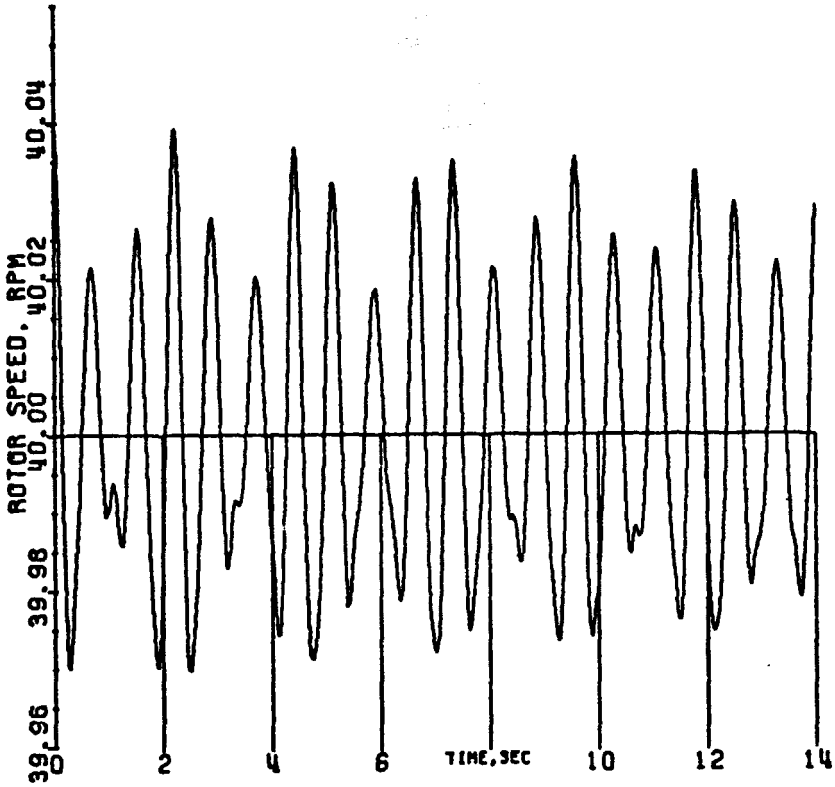

Fig. 11d: Case 2, Rotor Speed
Falk coupling, slip clutch, $X_L = 0.02$ p.u.

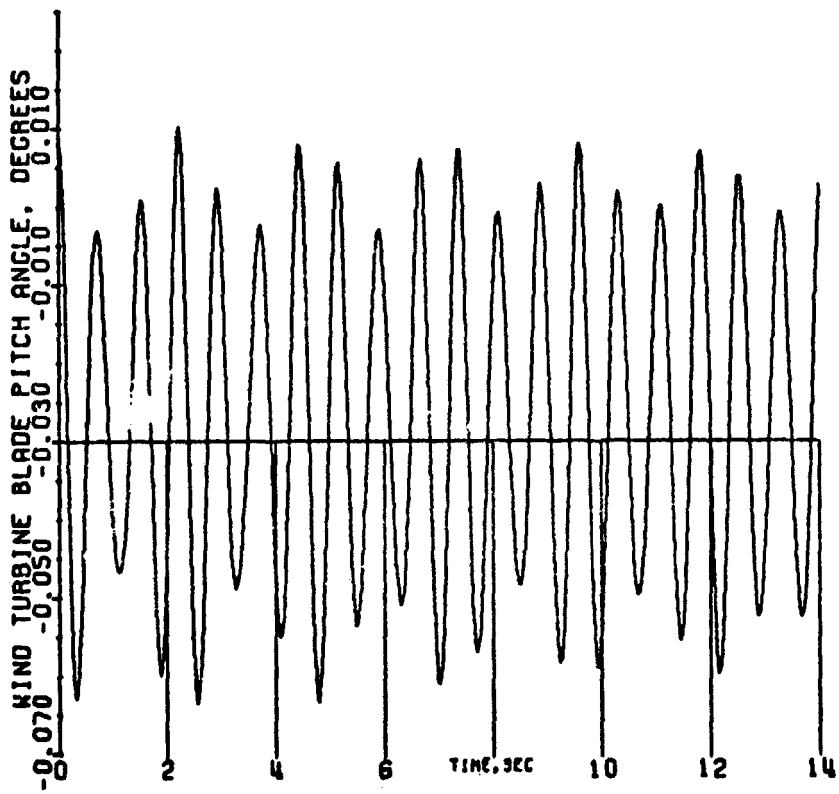

Fig. 11e: Case 2, Blade Pitch Angle
Falk coupling, slip clutch, $X_L = 0.02$ p.u.

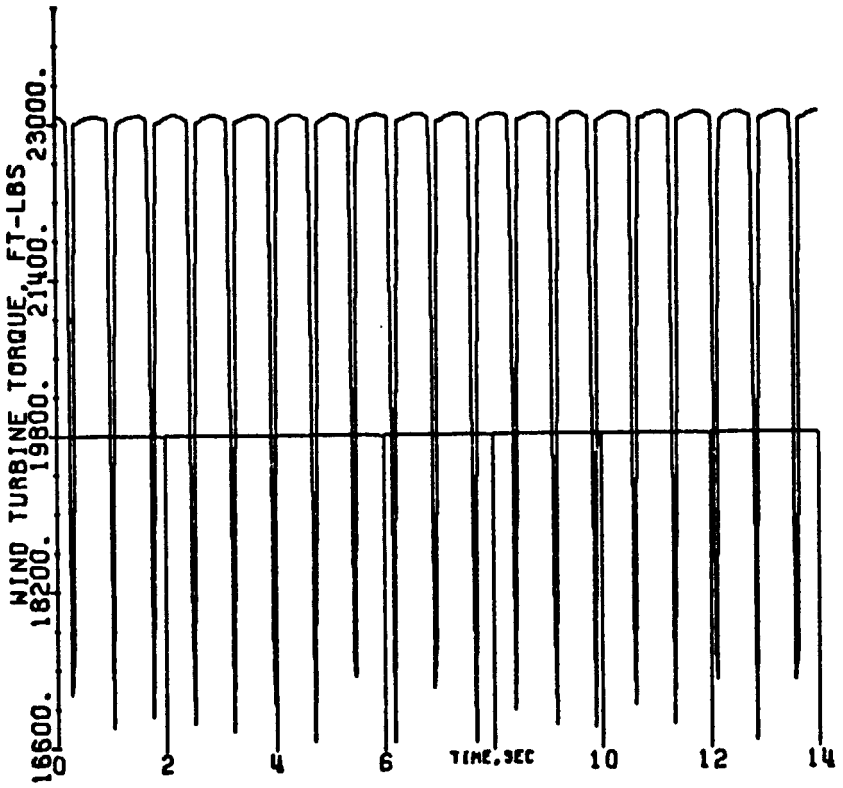

Fig. 11f: Case 2, Wind Turbine Torque
Falk coupling, slip clutch, $X_L = 0.02$ p.u.

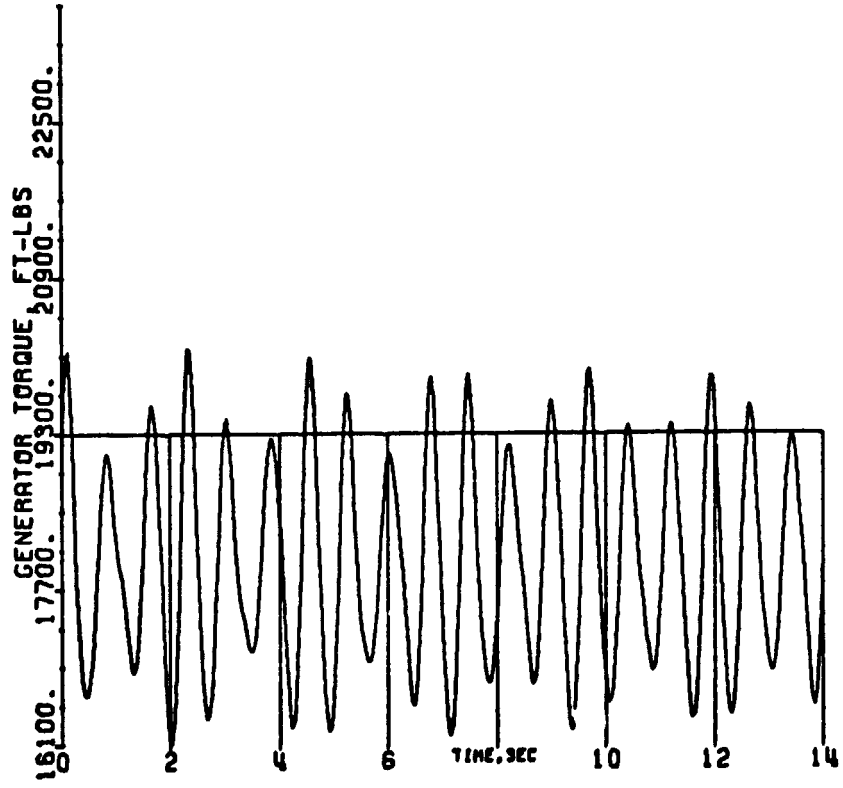

Fig. 11g: Case 2, Generator Torque
Falk coupling, slip clutch, $X_L = 0.02$ p.u.

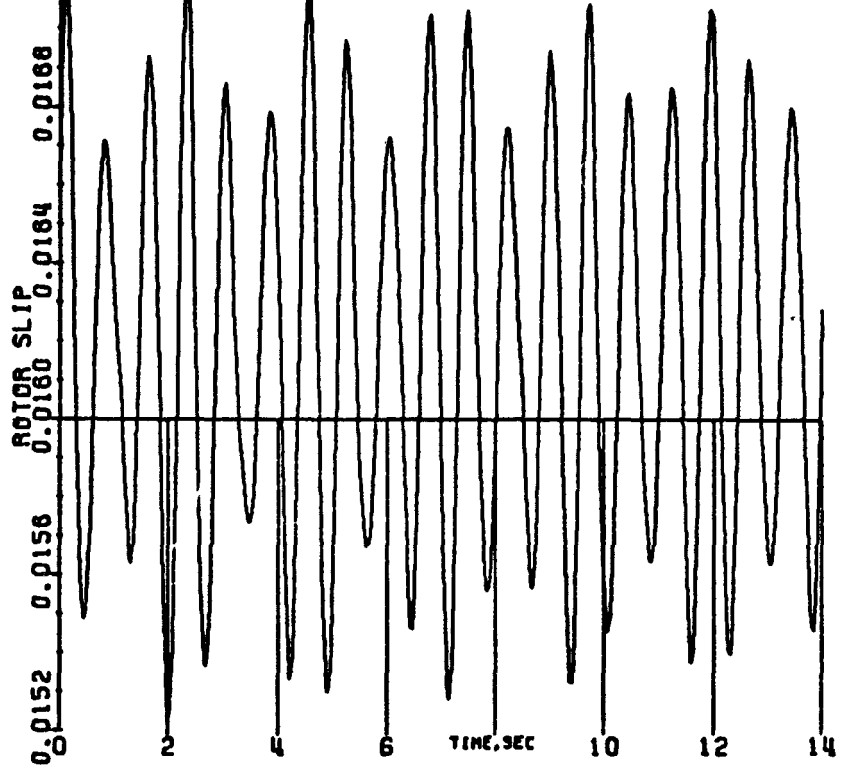

Fig. 11h: Case 2, Rotor Slip [S in Eq. (25)]
Falk coupling, slip clutch, $X_L = 0.02$ p.u.

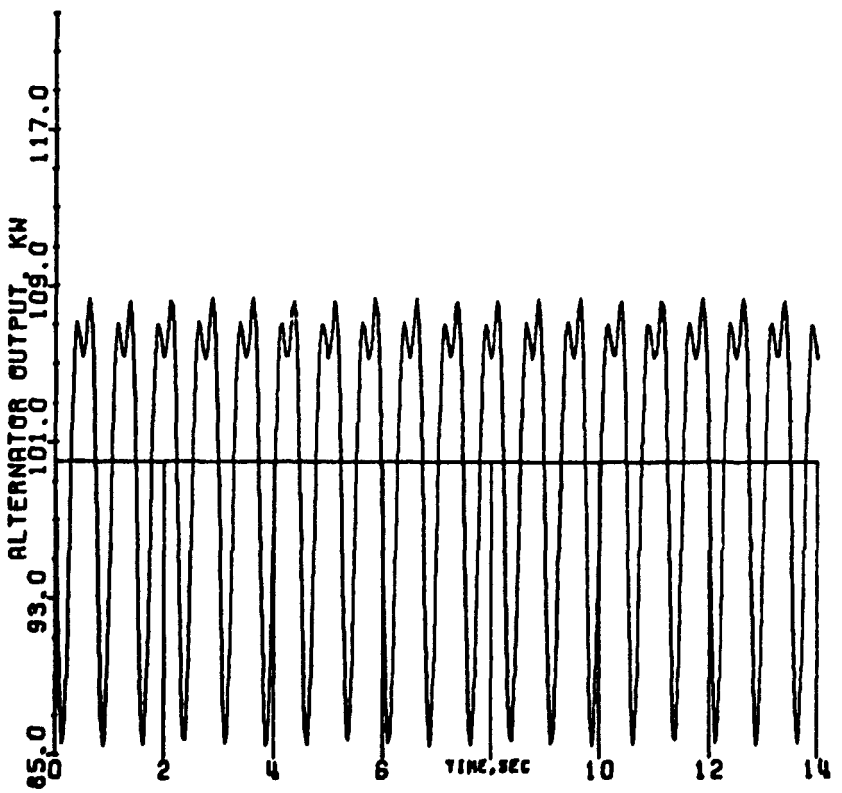

Fig. 12a: Case 3, Alternator Output
No Falk coupling, no slip clutch, $X_L = 0.02$ p.u.

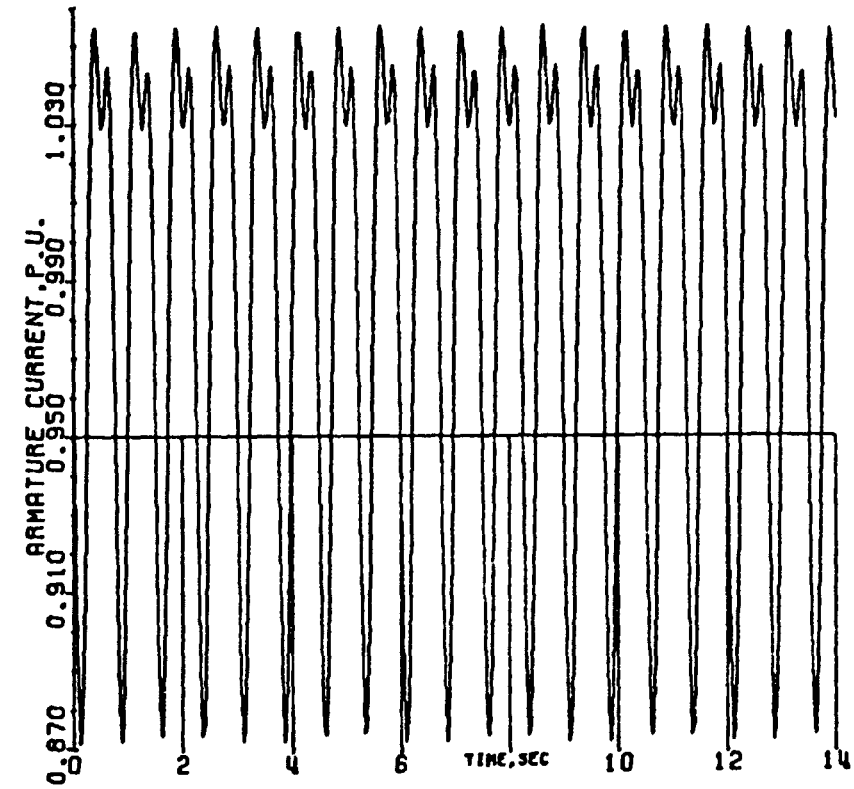

Fig. 12b: Case 3, Armature Current
No Falk coupling, no slip clutch, $X_L = 0.02$ p.u.

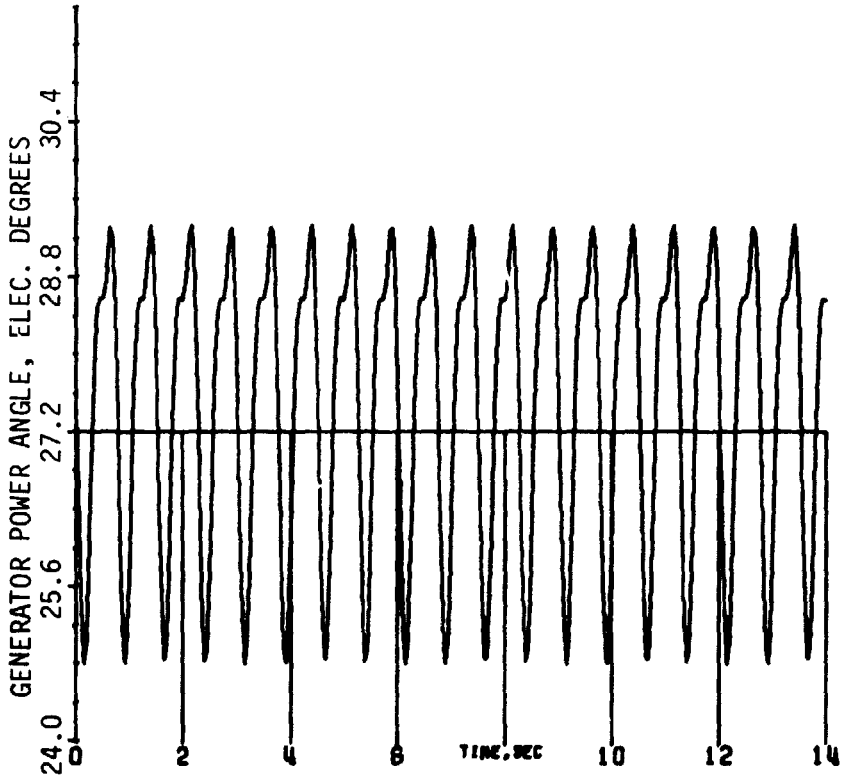

Fig. 12c: Case 3, Generator Power Angle
No Falk coupling, no slip clutch, $X_L = 0.02$ p.u.

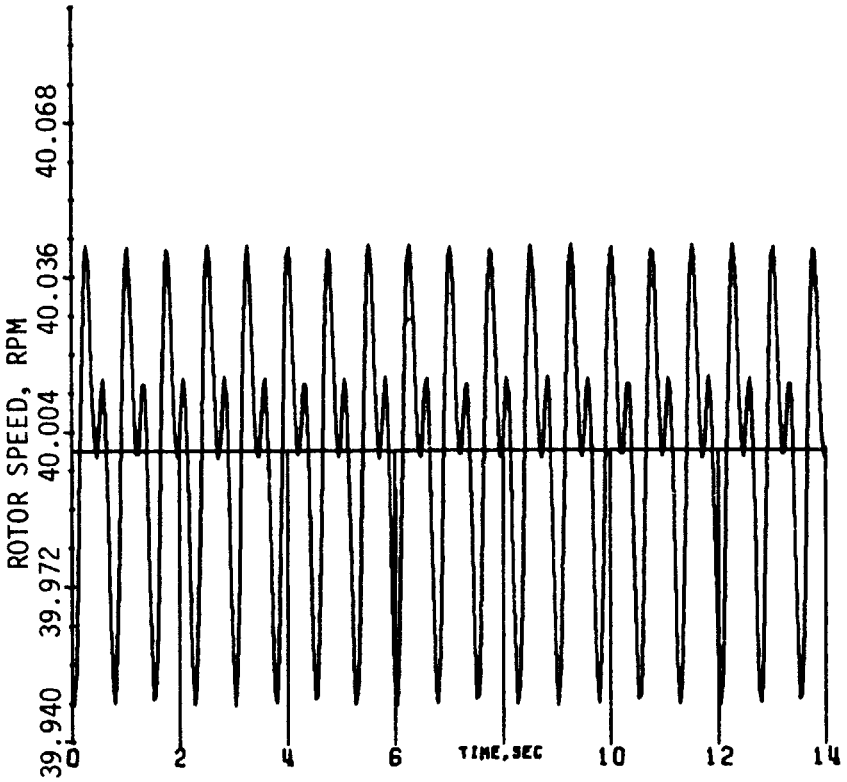

Fig. 12d: Case 3, Rotor Speed
No Falk coupling, no slip clutch, $X_L = 0.02$ p.u.

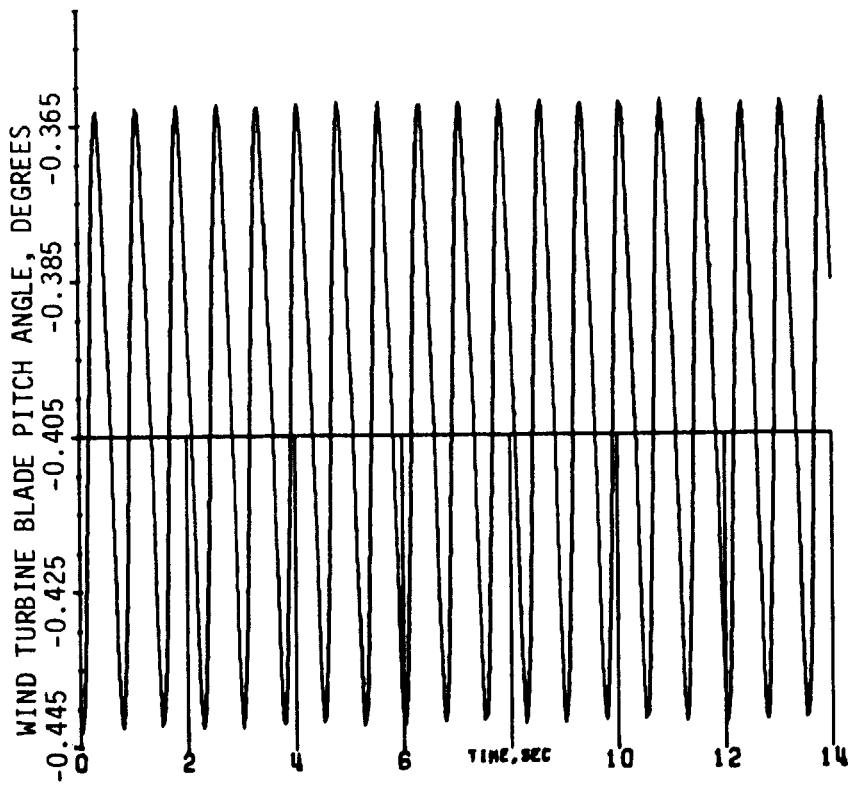

Fig. 12e: Case 3, Blade Pitch Angle
No Falk coupling, no slip clutch, $X_L = 0.02$ p.u.

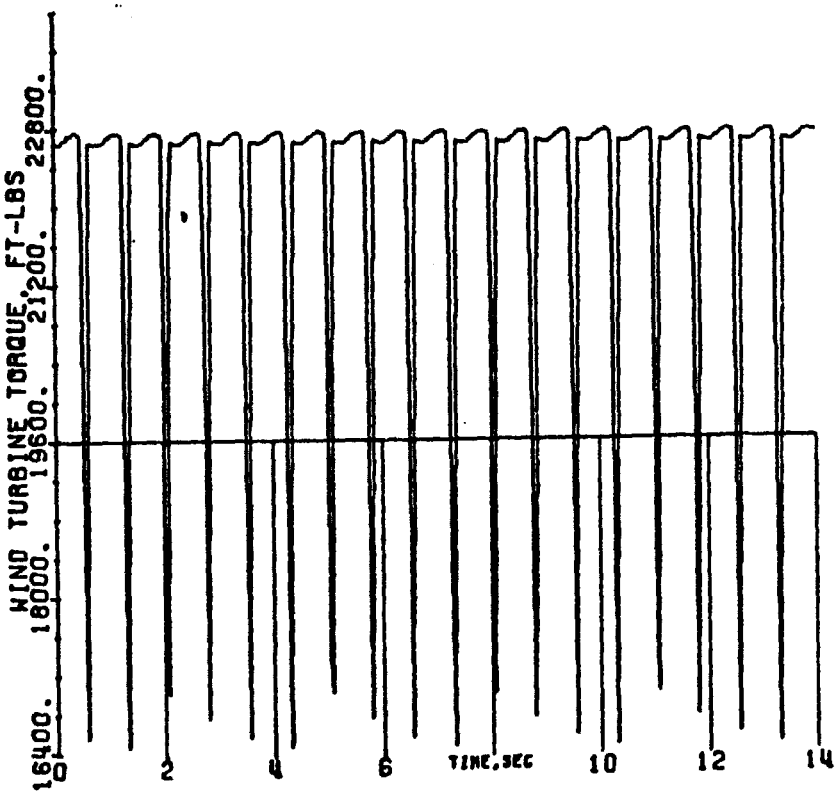

Fig. 12f: Case 3, Turbine Torque
No Falk coupling, no slip clutch, $X_L = 0.02$ p.u.

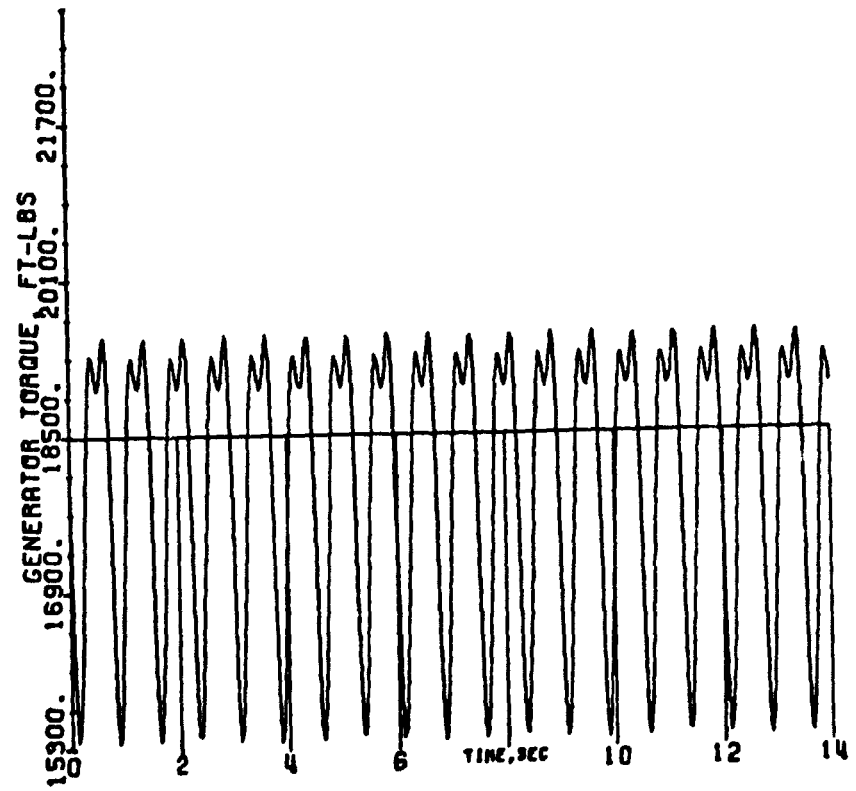

Fig. 12g: Case 3, Generator Torque
No Falk coupling, no slip clutch, $X_L = 0.02$ p.u.

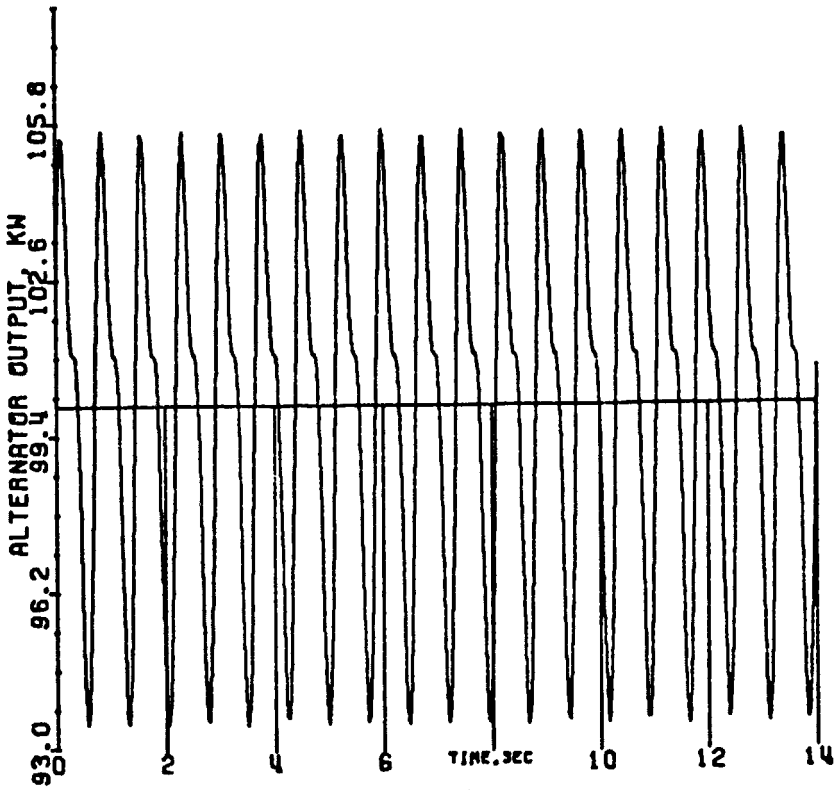

Fig. 13a: Case 4, Alternator Output
No Falk coupling, slip clutch, X_L = 0.02 p.u.

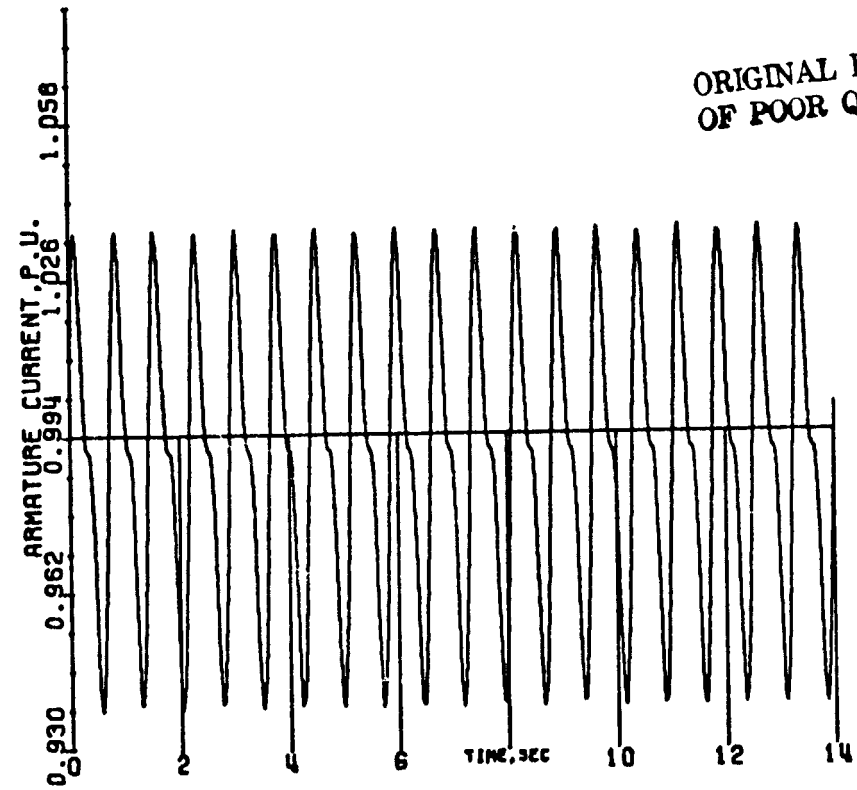

Fig. 13b: Case 4, Armature Current
No Falk coupling, slip clutch, X_L = 0.02 p.u.

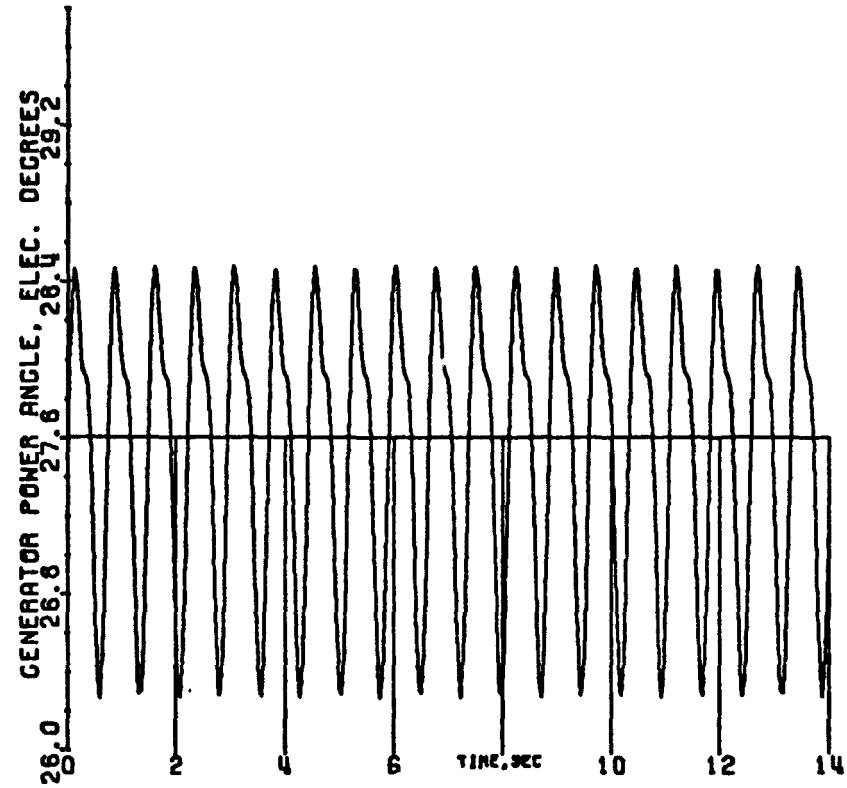

Fig. 13c: Case 4, Generator Power Angle
No Falk coupling, slip clutch, $X_L = 0.02$ p.u.

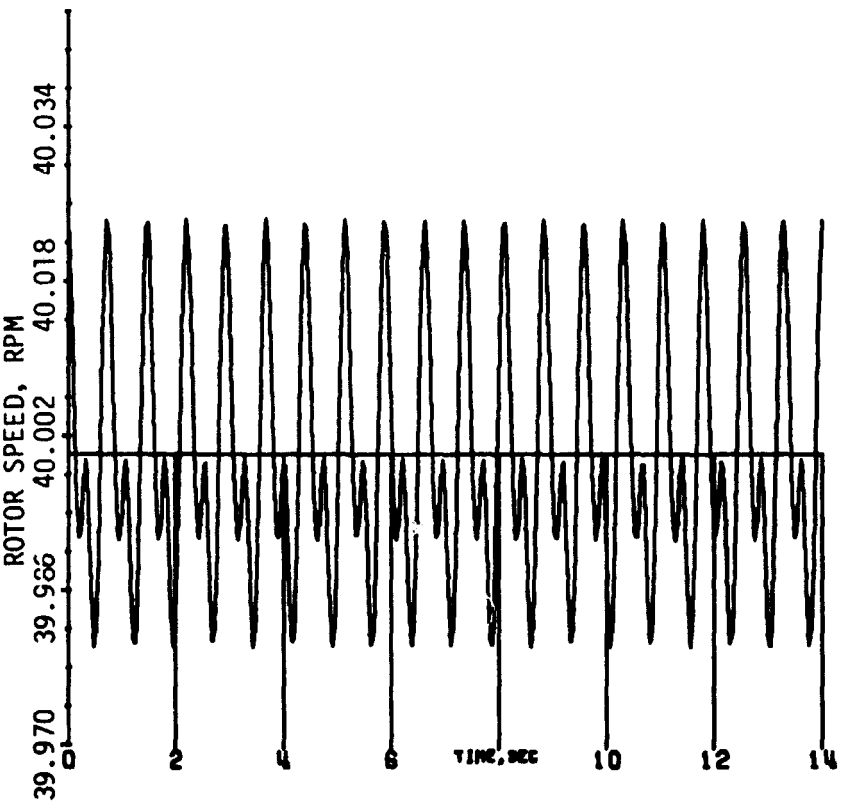

Fig. 13d: Case 4, Rotor Speed
No Falk coupling, slip clutch, $X_L = 0.02$ p.u.

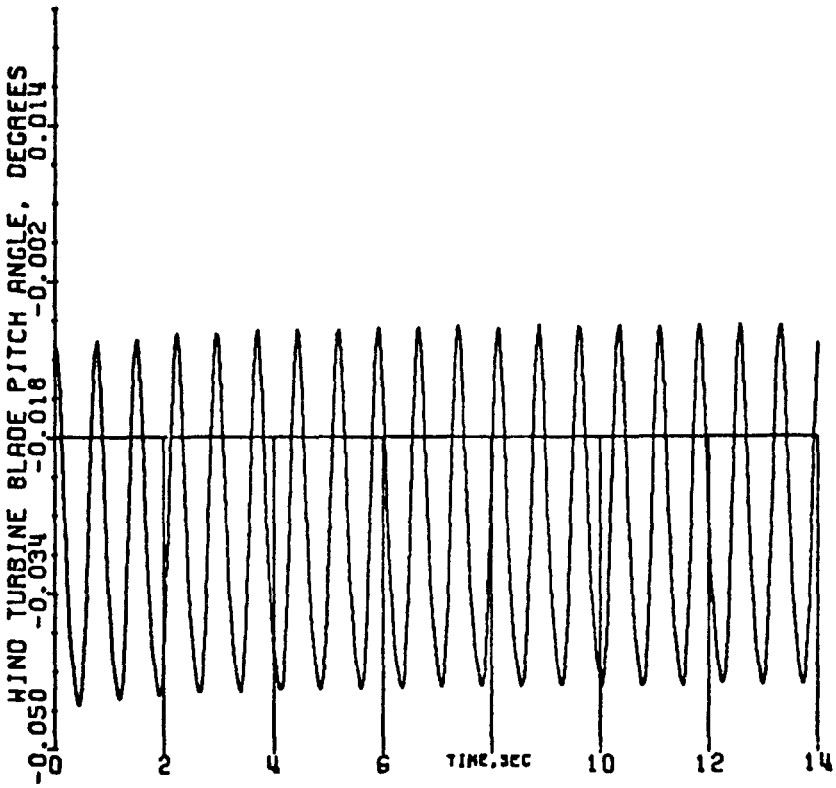

Fig. 13e: Case 4, Blade Pitch Angle
No Falk coupling, slip clutch, X_L = 0.02 p.u.

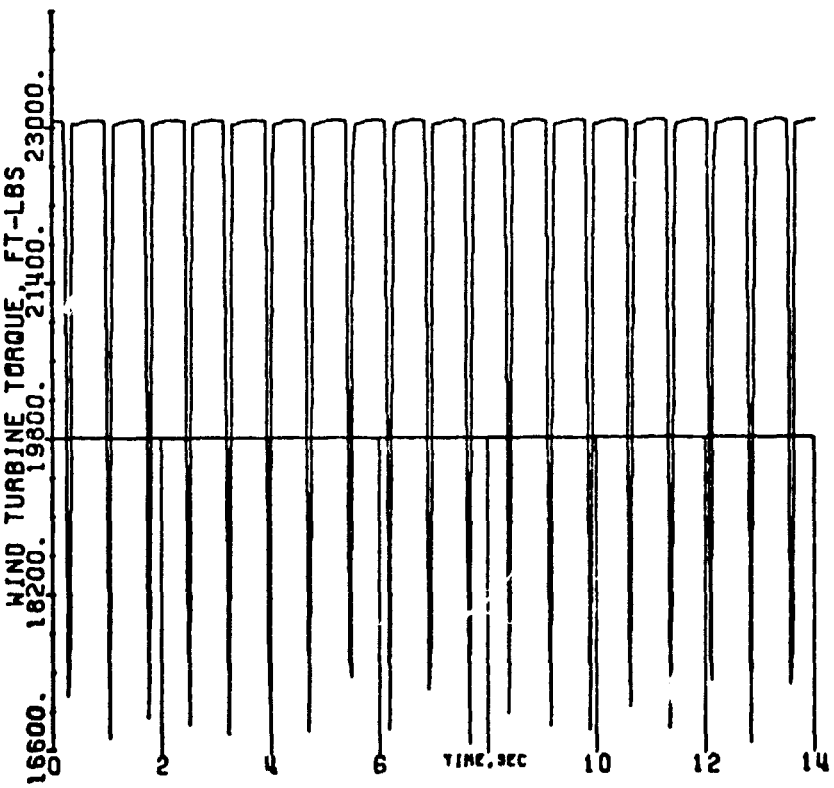

Fig. 13f: Case 4, Turbine Torque
No Falk coupling, slip clutch, X_L = 0.02 p.u.

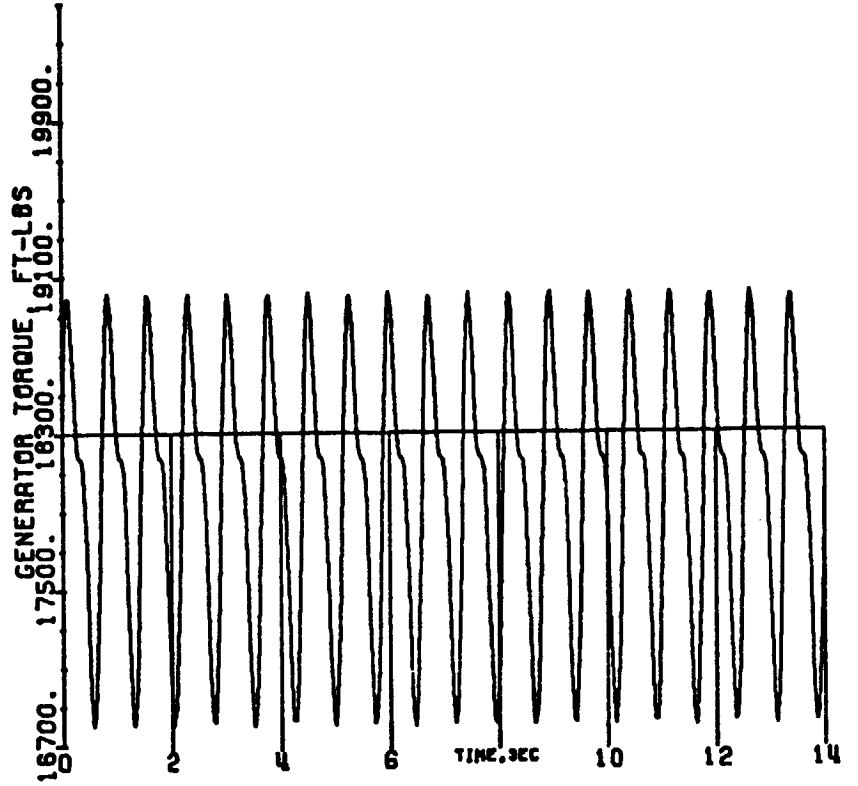

Fig. 13g: Case 4, Generator Torque
No Falk coupling, slip clutch, $X_L = 0.02$ p.u.

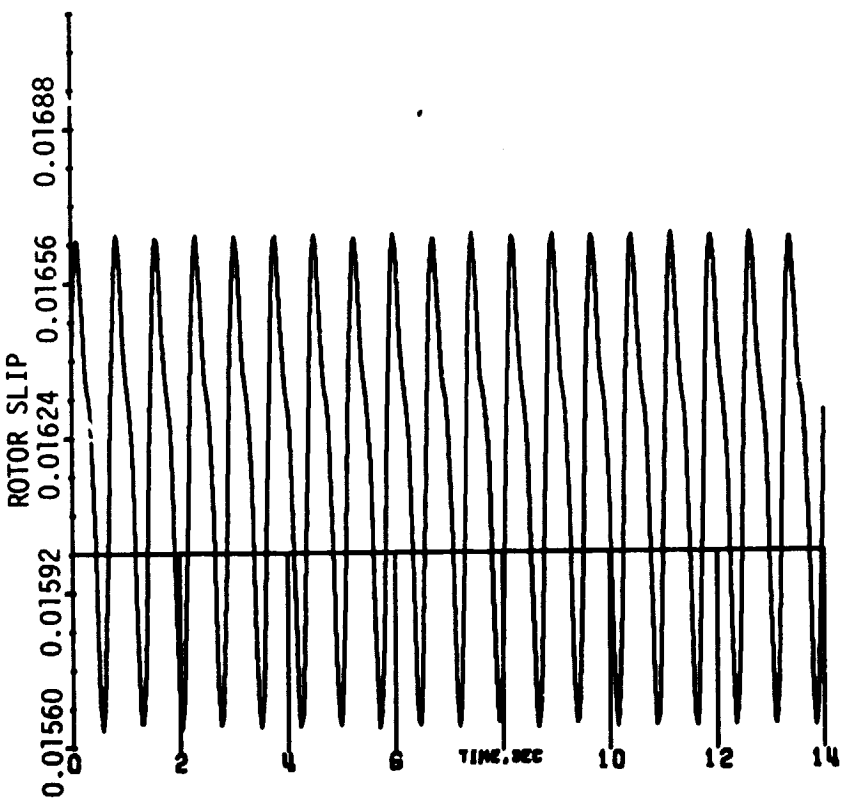

Fig. 13h: Case 4, Rotor Slip
No Falk coupling, slip clutch, $X_L = 0.02$ p.u.

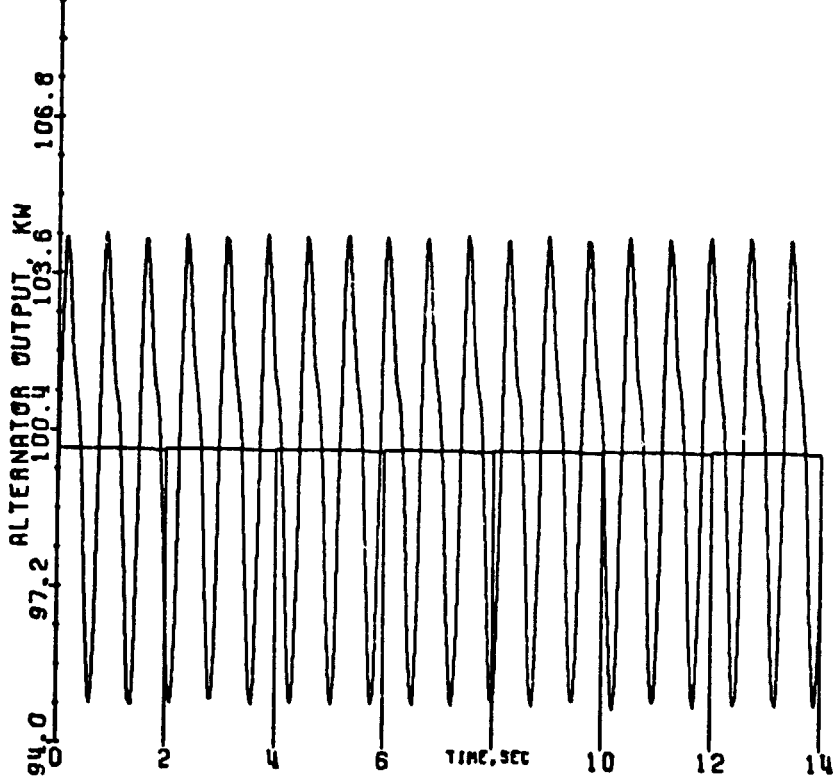

Fig. 14a: Case 5, Alternator Output
No Falk coupling, slip clutch, $X_L = 0.40$ p.u.

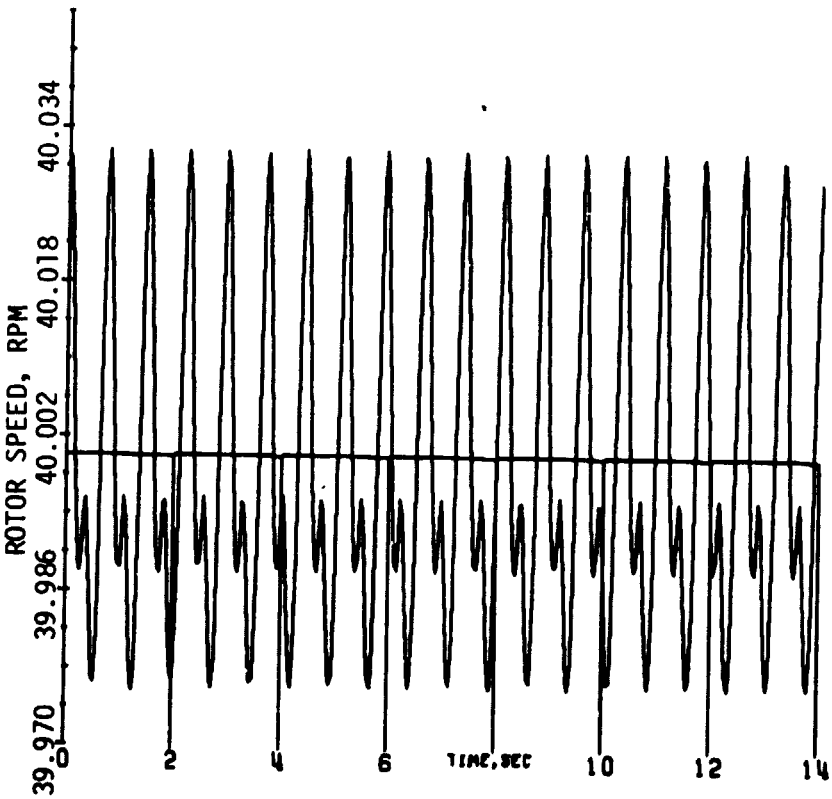

Fig. 14b: Case 5, Rotor Speed
No Falk coupling, slip clutch, $X_L = 0.40$ p.u.

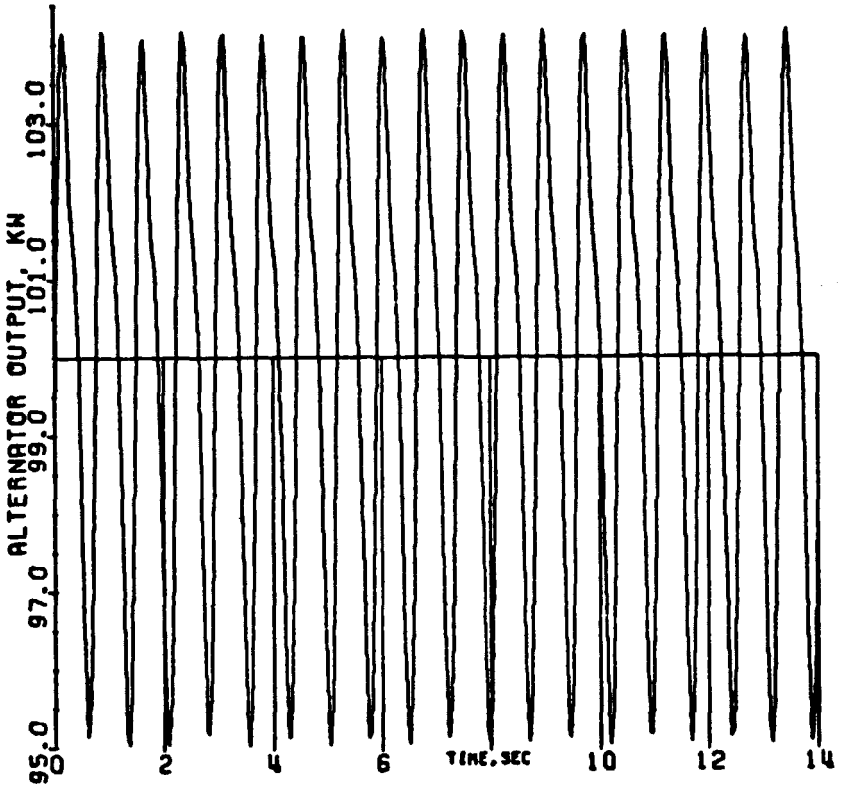

Fig. 15a: Case 6, Alternator Output
No Falk coupling, slip clutch, $X_L = 0.47$ p.u.

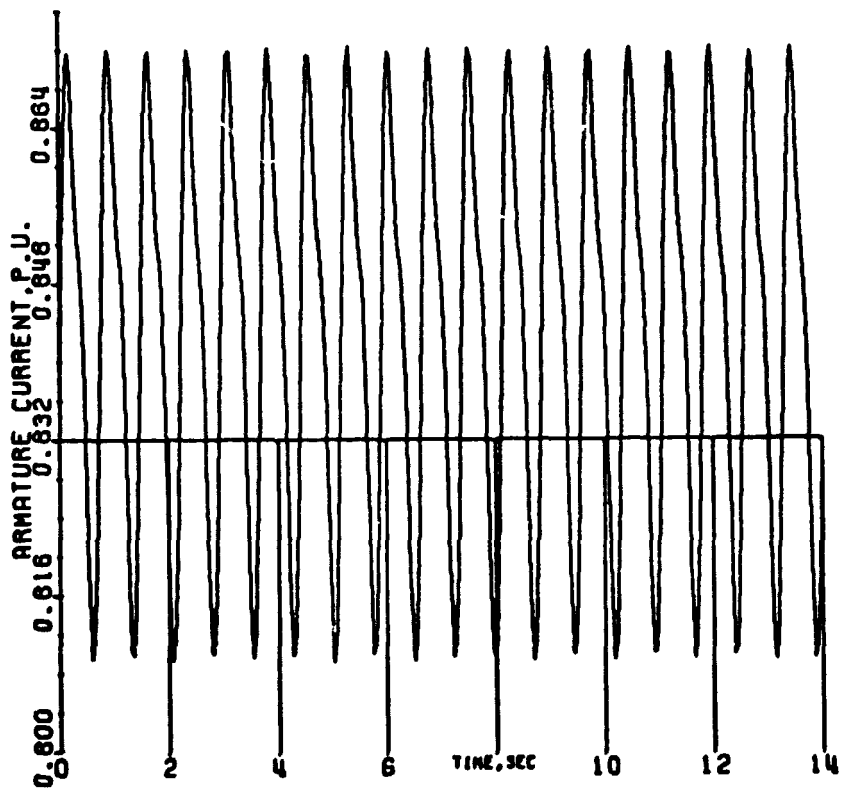

ORIGINAL PAGE IS
OF POOR QUALITY

Fig. 15b: Case 6, Armature Current
No Falk coupling, slip clutch, $X_L = 0.47$ p.u.

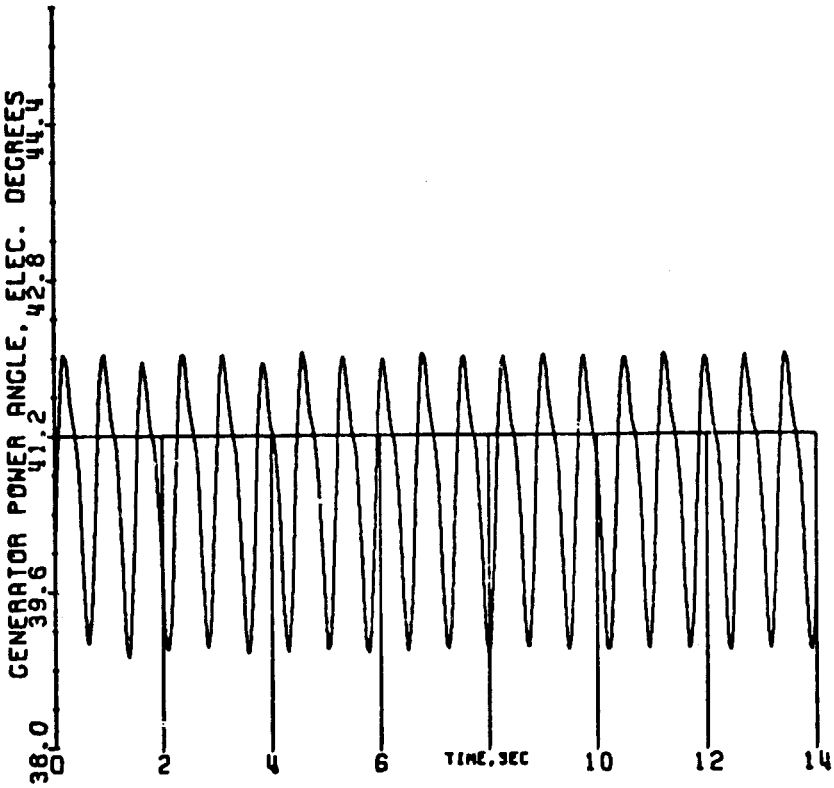

Fig. 15c: Case 6, Generator Power Angle
No Falk coupling, slip clutch, $X_L = 0.47$ p.u.

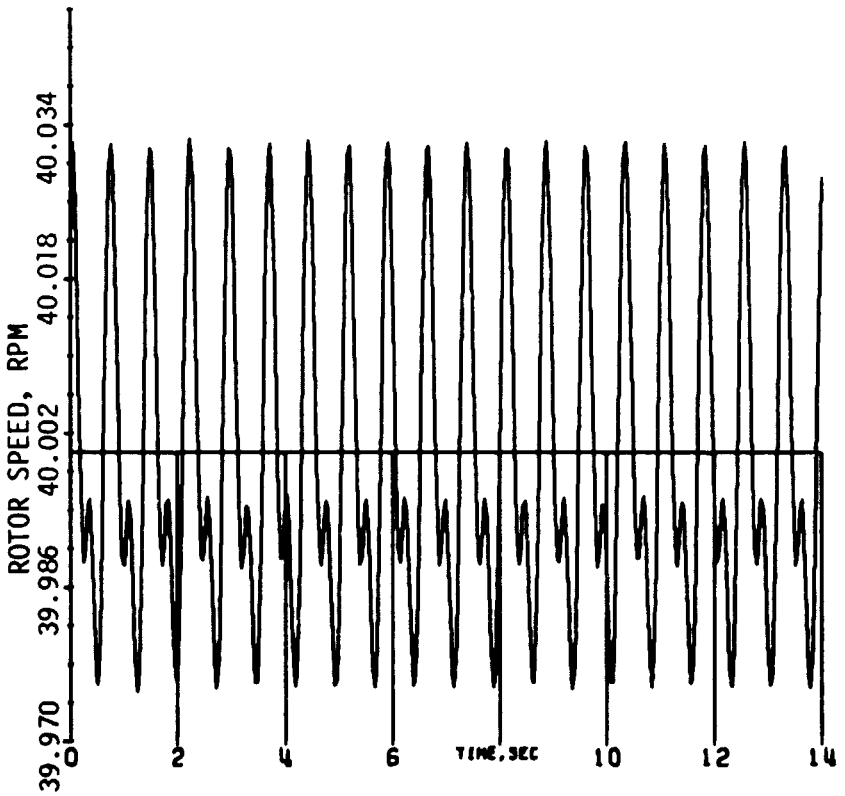

Fig. 15d: Case 6, Rotor Speed
No Falk coupling, slip clutch, $X_L = 0.47$ p.u.

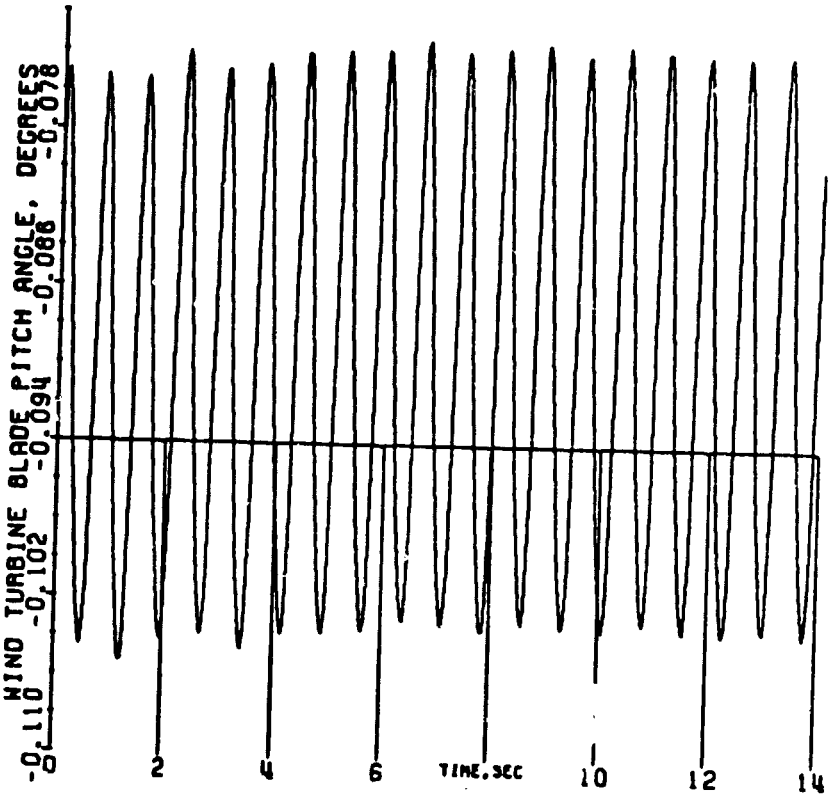

Fig. 15e: Case 6, Blade Pitch Angle
No Falk coupling, slip clutch, X_L = 0.47 p.u.

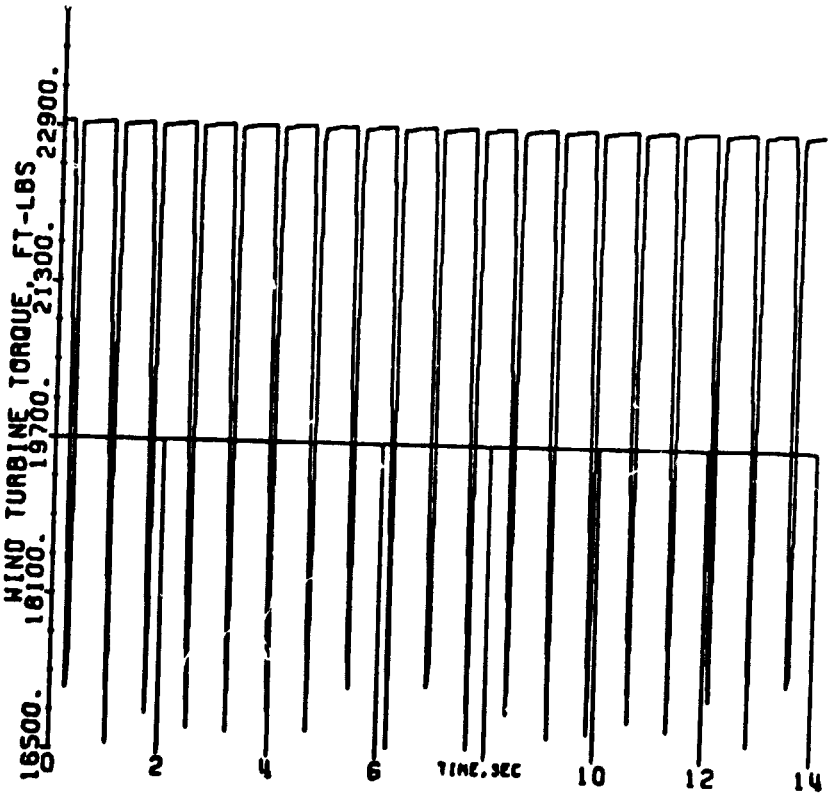

ORIGINAL PAGE IS
OF POOR QUALITY

Fig. 15f: Case 6, Turbine Torque
No Falk coupling, slip clutch, X_L = 0.47 p.u.

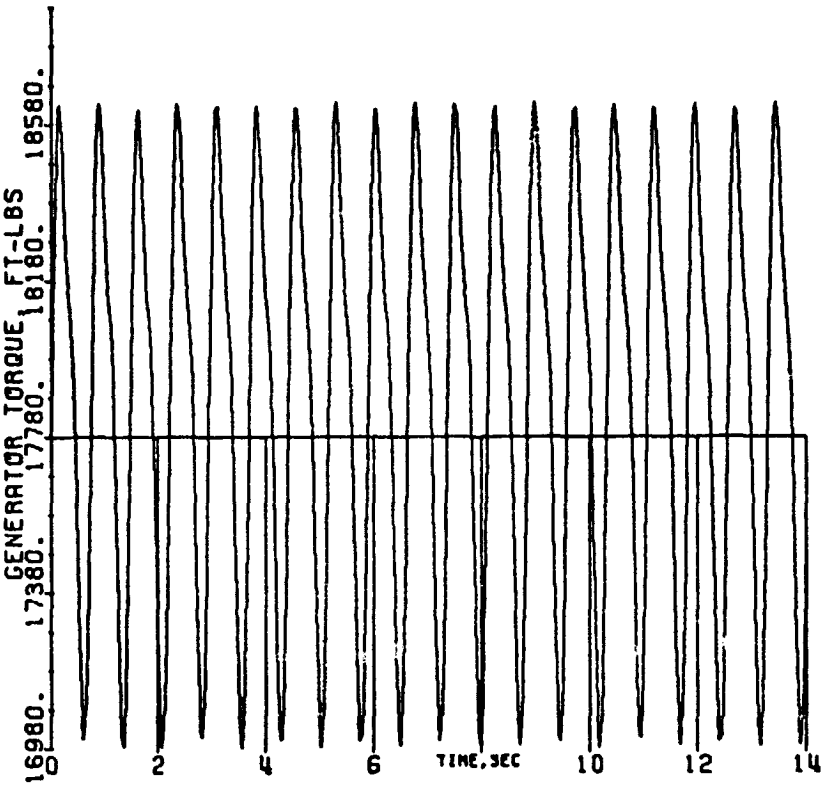

Fig. 15g: Case 6, Generator Torque
No Falk coupling, slip clutch, X_L = 0.47 p.u.

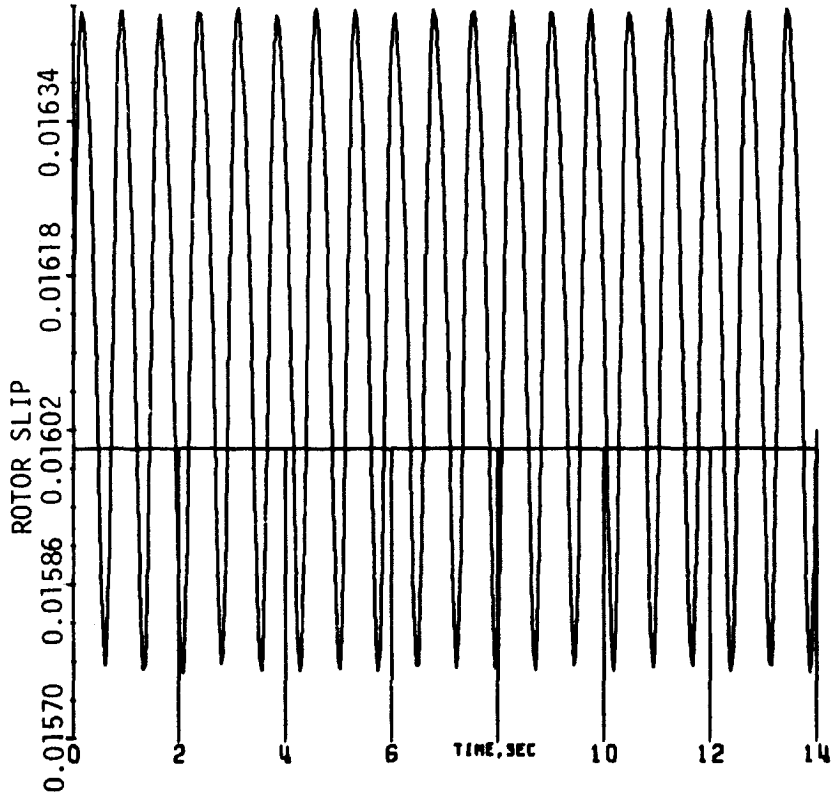

Fig. 15h: Case 6, Rotor Slip
No Falk coupling, slip clutch, X_L = 0.47 p.u.

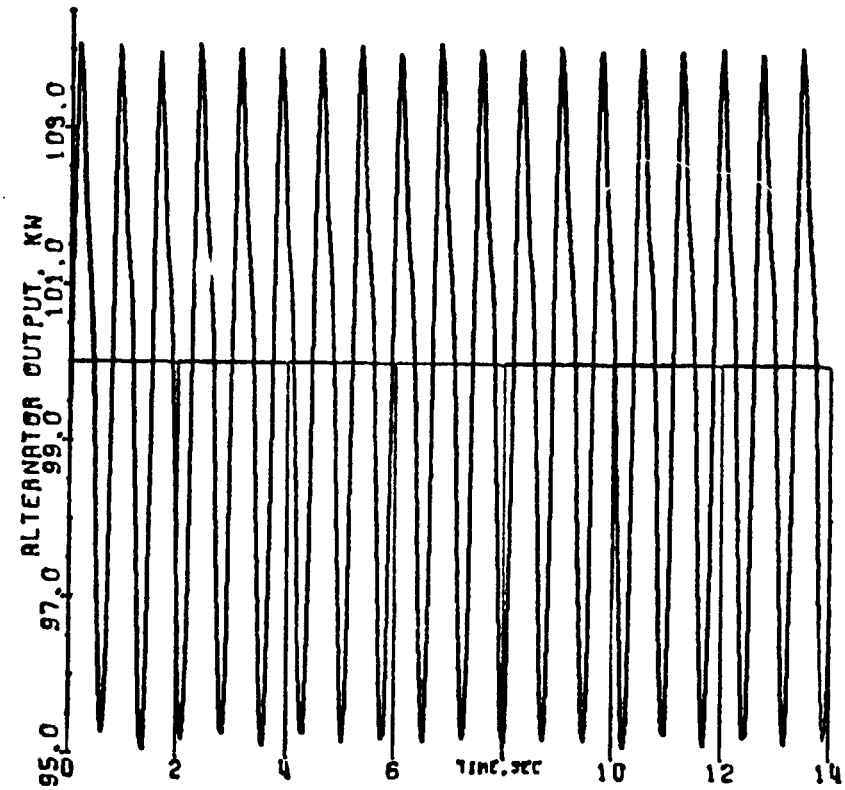

Fig. 16a: Case 7, Alternator Output
No Falk coupling, slip clutch, $X_L = 0.50$ p.u.

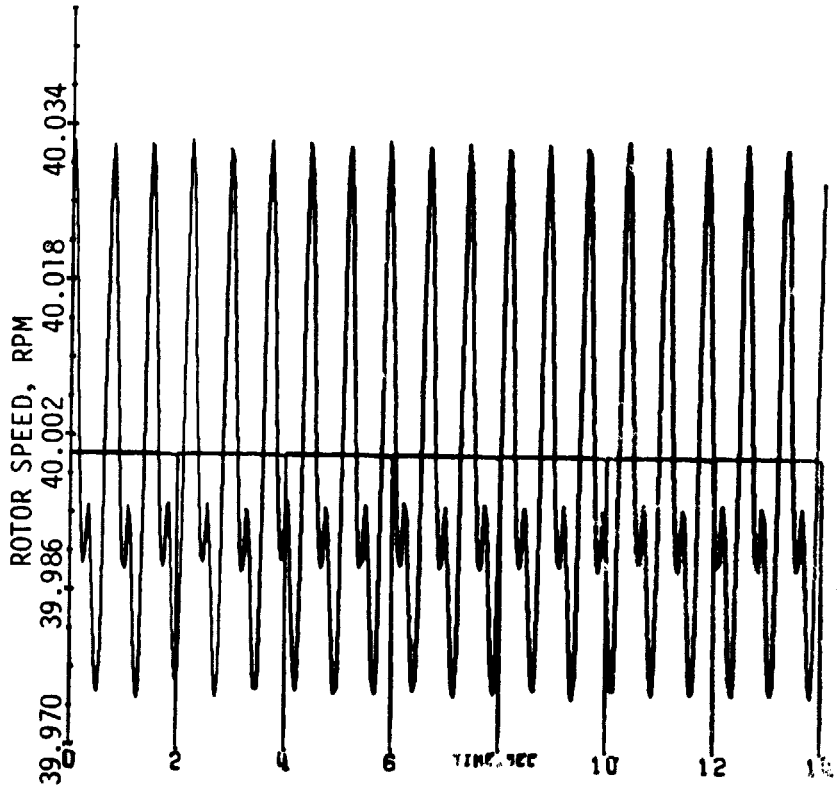

Fig. 16b: Case 7, Rotor Speed
No Falk coupling, slip clutch, $X_L = 0.50$ p.u.

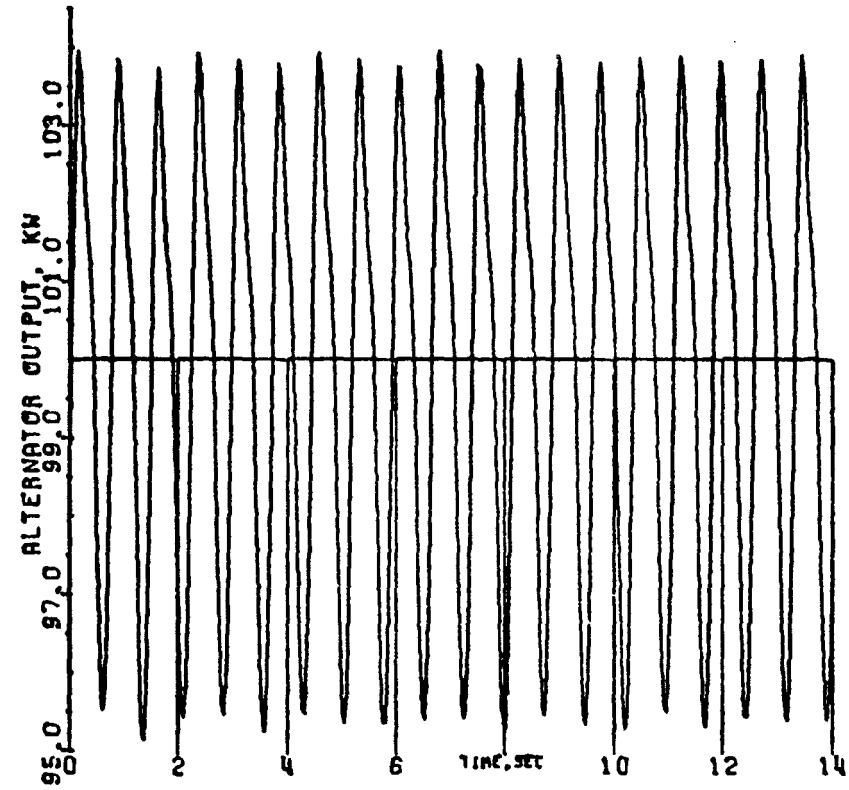

Fig. 17a: Case 8, Alternator Output
No Falk coupling, slip clutch, $X_L = 0.55$ p.u.

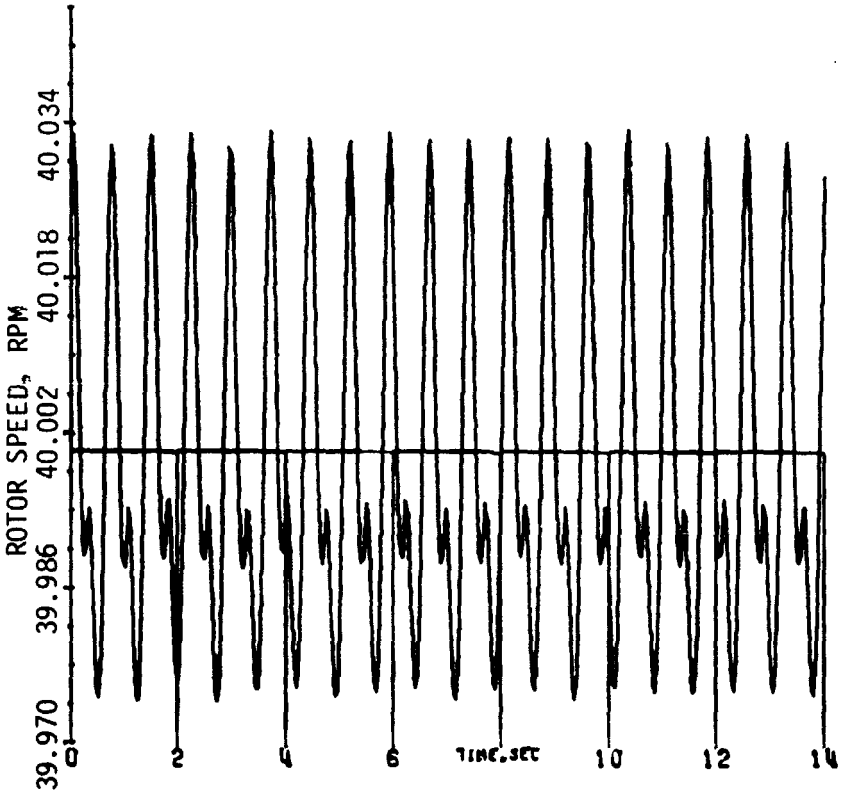

Fig. 17b: Case 8, Rotor Speed
No Falk coupling, slip clutch, $X_L = 0.55$ p.u.

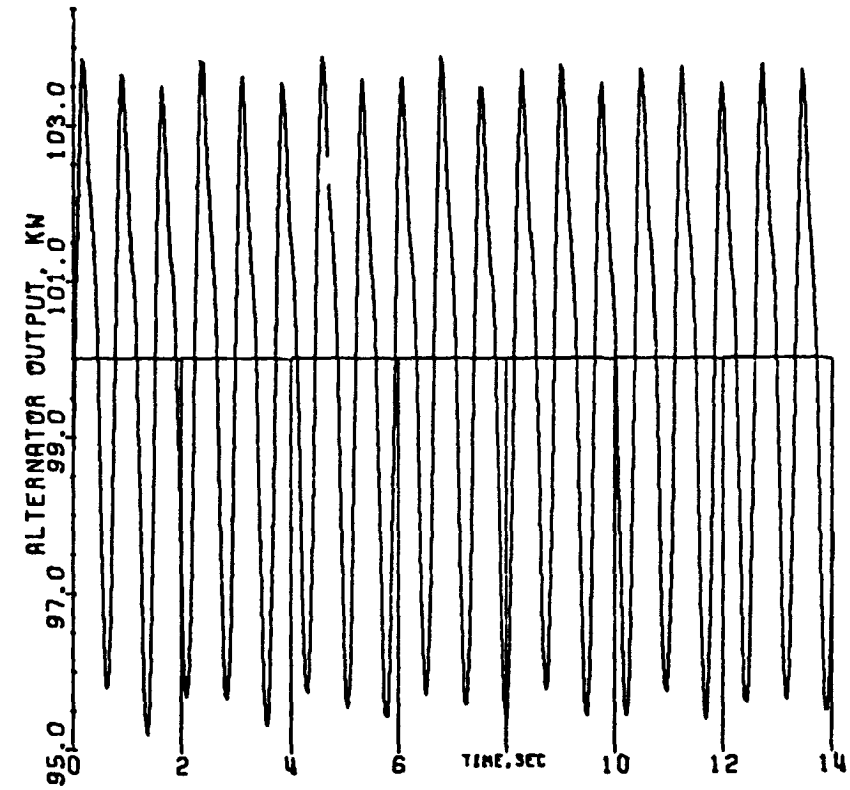

Fig. 18a: Case 9, Alternator Output
No Falk coupling, slip clutch, $X_L = 0.60$ p.u.

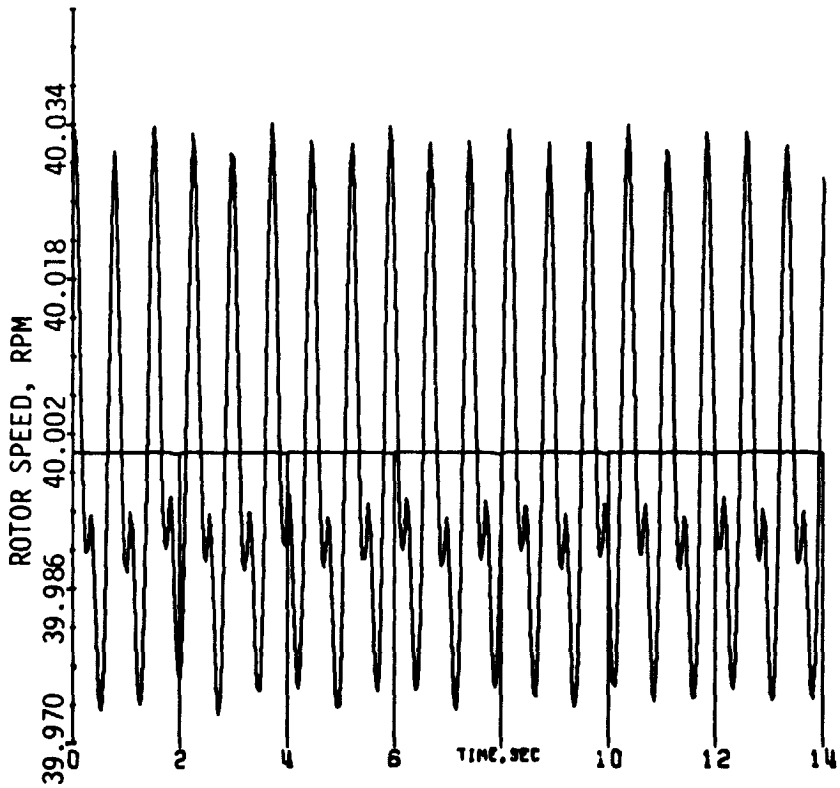

Fig. 18b: Case 9, Rotor Speed
No Falk coupling, slip clutch, $X_L = 0.60$ p.u.

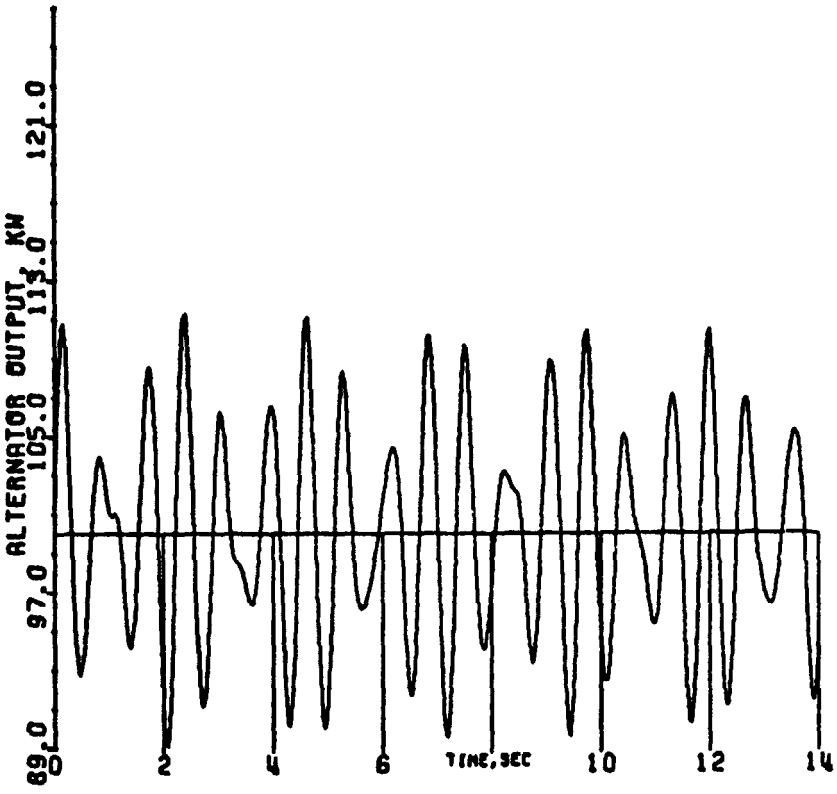

Fig. 19a: Case 10, Alternator Output
Falk coupling, slip clutch, $X_L = 0.47$ p.u.

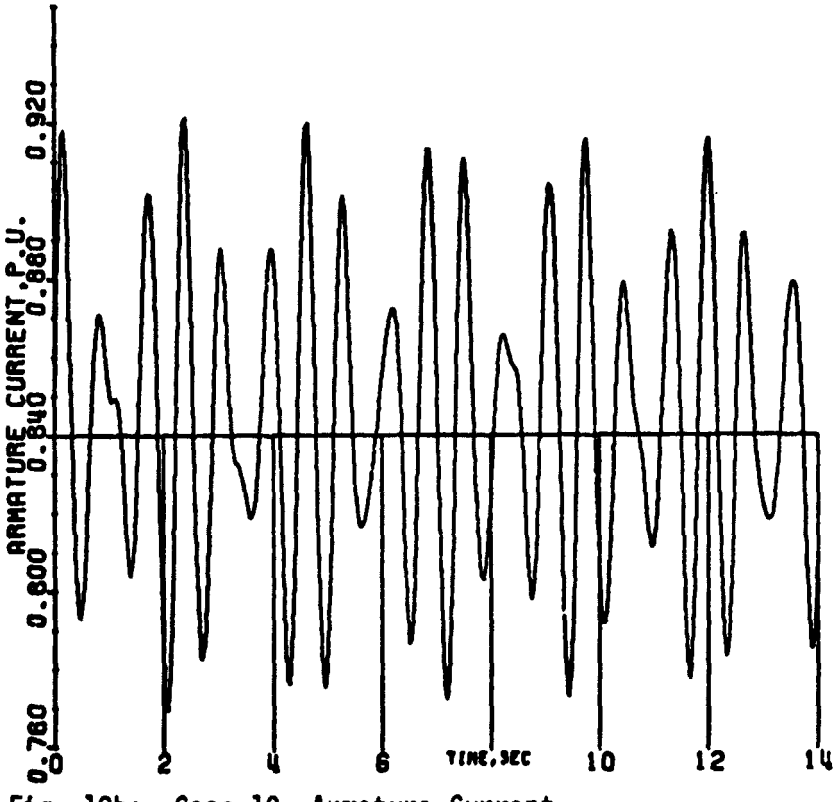

Fig. 19b: Case 10, Armature Current
Falk coupling, slip clutch, $X_L = 0.47$ p.u.

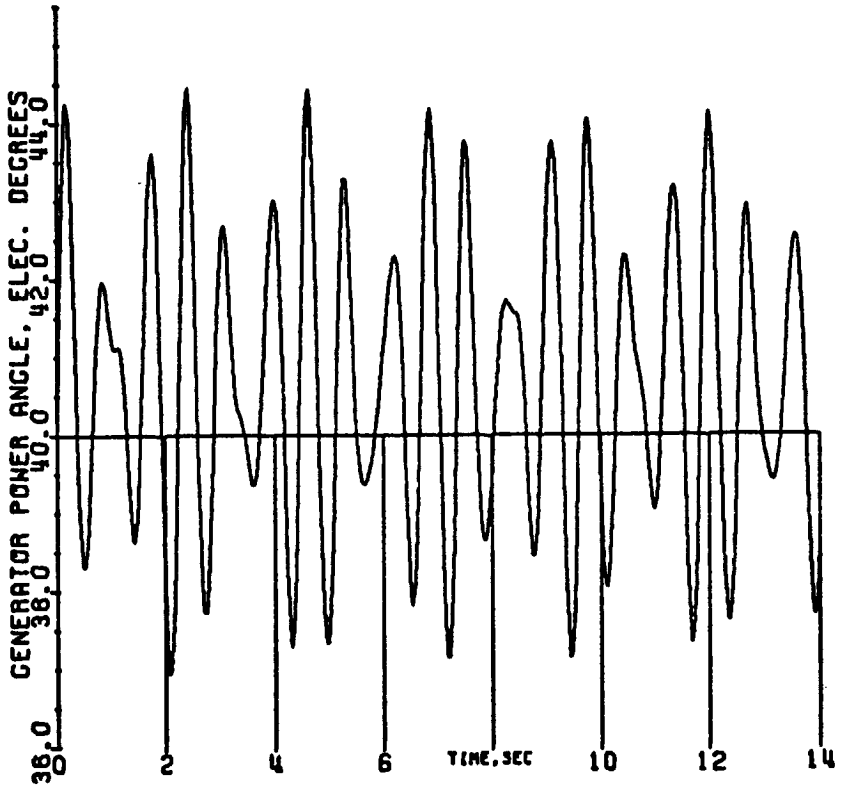

Fig. 19c: Case 10, Generator Power Angle
Falk coupling, slip clutch, $X_L = 0.47$ p.u.

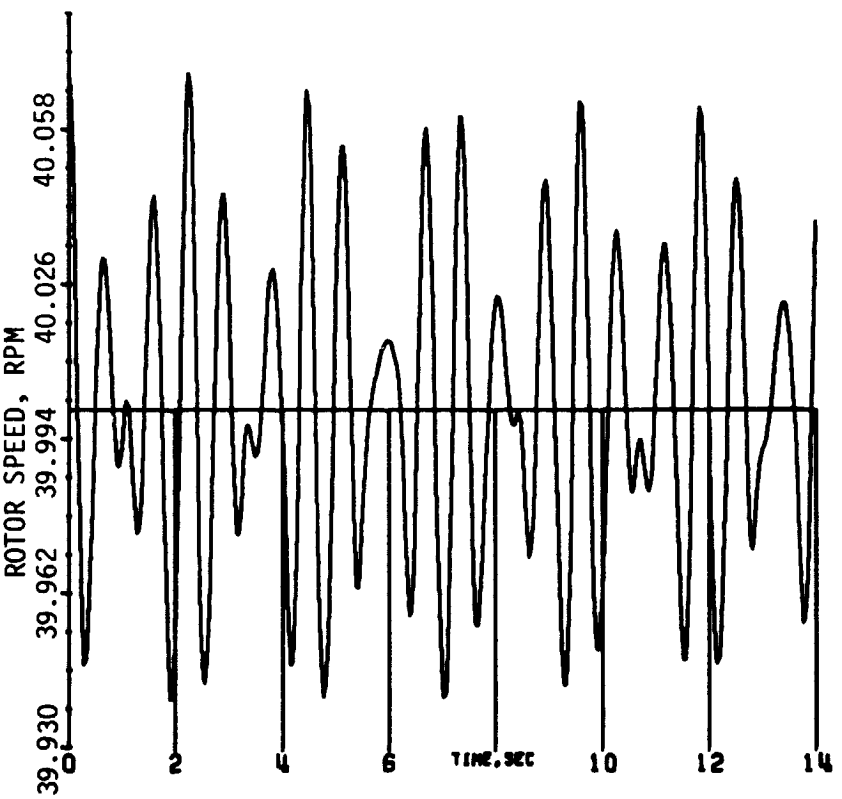

Fig. 19d: Case 10, Rotor Speed
Falk coupling, slip clutch, $X_L = 0.47$ p.u.

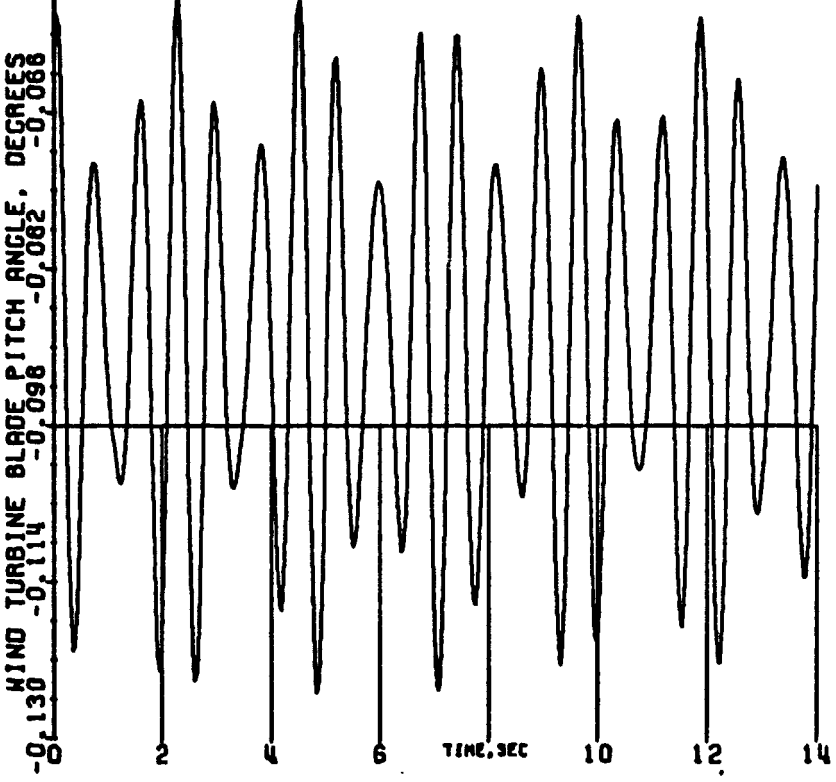

Fig. 19e: Case 10, Blade Pitch Angle
Falk coupling, slip clutch, X_L = 0.47 p.u.

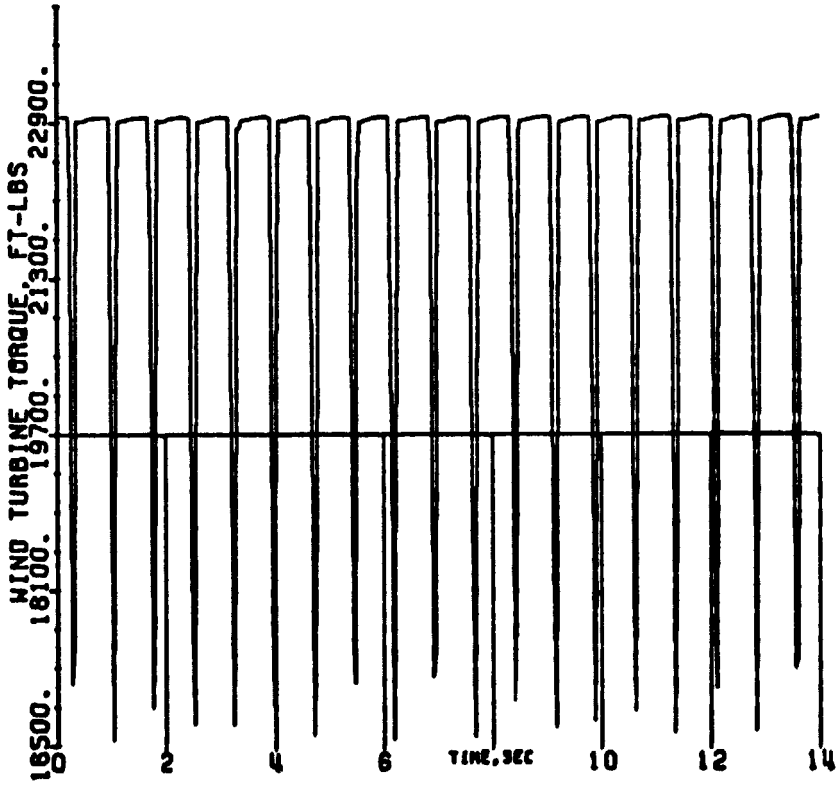

Fig. 19f: Case 10, Wind Turbine Torque
Falk coupling, slip clutch, X_L = 0.47 p.u.

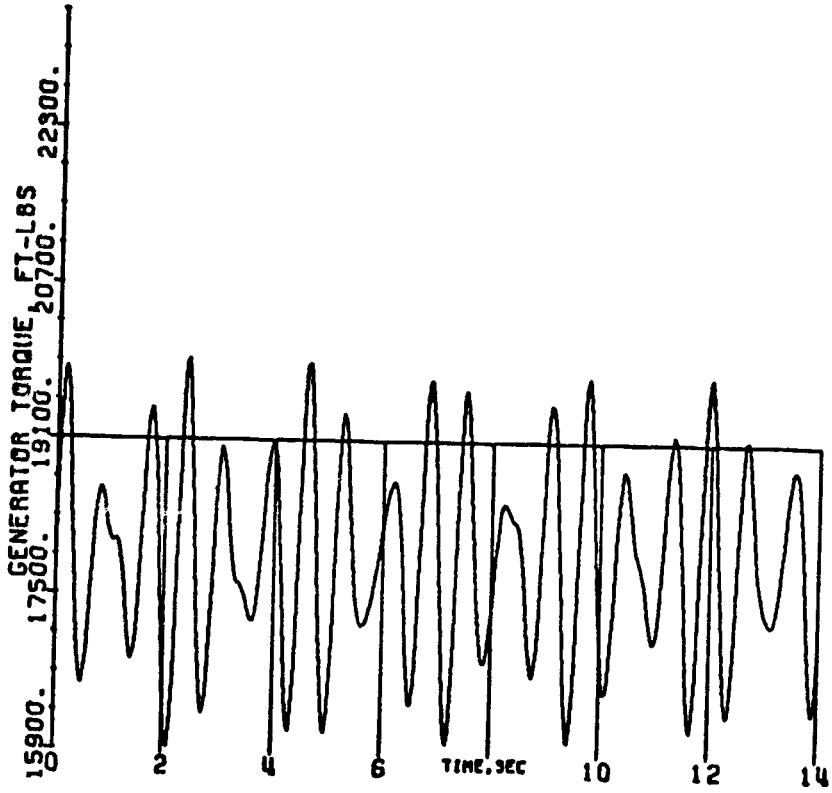

Fig. 19g: Case 10, Generator Torque
Falk coupling, slip clutch, $X_L = 0.47$ p.u.

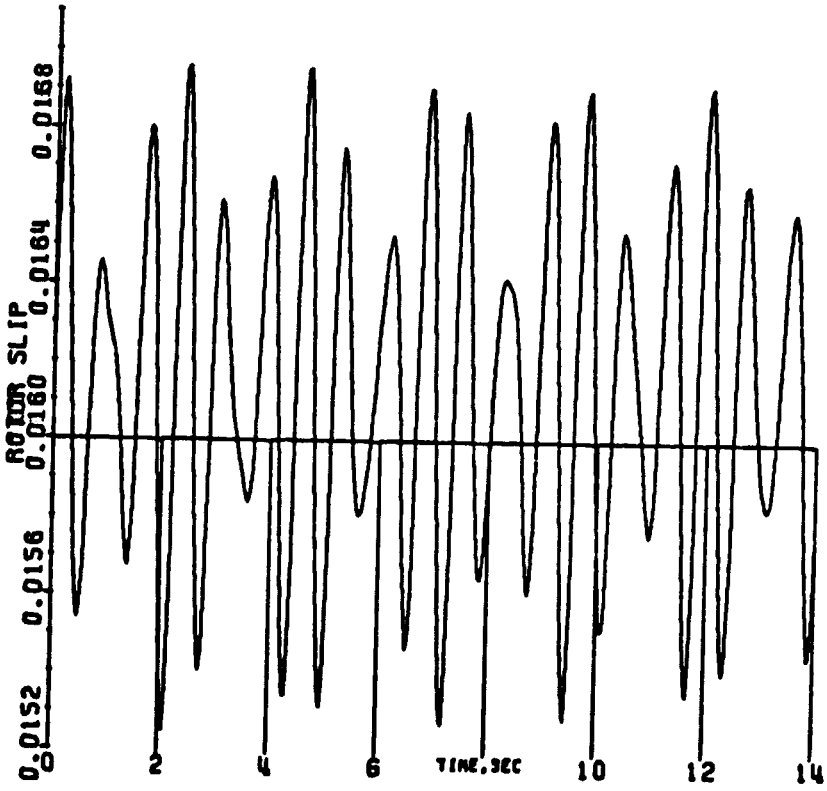

ORIGINAL PAGE IS
OF POOR QUALITY

Fig. 19h: Case 10, Rotor Slip
Falk coupling, slip clutch, $X_L = 0.47$ p.u.

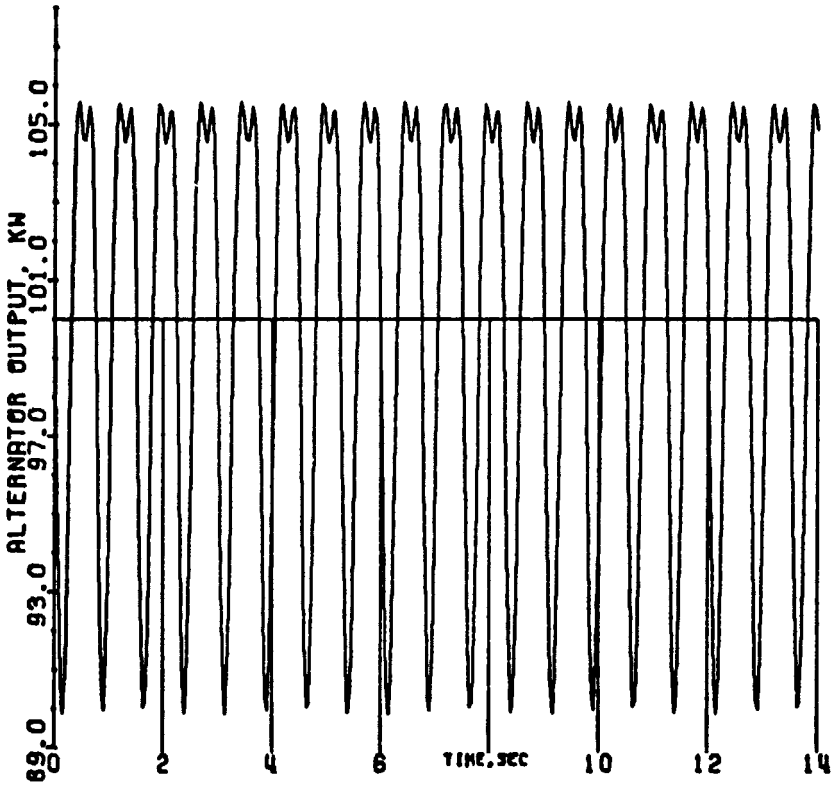

Fig. 20a: Case 11, Alternator Output
No Falk coupling, no slip clutch, $X_L = 0.20$ p.u.

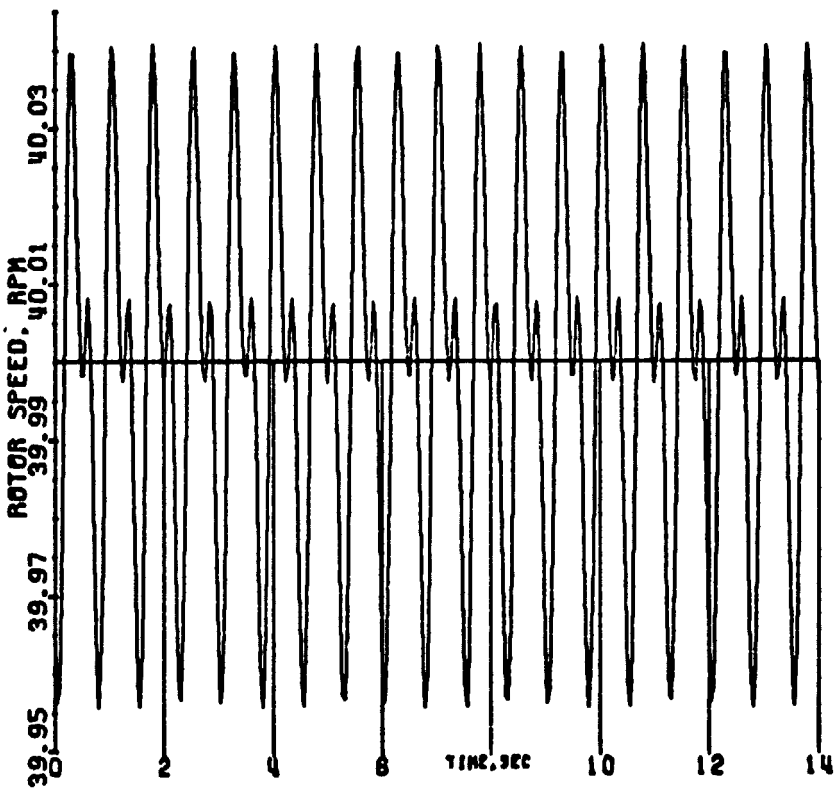

Fig. 20b: Case 11, Rotor Speed
No Falk coupling, no slip clutch, $X_L = 0.20$ p.u.

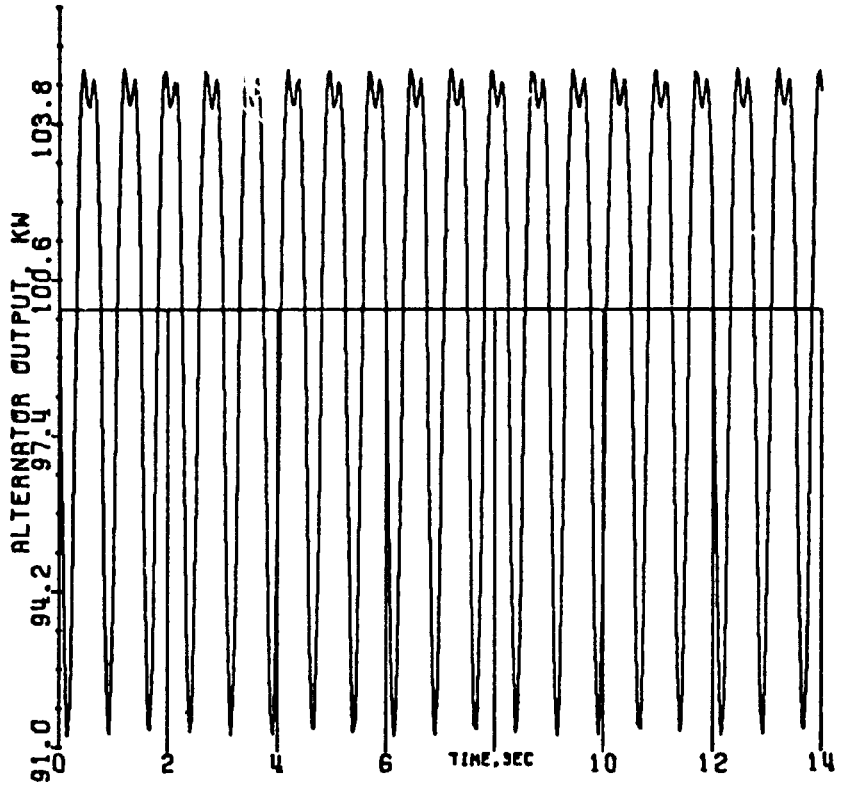

Fig. 21a: Case 12, Alternator Output
No Falk coupling, no slip clutch, $X_L = 0.30$ p.u.

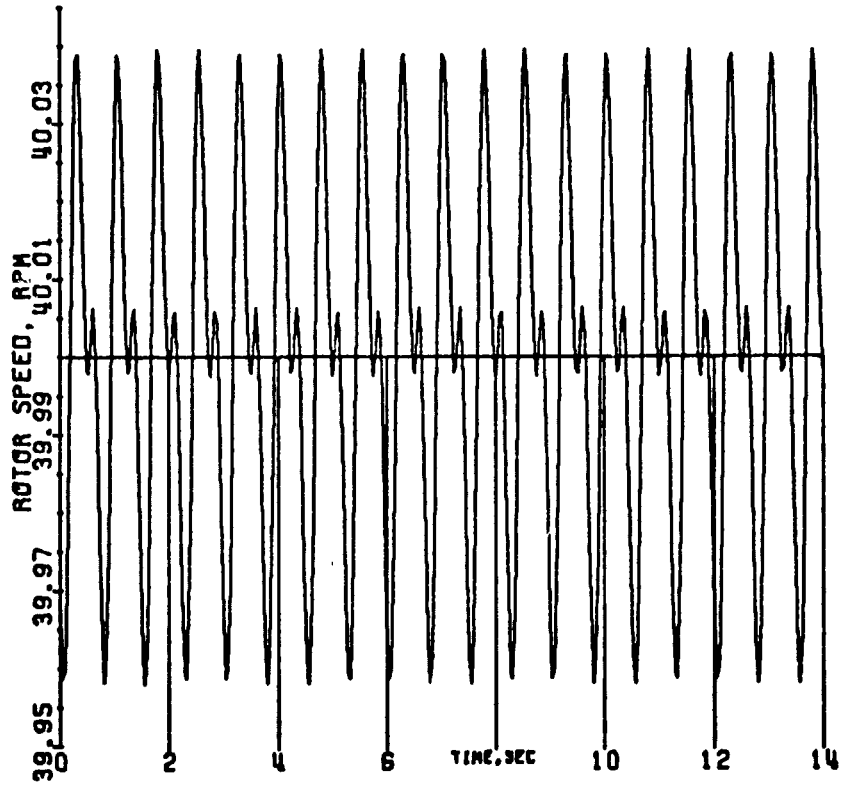

Fig. 21b: Case 12, Rotor Speed
No Falk coupling, no slip clutch, $X_L = 0.30$ p.u.

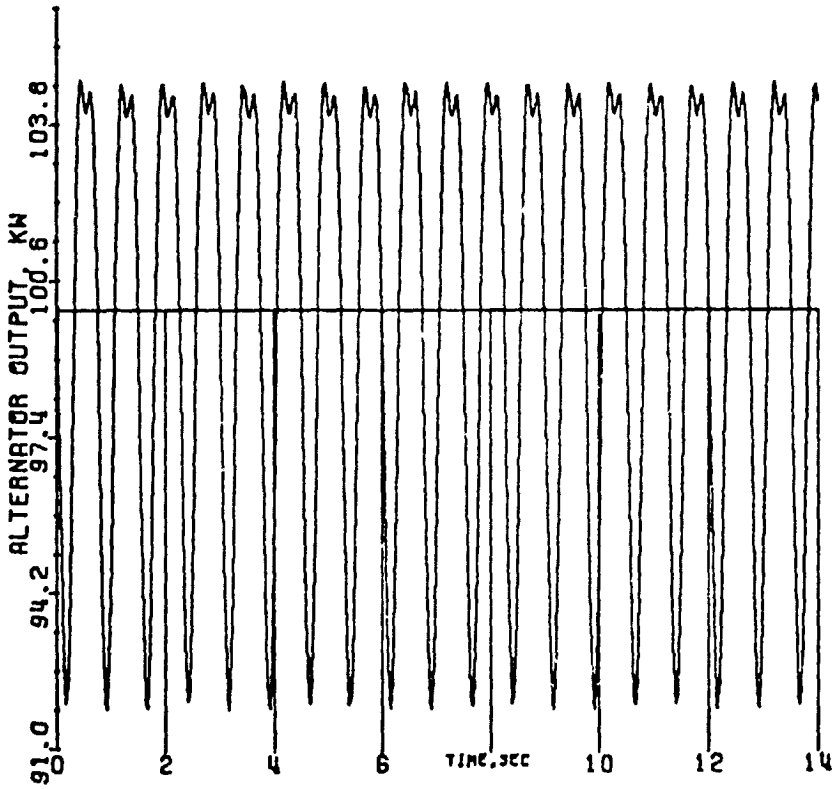

Fig. 22a: Case 13, Alternator Output
No Falk coupling, no slip clutch, X_L = 0.35 p.u.

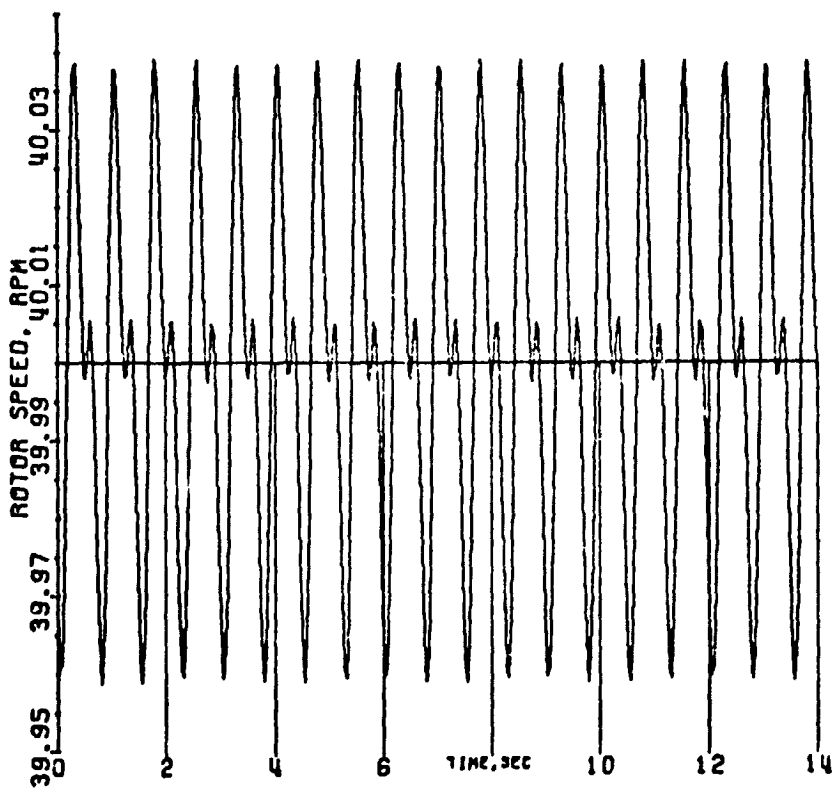

Fig. 22b: Case 13, Rotor Speed
No Falk coupling, no slip clutch, X_L = 0.35 p.u.

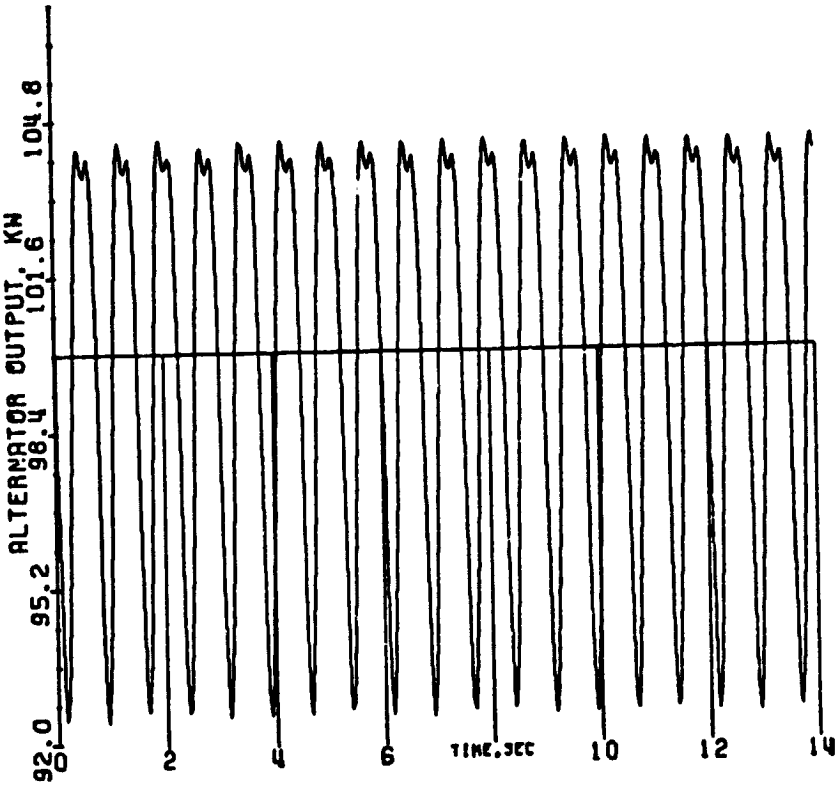

Fig. 23a: Case 14, Alternator Output
No Falk coupling, no slip clutch, $X_L = 0.40$ p.u.

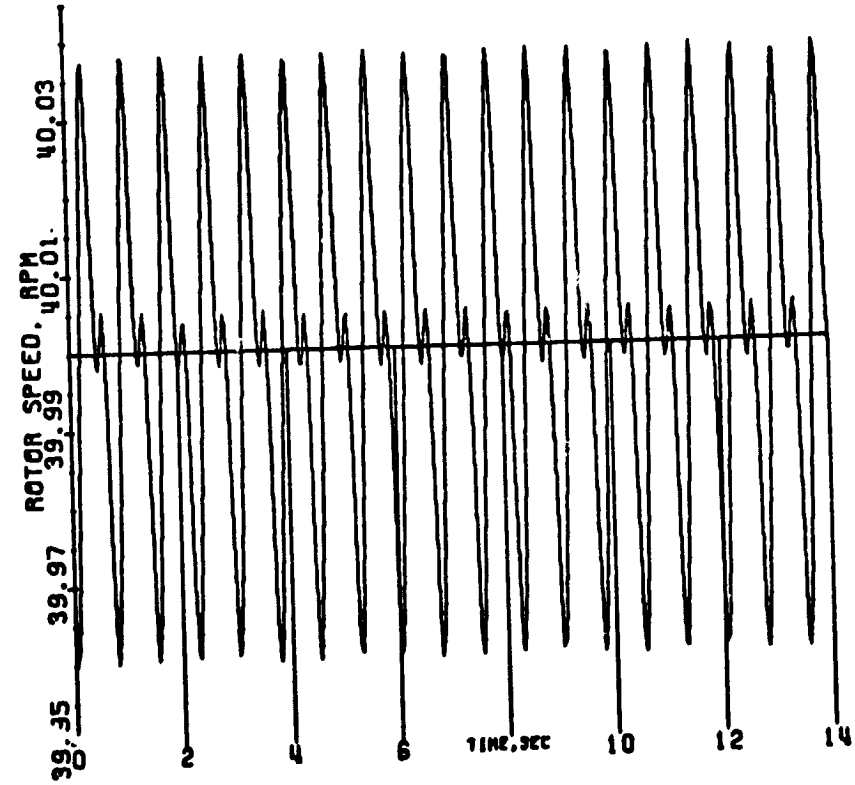

Fig. 23b: Case 14, Rotor Speed
No Falk coupling, no slip clutch, $X_L = 0.40$ p.u.

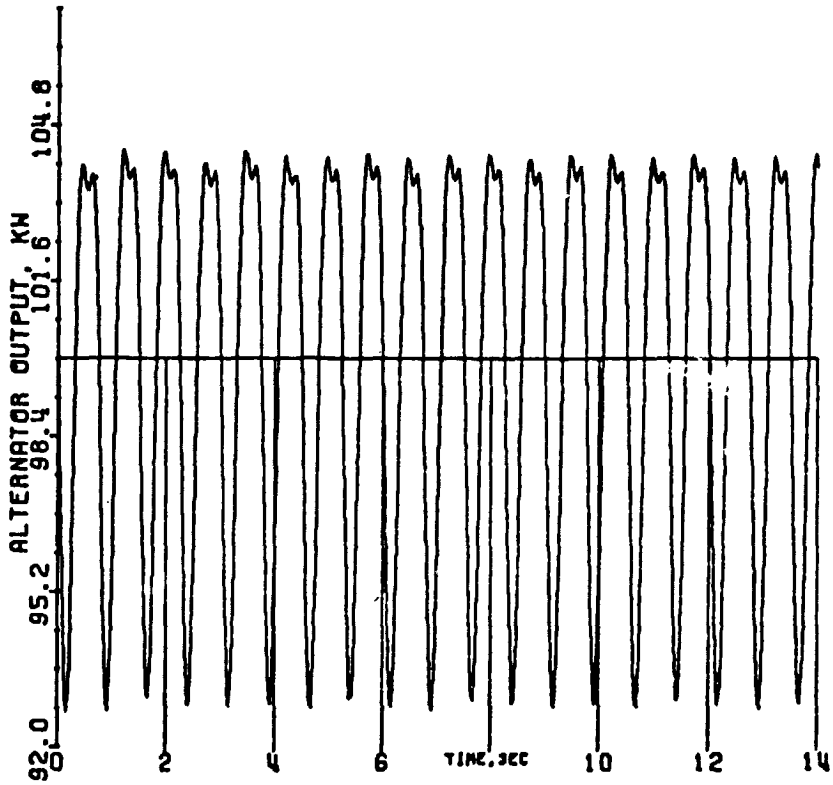

Fig. 24a: Case 15, Alternator Output
No Falk coupling, no slip clutch, X_L = 0.43 p.u.

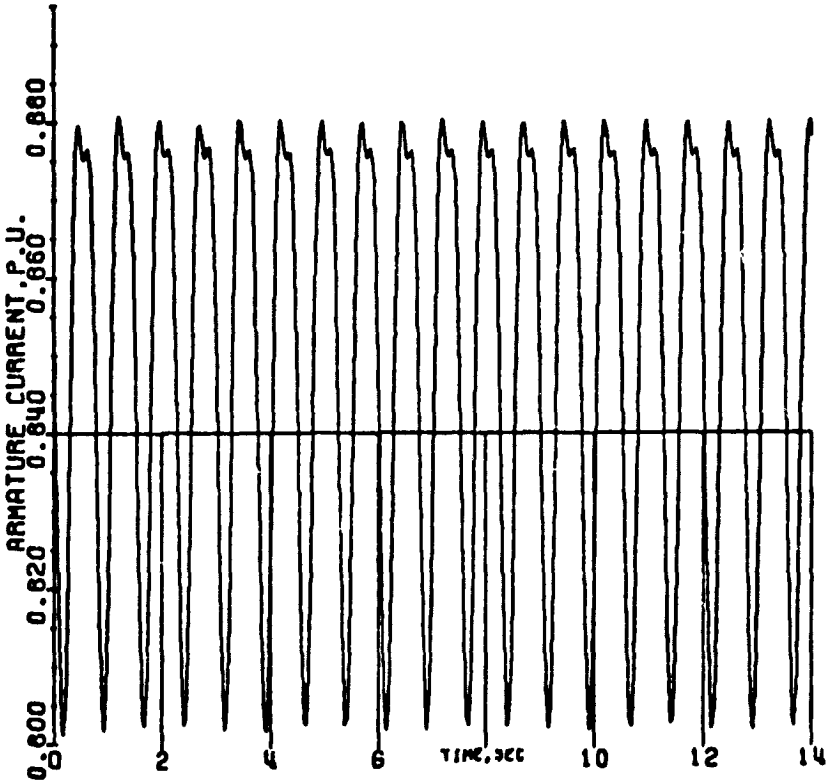

Fig. 24b: Case 15, Armature Current
No Falk coupling, no slip clutch, X_L = 0.43 p.u.

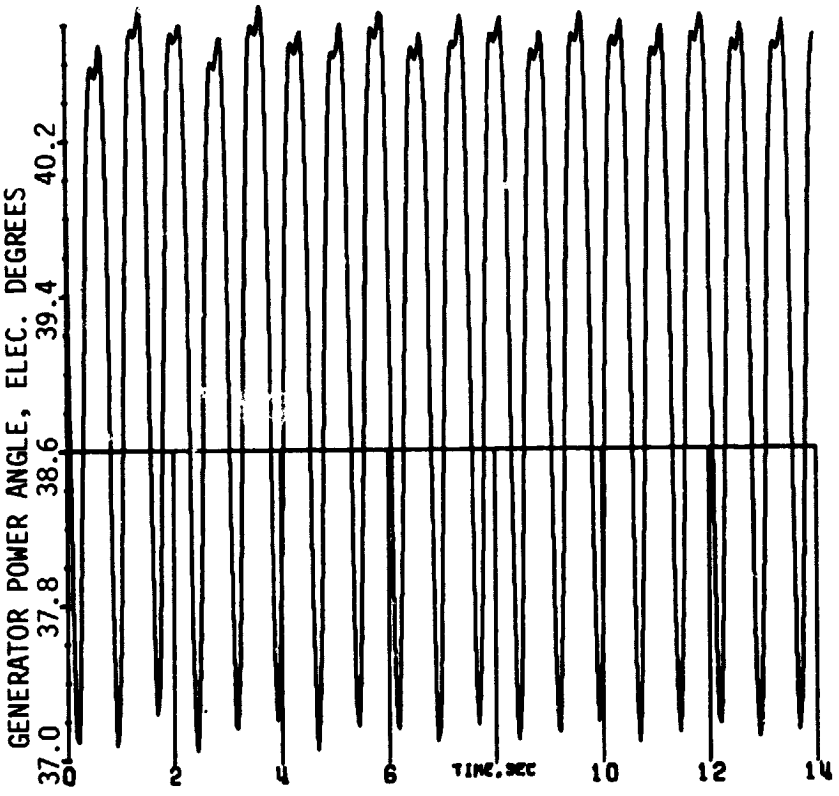

Fig. 24c: Case 15, Generator Power Angle
No Falk coupling, no slip clutch, $X_L = 0.43$ p.u.

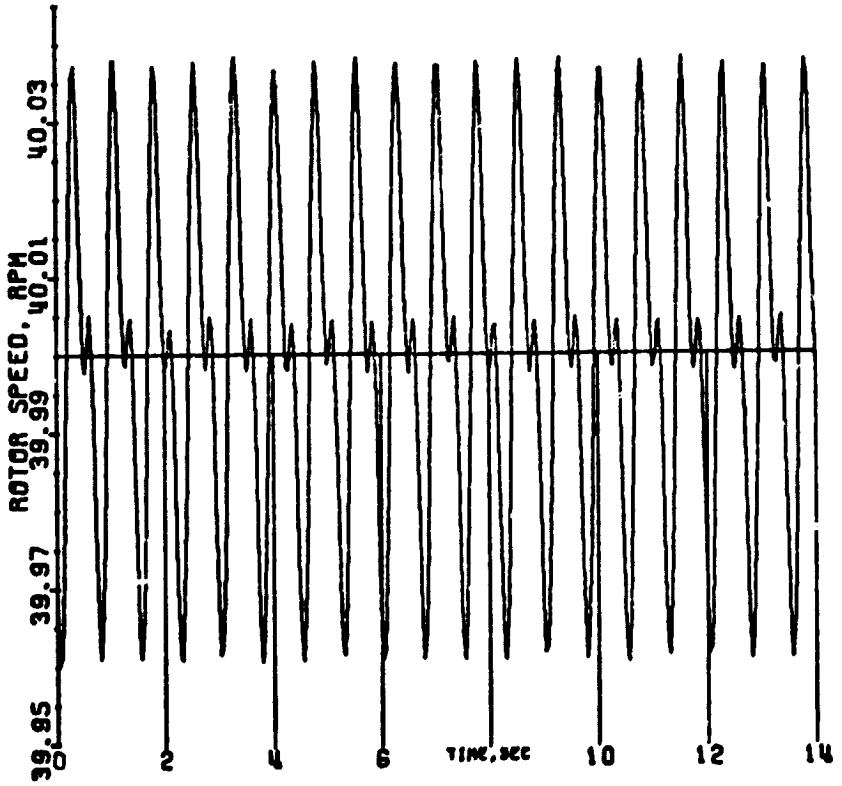

Fig. 24d: Case 15, Rotor Speed
No Falk coupling, no slip clutch, $X_L = 0.43$ p.u.

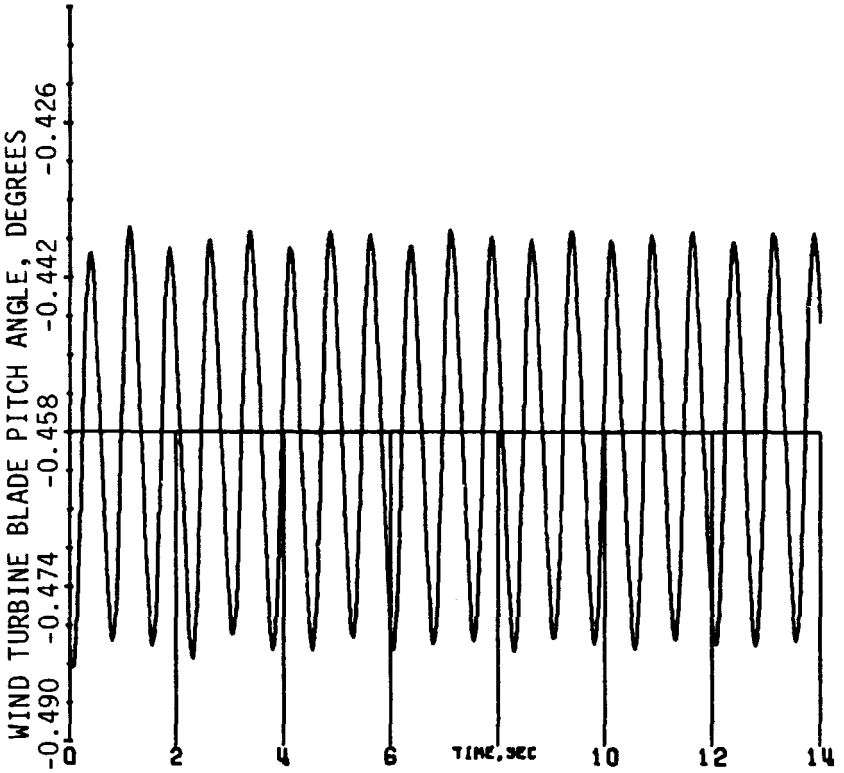

Fig. 24e: Case 15, Blade Pitch Angle
No Falk coupling, no slip clutch, $X_L = 0.43$ p.u.

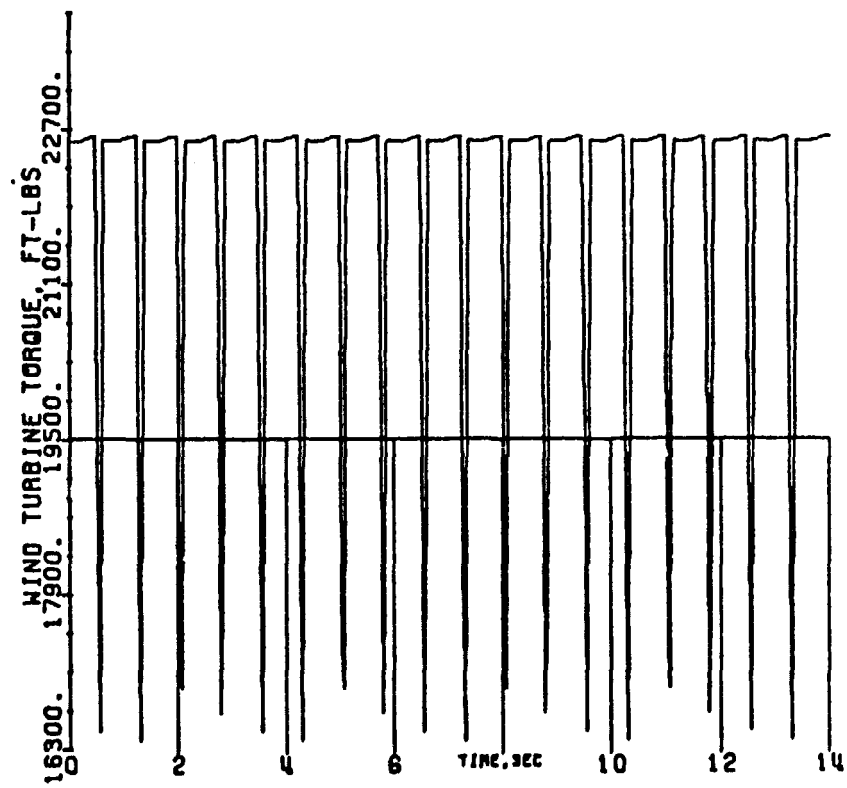

Fig. 24f: Case 15, Turbine Torque
No Falk coupling, no slip clutch, $X_L = 0.43$ p.u.

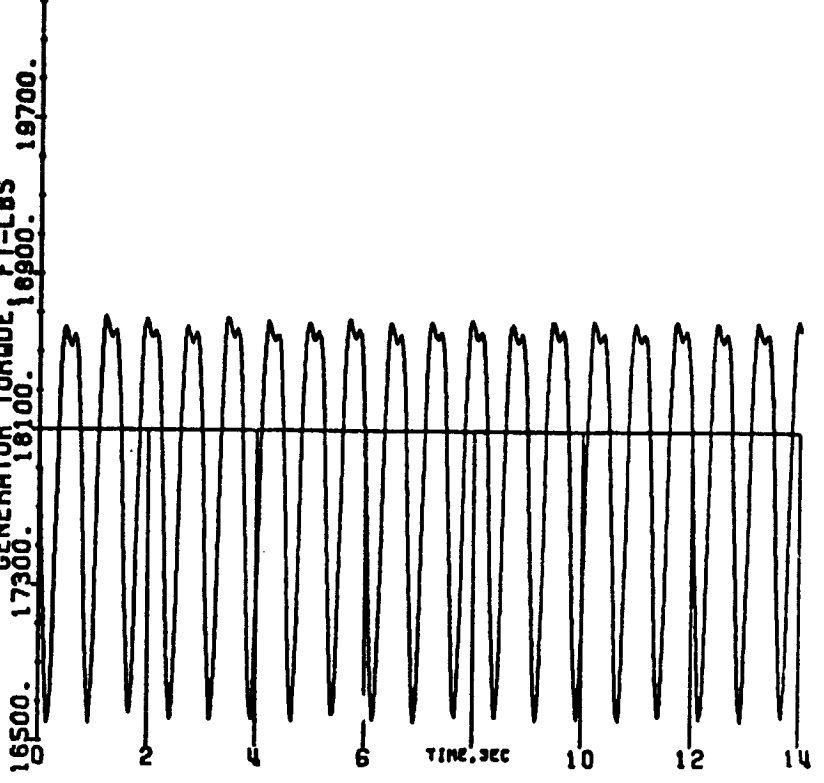

Fig. 24g: Case 15, Generator Torque
No Falk coupling, no slip clutch, X_L = 0.43 p.u.

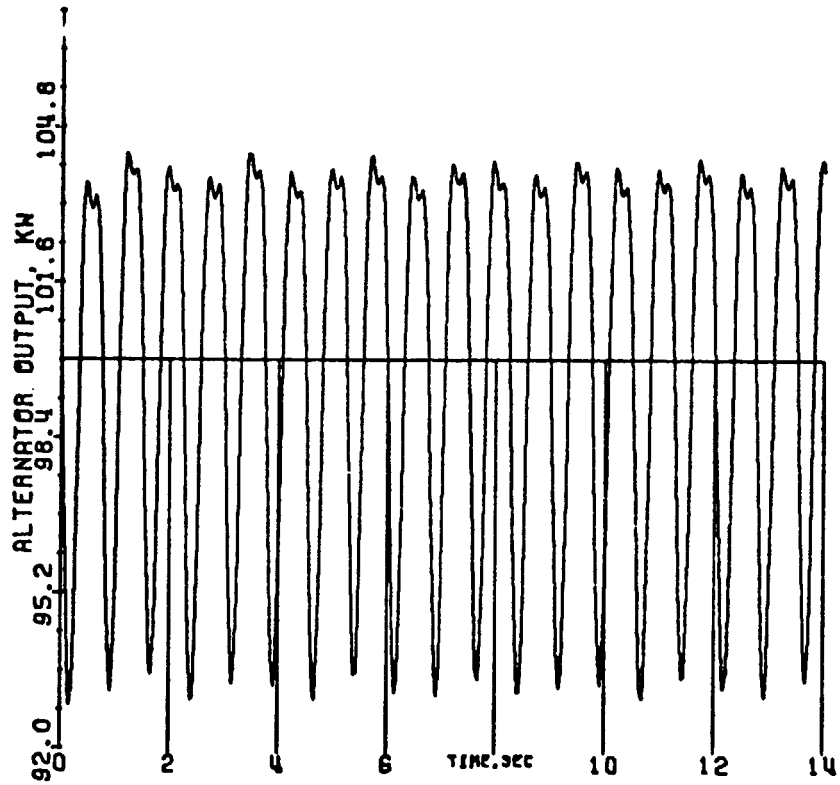

Fig. 25a: Case 16, Alternator Output
No Falk coupling, no slip clutch, X_L = 0.47 p.u.

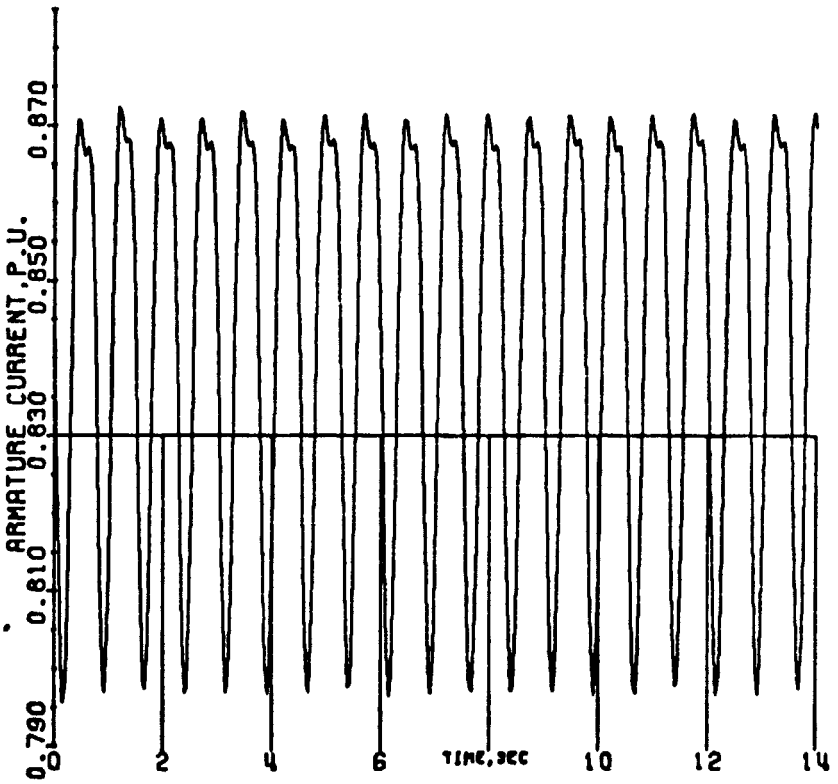

Fig. 25b: Case 16, Armature Current
No Falk coupling, no slip clutch, X_L = 0.47 p.u.

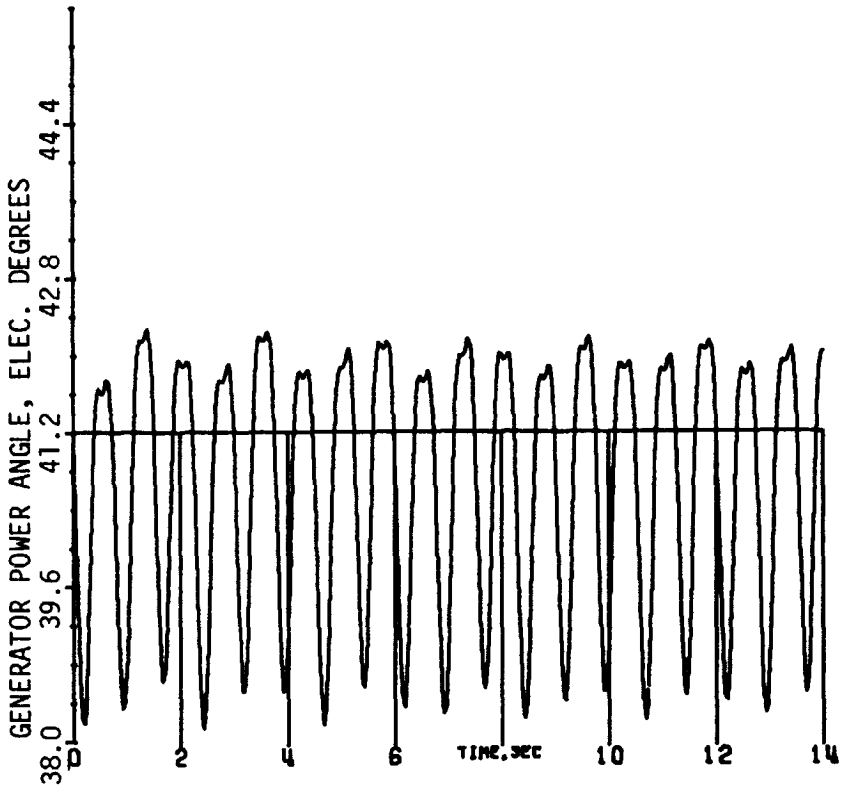

Fig. 25c: Case 16, Generator Power Angle
No Falk coupling, no slip clutch, X_L = 0.47 p.u.

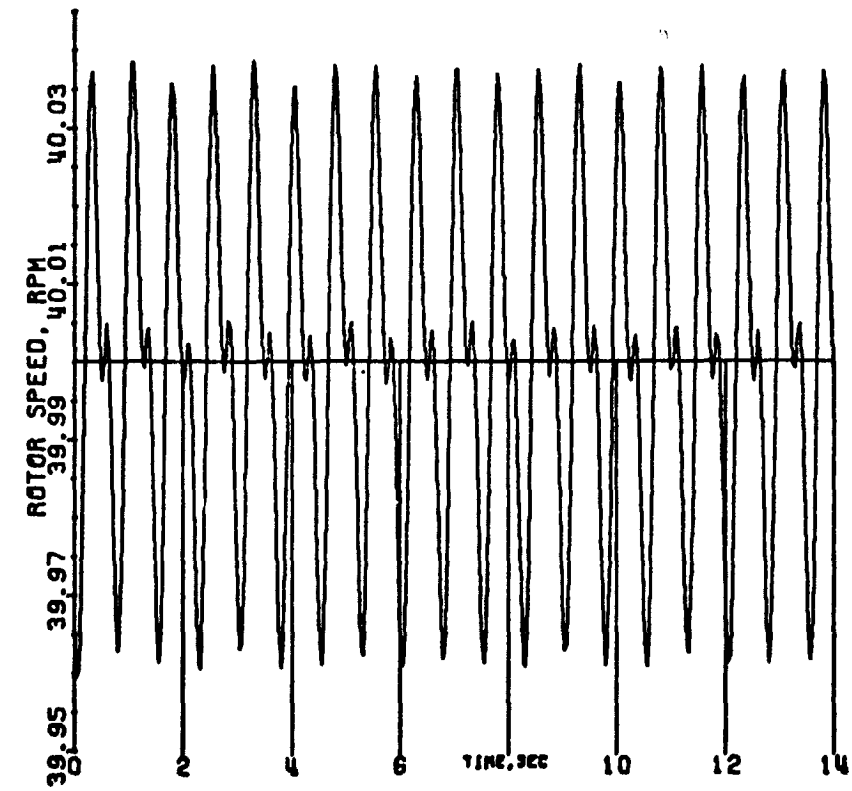

Fig. 25d: Case 16, Rotor Speed
No Falk coupling, no slip clutch, X_L = 0.47 p.u.

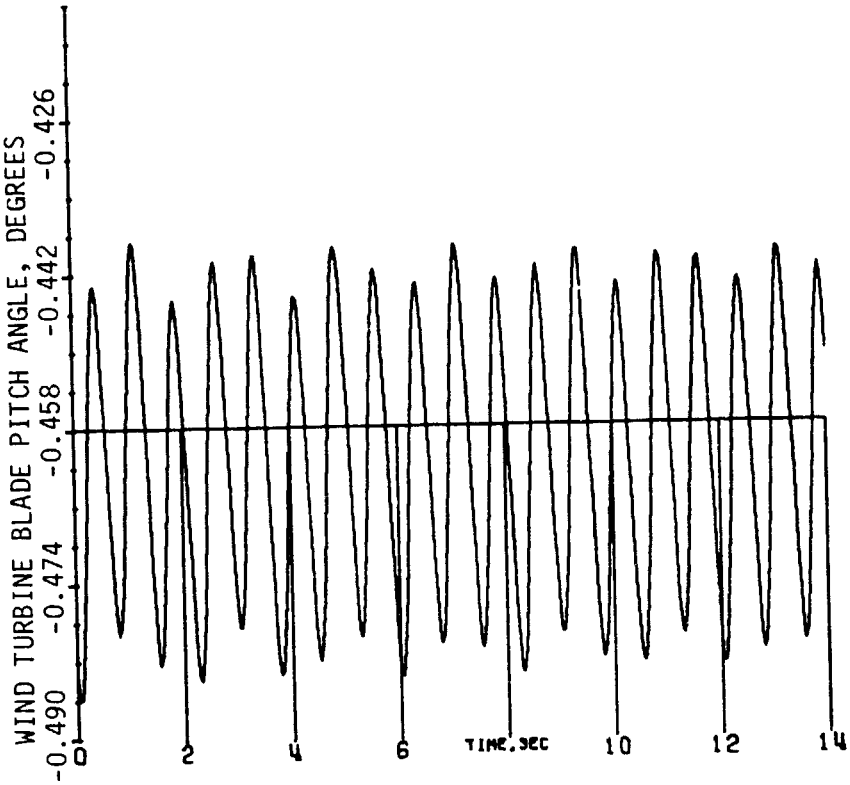

Fig. 25e: Case 16, Blade Pitch Angle
No Falk coupling, no slip clutch, $X_L = 0.47$ p.u.

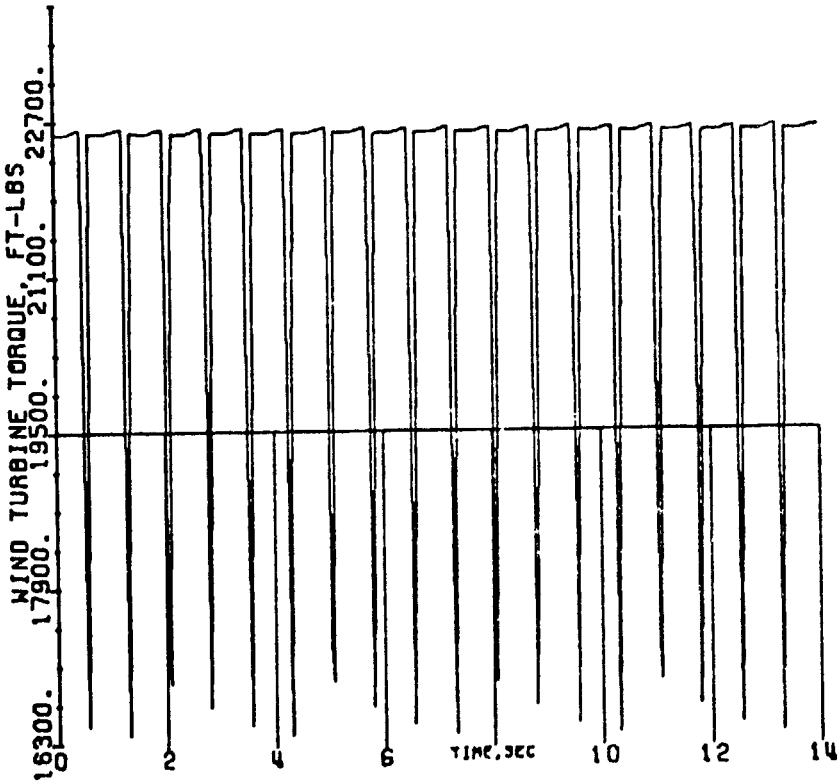

Fig. 25f: Case 16, Turbine Torque
No Falk coupling, no slip clutch, $X_L = 0.47$ p.u.

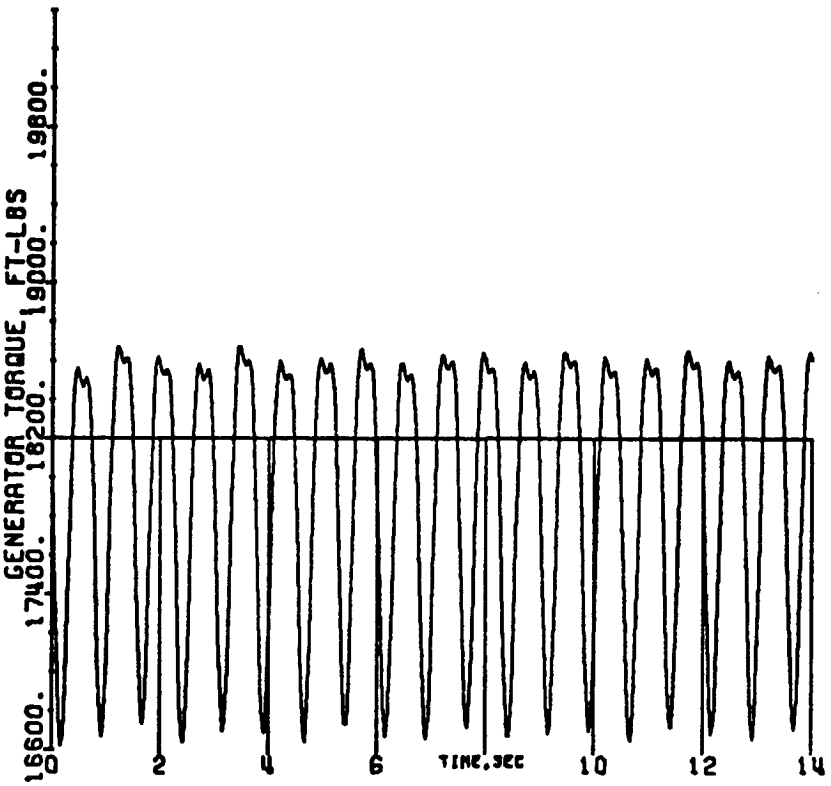

Fig. 25g: Case 16, Generator Torque
No Falk coupling, no slip clutch, $X_L = 0.47$ p.u.

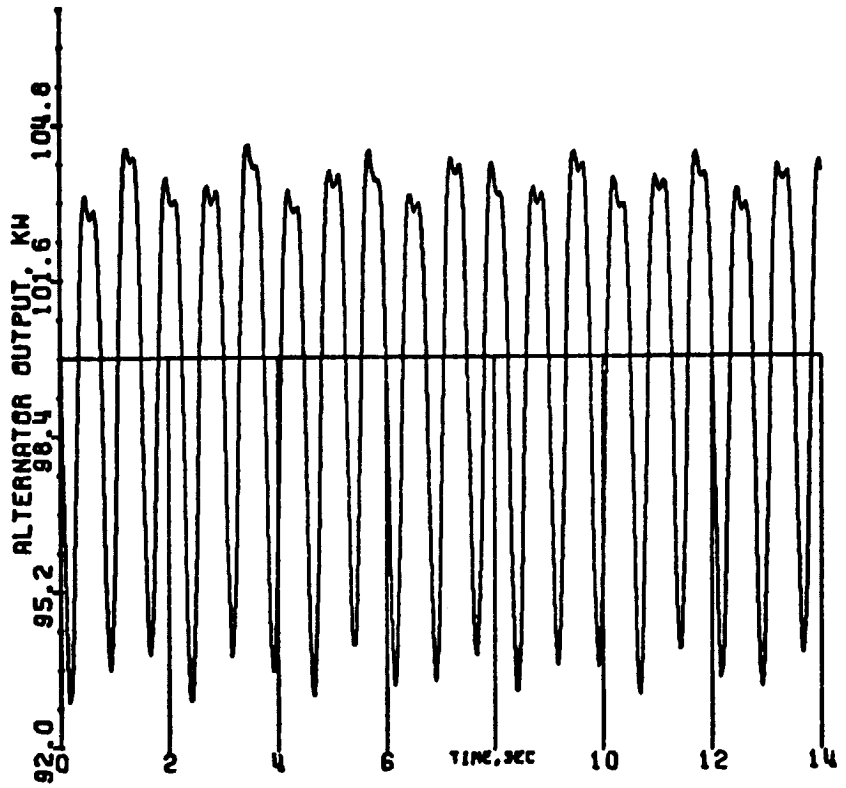

Fig. 26a: Case 17, Alternator Output
No Falk coupling, no slip clutch, $X_L = 0.50$ p.u.

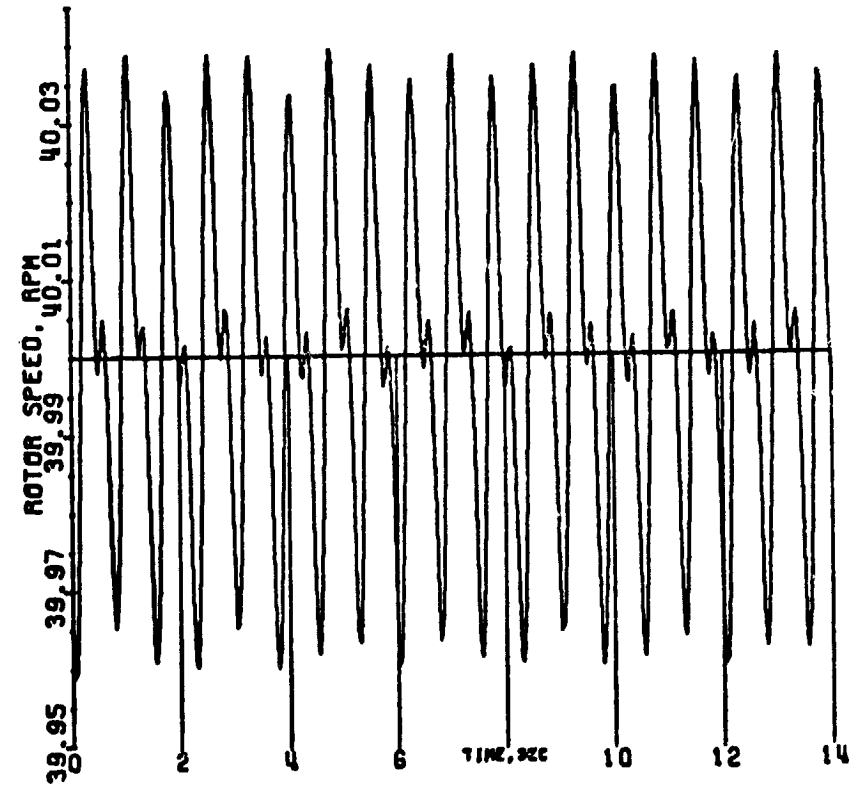

Fig. 26b: Case 17, Rotor Speed
No Falk coupling, no slip clutch, $X_L = 0.50$ p.u.

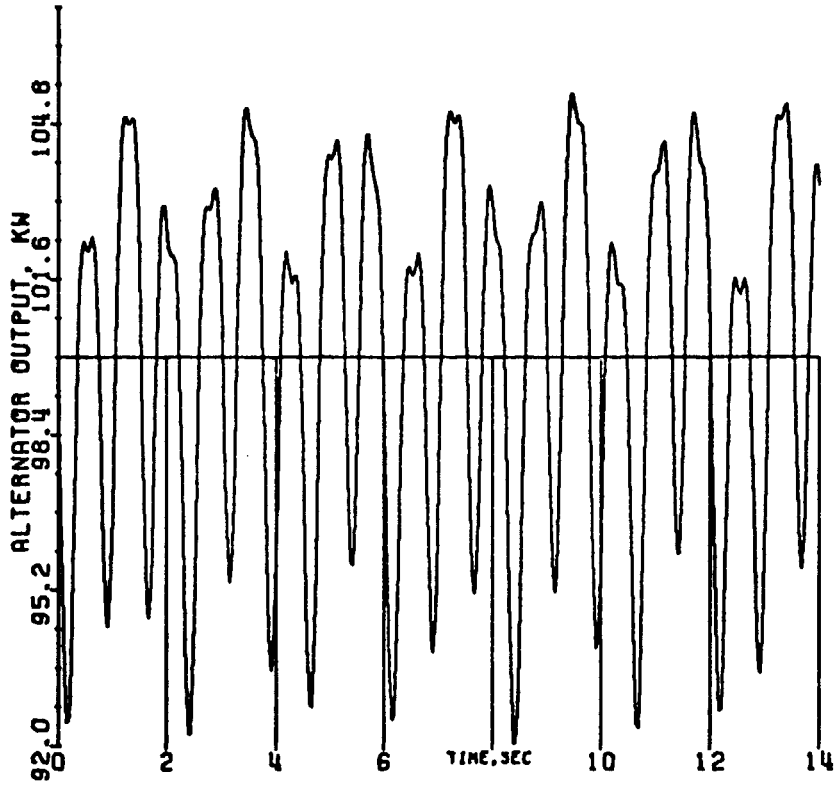

Fig. 27a: Case 18, Alternator Output
No Falk coupling, no slip clutch, $X_L = 0.55$ p.u.

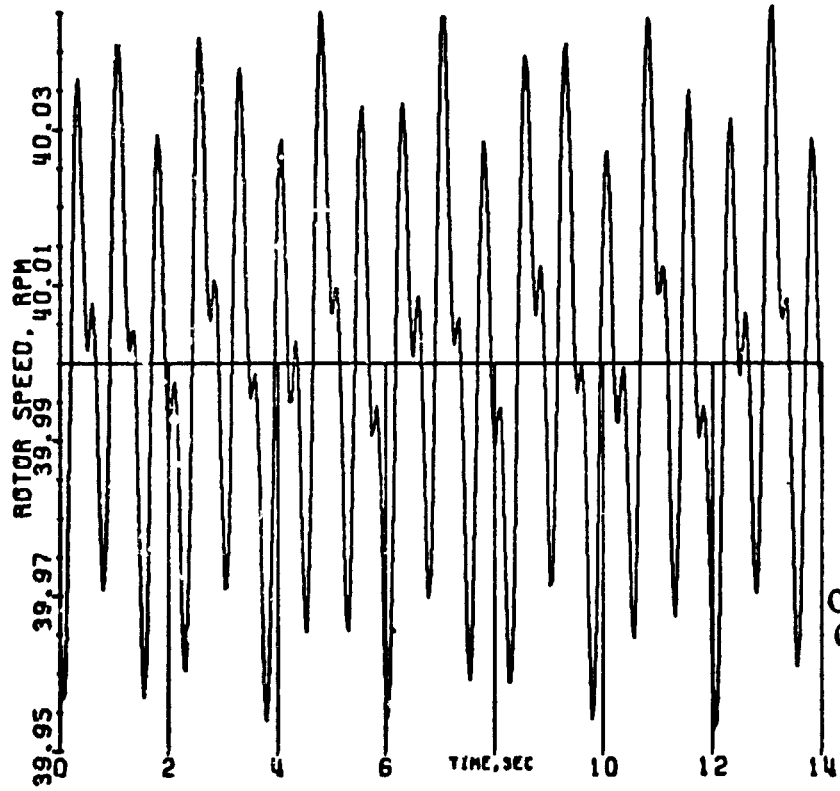

Fig. 27b: Case 18, Rotor Speed
No Falk coupling, no slip clutch, $X_L = 0.55$ p.u.

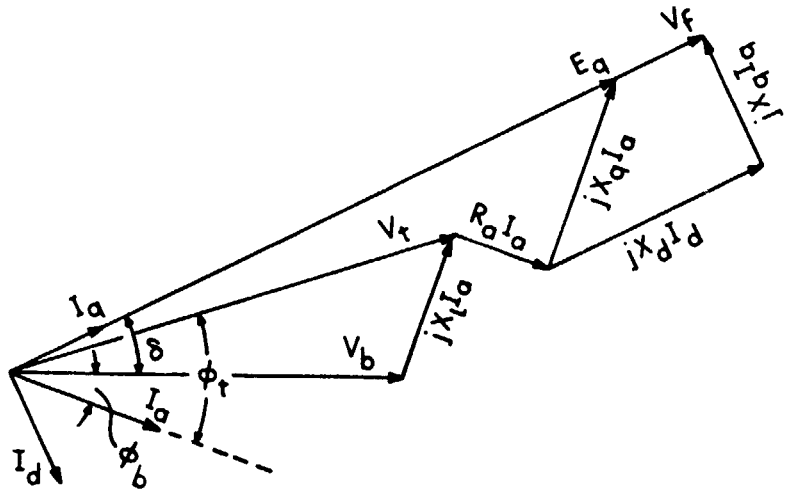

Fig. 28 Phasor Diagram of Synchronous Generator

★ U.S. GOVERNMENT PRINTING OFFICE 1978 - 757-139/6322